ALMA MATER STUDIORUM A.D. 1088
UNIVERSITÀ DI BOLOGNA

SCUOLA DI SCIENZE

Corso di Laurea Magistrale in Geologia e Territorio

Dipartimento di Scienze Biologiche, Geologiche ed Ambientali

Tesi di Laurea Magistrale

The fractionation of U-Th into the colloidal fraction in acid mine drainage conditions in the Río Tinto areas

Candidato:
Andrea Celeste Curcio

Relatore:
Prof. Enrico Dinelli

Correlatore:
Prof. Luis Carlos Barbero González

Sessione Dicembre 2016
Anno Accademico 2015-2016

To my family.

And in memory of Bruno Capaccioni.

ABSTRACT

Río Tinto provides ideal conditions for studying the role of colloidal particles in concentrating elements that could have environmental impacts like U and Th, and their influence on the transport of these radionuclides to Ría de Huelva estuary (Spain). To achieve this objective, ultrafiltration experiments were developed on the Río Tinto waters samples, in order to separate colloids by different sizes (50 kDa, 10 kDa, 5 kDa, 3 kDa). Samples obtained from the ultrafiltration performed with 50 kDa and 3 kDa were analysed to find out concentration using appropriate techniques (ICP-MS) and radionuclides activities have been determined for each of them. An ultrafiltration permeation model describes the relationship between log of concentration of the investigated element in the permeate solution plotted versus log of concentration factor (CF), which is the ratio of initial volume divided by the retentate volume. If there is a constant permeation, this relationship should result in a linear pattern and it can be used to predict the ultrafiltration behaviour of U and Th in this peculiar waters from Río Tinto acid mine drainage system. Experiments were carried out using concentration factor from 1,07 to 1,73, with the aim to investigate if a permeation model, already proved for higher concentration factor, could be applied for lower values too. The behaviour of U can be predicted by a permeation model that provides a permeation coefficient (P_c) of 0,813 for U < 50 kDa and P_c = 0,626 for U < 3 kDa. The permeation model can just show that little retention for U occurs and that the permeation behaviour of U can be considered the same even at low concentration factors. The application of the permeation model on Th 50 kDa samples failed because the membrane was not retaining in quantitative form, but it could be possible derived a P_c = 0,360 for Th from the 3 kDa experiments, result that, anyway, could be due to artefactual retentions. Using low concentration factors, the colloidal concentration cannot be estimated by the permeation model for both U and Th. Concentration of U amounts to values from 4,73 µg/L to 6,54 µg/L , while the range for Th is from 13,0 µg/L to 28,0 µg/L, but no significant differences among the permeate and the retentate were found. Both the elements are present in higher concentrations respect to their content in common natural waters, according to the predict character of the investigated elements in so acidic conditions, in which both can stay in dissolved form and even colloids and all of solid phases will be disintegrated. $^{234}U/^{238}U$ activity ratios range between 1,761 and 2,060. The disequilibrium among the ^{234}U and ^{238}U isotopes is attributable to the excess of ^{234}U related both to the recoil effect, and the preferential leaching of ^{234}U respect to ^{238}U by acidic waters from minerals in the mining areas. A range between 0,056 mBq/L and 0,169 mBq/L for ^{230}Th activity, whose presence in solution is mainly related to the decay of ^{234}U, was obtained. Its presence in solution again comes from the acidic environment that promotes the desorption of thorium from particles and colloids, as well as mineral phases undergo dissolution.

INTRODUCTION

The Río Tinto is one of the most important in the Huelva province, with a basin extended for 1676 km^2 and a length of about 100 km before reaching the Ría de Huelva estuary. It is well-known for its red coloured water, that gives it its name. Archaeological studies estimate the Río Tinto mining district has been exploited since 4500 years, first of all by the local population, then from Tartars and Phoenicians. It's since Roman Age that mining activity became more developed together with pollution increased (high Pb content was detected in ice level in Greenland, dated back to Roman age with isotopic compositions revealing that 70% of its contain came from Río Tinto mine); later, excavation activity decreased until the XIX century, when industrial revolution occurred and mining activity rose again, such a step provoked extreme damage to the environment due to the hundreds of mines that were operating during XIX and XX centuries producing sulphuric acid, copper and other base metals like Zn and Pb. The Río Tinto rises in Peña de Hierro, a mine located to the north-east of Río Tinto anticline. Even if it is less known respect to the Río Tinto mine and it dates Roman age, Peña de Hierro has a higher metal grade and it started to be profitable during the early XIX century, when several mining companies turned exploiting it. Like other mines advanced in Spain, it's located in the Iberian Pyritic Belt, rich in massive sulphide deposits, and Río Tinto path-flow is almost entirely delineated thru this area. The most common sulphide is pyrite (FeS_2), but it's associated with minerals of economic interest like chalcopyrite ($CuFeS_2$), sphalerite (ZnS), galena (PbS), arsenopyrite (FeAsS), etc.

The weathering on these sulphides during the last century caused the pH to fall down to values <2, favourable to the mobilization of heavy metals and natural radionuclides in waters and sediments (Borrego et al., 2001; Sánchez España et al., 2005; Hierro et al., 2011; Ketterer et al., 2011). Several studies were developed on this peculiar subject, with evidence of very high values of uranium concentration in acidic waters. As an example, Ketterer et al. (2011) revealed that dissolved ^{238}U activity varies from 10 to 850 mBq/L, with the highest ^{238}U activities and the highest $^{234}U/^{238}U$ ratios observed under the most acidic conditions.

All the processes of transfer materials from the continents to the oceans are constrained by the removal of reactive elements on to particles (Turekian, 1977). The *scavenging* process is the one by which elements are subtracted from dissolved form to particulate or colloidal form. It depends on particles composition and the probability of changing in its form is function of contact surface between particles and dissolved species, so it will be more significant in particles-rich environments, as those developing in acid mine drainage (AMD) conditions where colloids are very abundant due to the precipitation of Fe-oxyhydroxides and secondary sulphates as pH rises. Easy-absorbable elements and with low solubility will quickly remove from the water and will be deposited within the sediments, whereas elements which have the same residence time as mixing-time will be transported horizontally within to the particles-flow. Different results came out respect to the distinct affinity for sorption onto particles of each element (Osthols, 1995; Balistrieri et al., 1981; Lao et al., 1993), due to the scavenging residence times depending on composition and other uncontrollable factors. Chase et al. (2002) and Luo & Ku (2004) tried to go beyond this problem defining a partition coefficient which depends on the composition and describes the equilibrium partitioning of a species between the dissolved and the particulate phase. The dynamics of the system that regulate the delivery of the metals in the waters have been widely studied even though it's not always possible to study directly all of the elements.

Scientists have been able to carry out information thanks to the investigation on elements with similar physical-chemical behaviour or using tools such as ^{238}U-^{234}Th disequilibria to understand, for example, removal of Th.
Secondary minerals forming in acid mine drainage system are critical because of the increasing in the capacity for adsorption due to high surface area of the precipitation of Fe-oxyhydroxides phases (Jamieson et al., 2015). The latter are crystalline and amorphous colloidal forms that play an important role in acid rock drainage as carrier of metals and radioisotopes. Colloidal particles can be regarded as an intermediate of the precipitate formation process, since results show that only the degree of crystallization increases when particles are transformed into precipitates (Zänker et al., 2002). Nordstrom (2011) concluded that Fe(III), which is the major oxidant of pyrite under acid conditions, complicate the interpretation of dissolved concentrations species due to its colloidal form that passes through most filter membranes and alters the results respect to dissolved Fe(III). This phenomenon was pointed out in other works (Jamieson et al., 2005; Wang, 2014) who confirm that, high colloidal-content lead to an overestimation on the Fe-content and its associated elements. In acid drainage conditions, like in Río Tinto area, the abundant Fe-content colloidal fraction has high ability in ions absorption, and this fact was recognized by several authors (Dold & Fontboté, 2002; Andersson et al., 2001; Chen et al., 2001).

Aim of the work

Colloids act like ligands that influence speciation, removal, transport, bioavailability and toxicity of trace elements in aquatic system (Doucet et al., 2007), nevertheless their study is complicated because of its nature, since their instability, their minute size, their low concentration, their heterogeneous composition, their tendency to form carbonated complexes or to associate with clay minerals and their closed association with organic material (Lead & Wilkinson, 2007; Filella, 2007). That's why Río Tinto area is a perfect site for studying the influence of colloids on the dynamics of the system, since the following points:

1) In the Río Tinto prevailing conditions, pH neutralization, which occurs when strongly contaminated water get in touch with clear water from precipitation or of no-contaminated tributary, leads to the formation of the colloids, which result rich in sulphate complexes and ferric and/or aluminium disulphates.
2) At these conditions, colloids concentration tends to be very high due to the extreme ligands concentrations in the contaminated water.
3) There is no carbonate or bicarbonate dissolved in the acid water of Río Tinto basin.
4) At so low pH order, organic matter may be considered negligible.

All of these aspects make Río Tinto conditions ideal to assess the role of colloidal particles on the carriage of significant amount of radionuclides and to evaluate their role on the natural remediation of the system. To achieve this goal, ultrafiltration experiments on collected water samples was developed using 50 kDa, 10 kDa, 5 kDa and 3 kDa membranes. U and Th were investigated, measuring their activities for each of the samples obtained. Lastly, a permeation model was established for the discussed elements.

1 - STUDY AREA

The study area is located in the south-west of Spain, in the mining district of Río Tinto (fig. 1). Río Tinto is the name of a river that rises in Peña de Hierro, next to Nerva, in the north-east of the Huelva province and flows across the Iberian Pyrite Belt, one of the most relevant volcanogenic massive sulphide district in the world. The study was developed to a close area of approximately 60 m^2, delimited by a big tailing of the Peña de Hierro mine to the west, the headwaters of the Río Tinto to the north, the slope coming down the HV-5011 road to the east and the street that goes from the HV-5011 to the Peña de Hierro mine entrance on the south. In this restricted basin, Río Tinto water catch two different water contributions: one of them arises from the tailing dump and flows along the west-side into the Río Tinto, whereas the other one join the segment resulted by this first water mixing about 7 m further to the south than the first one, but running from the east-side of Río Tinto and generating another mixing.

1.1 Geological setting

The investigated zone is included in the 1:50000 sheet number 938 (Nerva), resulted from the MAGNA project (NAtional Geological MAp) conducted between 1972 and 2003 by the Spanish Geological Survey (IGME), and situated in the central-east part of the Huelva province, in Sierra de Aracena foothill. It's located in the eastern extremity of the Iberian Pyrite Belt, which is extended from the Baixo Alentejo province in Portugal towards the Spain with a NW-SE direction, forming an arch 240 km long and 35 km wide that belongs to the South-Portuguese Zone, the southernmost domain of the Iberian Massif. The area is characterized by deposits dated back to Upper Devonian and Lower Carboniferous, that can be resumed in a relatively simple succession, shown in the schematic section in fig. 2: the Devonian Phyllite and Quartzite Group (PQ), the Volcano-Sedimentary Complex (CVS) and a Carboniferous flyschoid sequence named the Culm formation, that is the base of the Baixo Alentejo Flysch Group (the following Carboniferous component of the South-Portuguese Zone) but included in this domain. The oldest rocks observed are organized in the PQ group and they consist in a detrital sequence of more than 2000 m of slate alternated with sandstones, with facies revealing a stable continental shallow platform deposition during the Frasnian and Famennian ages. Formation of half-graben basins, related to the Hercinian compressive tectonic just started, led to a period of instability in which, heterogeneous and high energy sedimentation prevailed, determining the deposition of subaerial, delta fan and gravity flows deposits, recorded now in the PQ hanging wall and representing the Fammenian transition with the overlying Volcano-Sedimentary Complex (VSC) (Moreno et al., 1996). The VSC include a complex bimodal volcanic unit intercalated with shales, volcanogenic facies and Mn-rich chert deposits of late Fammenian-middle Visean ages. The activity was submarine and, despite the fact that it is a discontinuous unit and it varies frequently and quickly both in thickness and in lateral and vertical facies distribution, it can be differentiated in two felsic volcanic cycles separated by two mafic cycles. On a regional scale, the unit hold a Mn-rich bed of purple shale associated to jasper and forming a continuous marker in the uppermost part of the succession. The thickness range of VSC is 0-1300 m, due to the differences in the intensity of the volcanism within the intracontinental basin wherein it occurred, and the characteristics of the northern domain widely differ from those of the southern domain. The latter reflects a continental influence deposition, proved

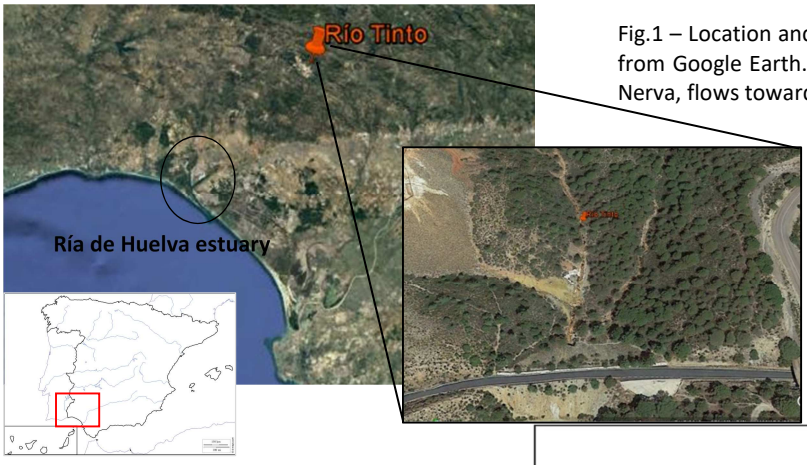

Fig.1 – Location and detail of the study area in Spain , images from Google Earth. Río Tinto rises in Peña de Hierro, next to Nerva, flows towards SW and reaches Ría de Huelva estuary.

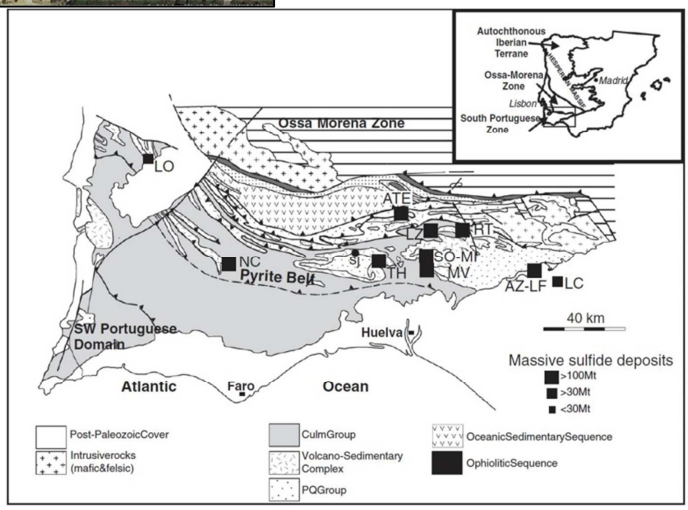

Fig. 2 – On the right, schematic geological map showing the location of the major massive sulphide deposits. AZ-LF: Aznalcóllar-Los Frailes; LC: Las Cruces; LO: Lousal; LZ: La Zarza; NC: Neves Corvo; MV: Masa Valverde; RT: Rio Tinto; SO-MI: Sotiel-Migollas; TH: Tharsis. Modified from Tornos (2006). From Menor-Salvan et al. (2010).

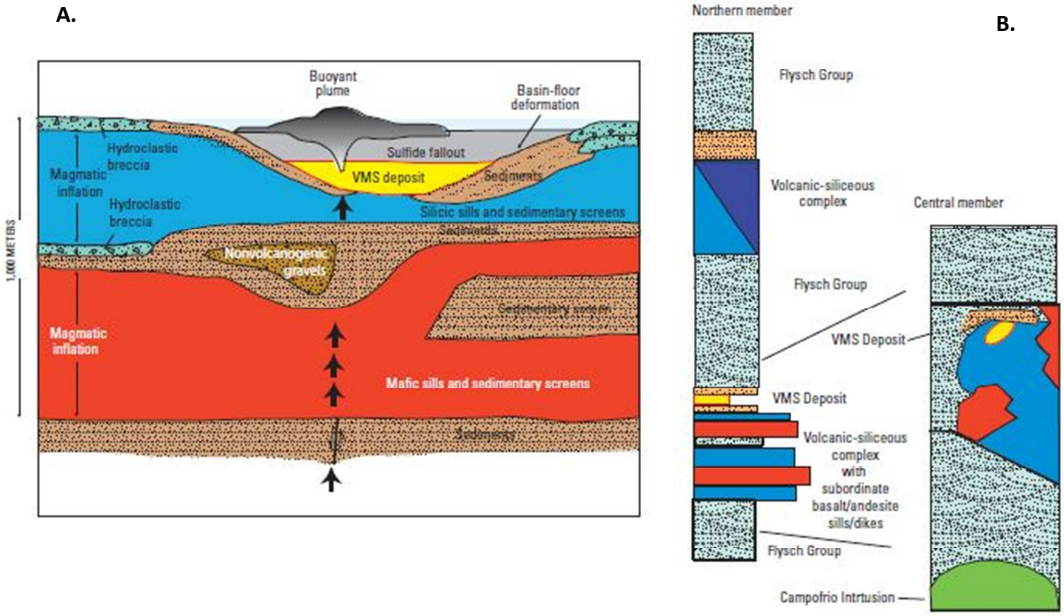

Fig. 3 - The Iberian Pyrite Belt, where volcanogenic massive sulphide mineralization has occurred in a siliciclastic-felsic suite, is shown in a schematic geologic cross section (A) and generalized stratigraphic sections (B). A: schematic cross section of the Rio Tinto mine showing the location of the volcanogenic massive sulphide deposit and sediment-sill complexes. B, stratigraphic sections of the northern and central members of the Iberian Pyrite Belt. From Franklin et al.(2005).

by the abundance of shale and siliciclastic sediments, whereas the northern area shows a thick volcanic sequence with lower content in shale. Felsic terms dominate, with andesitic-rhyolitic range composition (with a prevalence of the dacitic one) of the formed domes and sills and their associated volcanoclastic deposits, constituted by hyaloclastites and pumice- and glass-rich rocks. These rocks are calc-alkaline with low Al-content and high Nb-content, though the less common mafic rocks consist in tholeiitic and alkaline basaltic and andesitic-basaltic lava flows and pillow-lavas (Mitjavila et al., 1997). Volcanoclastic rocks occupy low topographic places and they are interpreted as resulting from the dismantling of the volcanic structures, which were building up meanwhile the interaction with sea-water. The massive sulphide deposits of the Iberian Pyrite Belt are enclosed in the VSC (fig. 3) and orebodies show distinct relationships with their host rocks. They reflect the previously described two domains of the succession, because of their paleogeographic control: the black slate-related are mainly spread in southern part, reflecting deposit formed in anoxic third-order basins, like brine pools, where the hydrothermal activity was very efficient despite the shortness of the time interval (less than 5 million years) during which the deposits were developed; the felsic volcanoclastic rocks-related are located in the north part and they were originated by the replacement of the below seafloor volcanic rocks. A submerged sedimentation environment has been proposed for the PQ Group and the VSC (Quesada, 1996; Sáez et al., 1996), but due to the different depths revealed by several depositional setting of rocks, Sáez et al. (1996) suggest the Iberian Pyrite Belt as including several deep basins separated from deeper zone and other emerged ones during the massive sulphide formation. In the Culm formation, that overlays VSC, shales and sandstones deposited from turbidity currents are the main lithologies. They have Carboniferous age (upper Visean) and their thickness reach 3000 m. The formation represents a sinorogenic flysch sedimentation related to the Variscan collision and their reversal tectonic (Moreno, 1993). All of the rocks constituting the IPB were metamorphosed and deformed by Variscan orogeny, so they suffered a regional low grade metamorphism in green-schist facies, that increase from the south to the north of the belt and towards the base of the sequence (Munhá, 1990), due to the subsequent intrusion of large granitic, tonalitic and dioritic bodies. The Variscan tectonic produced a '*thin-skinned*' deformation which affected the shallower part of the crust, developing a thrust and fold belt with a southward and south-westward vergence and the consequent foliations parallel to the folds structural axis oriented WNW-ESE. Other important manifested metamorphism is the hydrothermal one, resulted from the interaction between rocks and circulating fluids, heated by the anomalous geothermic conditions existing during the Upper Devonian and the Lower Carboniferous.

1.1.1 Metallogeny

Massive sulphide deposits occur within the VSC and exhibit the classical configuration of Volcanic Massive Sulphide deposit, that is a lens of massive sulphide superimposing a wide sector with rocks interested by an important hydrothermal alteration. "*Stockwork"* mineralization is disseminated in the body nucleus, it consists in a network of widespread sulphide-rich veins as a consequence of hydrothermal fluid flows exhaled out of the sea floor (fig. 4). Mineral paragenesis comprehends pyrite as the prevailing phase, with sphalerite, galena and chalcopyrite as accessories, together with many other minor minerals. These massive sulphide deposits can be grouped into two different styles of mineralization,

reflecting the formation in contrasting geological settings (Tornos, 2006). The southern part includes deposits that are in direct relationship with shale, sedimentary component prevailing in this sector of VSC, with features developed in a low-topographic zone suggesting an exhalative environment evolved in third order basins: this kind of basins, with their reduced extension, their euxinic and low-energy deposition that build-up organic-rich, pyritic, fine-grained shale and mudstone, it is the best environment providing ideal bathymetric and chemical conditions for dense, sea-floor-closely, metalliferous and sulphur-depleted upwelling brine to accumulate and react with locally H_2S derived from sulphur-rich seawater, so as to lead to the precipitation of the sulphide minerals that compose the ore. These massive sulphides are characterized by a high (10-20) aspect ratio (longitude/thickness) due to their stratiform morphology, large tonnages, abundance of pyrite but low total base metal content, abundance of sedimentary structures but absence of sulphate. The sulphides are composed by fine-grained anhedral to subhedral pyrite, with interstitial sphalerite, chalcopyrite and galena. Carbonates are also present as widespread siderite-cemented breccias (Tornos & Conde, 2002) or as a pervasive ankerite-rich hydrothermal alteration. Other characteristic features are the presence of a large underlying stockwork and no evidence of clear metal zonation. Northern part deposits are hosted in a felsic volcanoclastic sequence with low level of mudstone, so they are poor in sedimentary structures. They show replacive fronts on felsic volcanic rocks and a hydrothermal alteration around the massive sulphides. The most recent model proposes these massive sulphides are formed by replacement of the sub-seafloor volcanic rocks, explaining their greater base metal richness with the efficiency of the geochemical trap of this environment (Doyle and Allen, 2003). They are hosted by high-energy volcanoclastic rocks like transported hyaloclastites or pumice/crystals/glass-rich breccias. At regional scale, the formation of massive sulphides was determined by the Variscan '*thin-skinned*' tectonic that furthered intrusion of basic magmas into the crust: these conditions let the geothermal gradient increase, as well as they led to acid magmas production and aided diagenetic and metamorphic evolution of the PQ group with the expulsion of saline water fluids full of metals in the convective cells generated by acid magma intrusions. As like as the southern shale-related deposits, the distribution of the massive sulphides follows the regional setting, so they are clustered along E-W trending zones forming isolated groups. The regime developed stacking lens of these massive sulphides, giving rise to intermediate (5-10) aspect ratio deposits, that present generalized recrystallization due to their intense deformation and a host rock with a pervasively silicic and sericitic alteration. Northern deposits are rich in sphalerite, galena, tetrahedrite and gold, they typically contain sulphates like barite and gypsum and oxides like magnetite. Grain size ranges from medium to coarse and remnants of silicified and chloritized host rocks are frequent within whole deposits. Tectonic banding is determined by distinct sulphur-enrichments layers alternation; such an origin is moreover confirmed with the existence of widespread S-C structures, composition and texture of banding, as well as the presence of angular fragments of pyrite hosted by the more ductile sphalerite-galena matrix. Here the metal zonation is well-defined and show differentiated Cu- and/or Zn-/Pb-rich zones. The supergene alteration of these massive sulphides originated large gossan outcrops, usually enriched in Au and Ag, but without showing any obvious zoning.

Fig. 4 - Stockwork mineralization in pyrite (a) , highlighted by the oxidation. In detail (b) the small minerals are disseminated in a network of widespread veins.

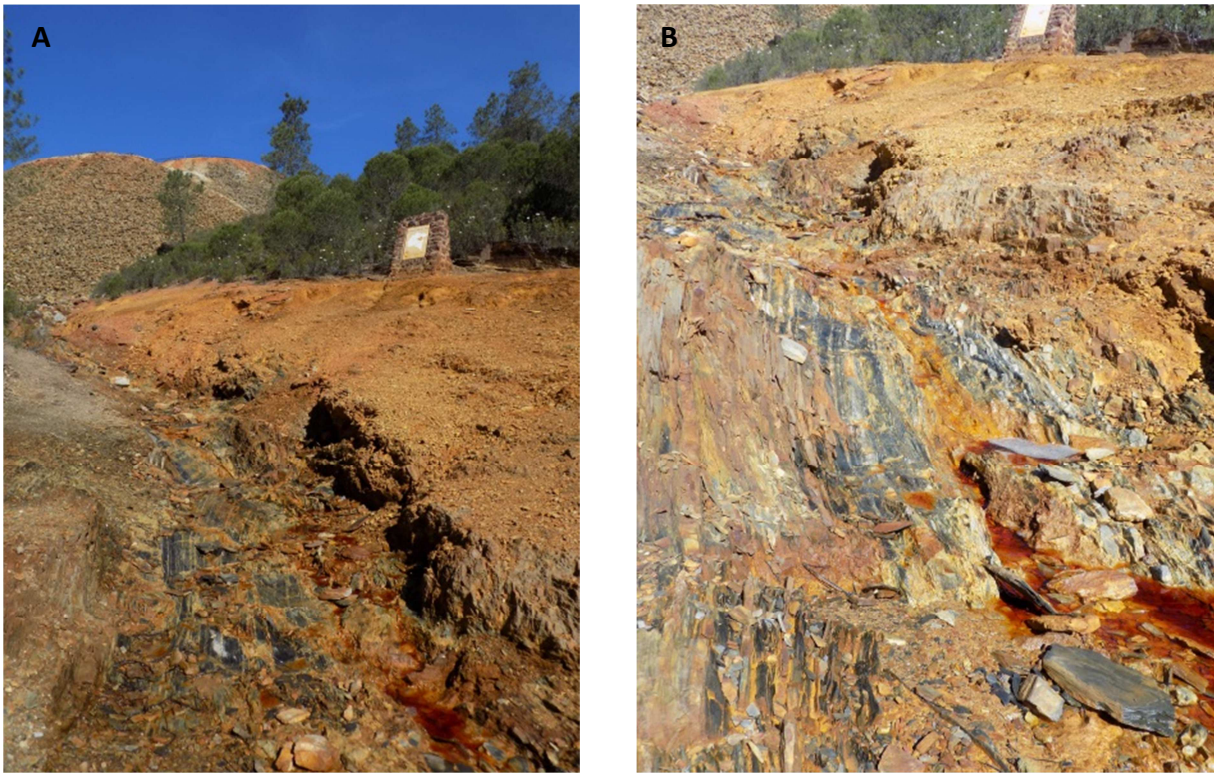

Fig. 5 – A) Branch of water flowing from the big waste pile of Peña de Hierro mine. B) The drainage in this area is developed in shale, prevailing sedimentary component that, together with all of the rocks of the IPB, suffered the Variscan orogeny

Fig. 6 – Ochre and brownish coloured precipitated typical of the acid mine drainage sites.

Fig. 7 – Acid mine drainage (AMD) contamination starts with the oxidation of pyrite and goes on with a series of reactions that release more and more acidity, sulphate and an elevate amount of metals and metalloids, leading to a toxic and highly contaminant solution (a e b). When pH rises, precipitation of Fe-oxyhydroxides and secondary sulphates occurs, developing a particles-rich environment characteristic of AMD conditions (c). In d: efflorescent sulphates formed in the course of a dry period that temporally store acidity, SO_4 and metals.

1.1.2 Río Tinto district

Río Tinto synclinal is a Carboniferous structure with W-E direction, with a main gentle folding and several minor folding, one of whom constitutes the Río Tinto volcanic anticline with its related mineralization. Faults and thrust are abundantly present, together with a pervasive hydrothermal alteration often hiding original formational relationships. In Río Tinto district we can find deposits showing both northern and southern characteristics, reflecting their different original environment, in fact the mineralization in Northern Vein is dacite-hosted displaying replacement structures with it, while the one of Southern Lode is slate-related (fig. 5) and has sedimentary structures formed in a exhalative scene. So we get the mineralization as disseminated or in small veins in the stockwork areas, as well as in lenses in massive form above or comprehended in the stockwork zone, or in gossan area representing the supergene alteration.

1.2 Geochemistry of the acid mine drainage

1.2.1 AMD contamination

A common aspect of the study area is the pervasive presence of yellow-ochre to reddish-brown sediments in the riverbanks, consisting of Fe-precipitated due to the pyrite oxidation in mine sites (fig. 6). In reducing conditions sulphides are extremely insoluble. They remain stable in the subsoil as long as they don't react with oxygen, but once they get in touch with it and with water, the oxidation of pyrite takes place:

$$FeS_{2\ (s)} + 7/2\ O_2 + H_2O \rightarrow Fe^{2+} + 2H^{+} + 2SO_4^{2-}$$

This reaction origins acidity (H^+) and produces a large amount of sulphate (SO_4^{2-}) and ferrous iron (Fe^{2+}), leading to a toxic leached solution with an extreme contaminant capacity. However, when ferrous iron (Fe^{2+}) flows over the contact surface with the oxygen, oxidation to ferric iron (Fe^{3+}) occurs, according to the following reaction:

$$Fe^{2+} + 1/4\ O_2 + H^{+} \rightarrow Fe^{3+} + 1/2\ H_2O$$

this reaction is catalysed by bacteria which increase the rate of the reaction by a factor of 10^6.
Ferric iron (Fe^{3+}) can persist as dissolved form at pH < 3 or it can precipitate as Fe-hydroxide producing more acidity:

$$Fe^{3+} + 3H_2O \rightarrow Fe(OH)_{3\ (s)} + 3H^{+}$$

1.2.2 AMD chemistry

As seen above, Fe^{3+} and hydroxides precipitated give the typical red/yellow colour to the rivers affected by this process, as typically manifested in acid mine drainage rivers. Further, oxidation of accessory sulphides (e.g. As or Se in pyrite; Co and Ni in pyrrhotite) takes place

and an elevate amount of metals and metalloids like Cd, Cu, Pb, Zn, etc., some of them extremely toxic, are released. In the literature several case studies reporting the typical AMD chemical composition of waters draining massive sulphide deposits can be found, all of them suggesting a strong geologic control on its chemistry dictated by the deposit geology and mineralogy (Ball & Nordstrom, 1989; Goldfarb et al., 1996; Plumlee et al., 1999; Nordstrom & Alpers, 1999). One more interesting feature of the AMD chemical composition is the high U and Th contents. Studies demonstrated the good correlations between U and elements such as Al, Mg, Mn, and Zn, Cd and SO_4, whom suggest that U could be derived 1) from the dissolution of aluminosilicates of the acidic volcanic lithologies present in the area and 2) other phases related with sphalerite-rich complex ores (Sánchez España et al., 2005). The concentration of metals in the acid solutions decreases the further you move away from the discharge point, since their co-precipitation with Fe-oxyhydroxides that always formed due to solution supersaturation in Fe, though this acidic leached reacts with the surrounding rocks and produces dissolution by hydrolysis of other gangue minerals. This explains the abundance of elements like Al, Ca, Mg, Na and K in acid mine waters. These reactions, normally very slow, are catalysed by microorganisms, identified by several microbiological studies (López-Archilla & Amils, 1999; López-Archilla et al., 2000; González-Toril et al., 2003) as chemiolithotrophic acidophilus bacteria that use minerals as their source of energy in addition to elements from atmosphere. In fact, sulphide oxidation would not be a problem without these bacteria, since the produced acidity could be neutralized by the environment. Field and laboratory investigations confirm that the oxidation rates measured in sectors with dense biofilms of acidic slime streamers are remarkably faster than those measured in sites where streamers are not present (Nordstrom, 1985; Williamson et al., 1992; Kirby & Elder Brady, 1998; Kirby et al., 1999; Sánchez España et al., 2007). In acidic conditions, they will reproduce very fast and the consequence will be an increasing in acidity in order to generate a negative feedback system, with a leached solution characterized by very low pH and very high metals and metalloids concentration. Anyway, the composition of AMD suffers seasonal variations: during the summer, a lower flow rate and a decrease in pH are observed, so they could be factors in determining the changing in elements concentrations. Efflorescent sulphates form in the course of the dry period (fig. 7), so they act like a temporal store of acidity, SO_4 and metals that will be dissolved in the more raining winter, determining increase in acidity, SO_4 and metals content (Sánchez España et al., 2005).

1.2.3 Anthropic effects

The anthropic activity strongly accelerated the natural oxidation of pyrite due to actions linked to the mining activity. Mineral resources exploitation involves different workings settings, each of them leads to an increase in the surface area exposed to the oxidation. Looking to an update of Nordstrom et al. (2015), the anthropic impact on the drainage water can be appreciated. For example, underground workings is a mining technique made up of various features, excavated usually into relatively intact rock in order to gain access to the orebody. Blasting and collapses of the wall-rock develop uneven unsheltered surfaces, together with widespread fracture networks, that carry out enlarged revealed surface areas in contact with water and oxygen. The increase in the reactive surfaces causes an increase in the sulphide oxidation and in the rate of the release of leached solution into mine waters. The difference between this technique and open-pit operations is that the latter are developed to extract near-surface orebodies and are made of a series of benches that allow

the stability of the pit walls. During mining activities, operations of dewatering are necessary, so they conduct to the uncovering of the pit-walls. Because they are irregular and fractured as well, the consequence is the same: more sulphide minerals and gangue minerals exposed to water and oxygen and more release of dissolved components into mine waters. The closure of an open-pit carries out a pit lake, wherein atmospheric water and groundwater will be collected, together with the previously stocked oxidation products that will impact water quality. Another problem affecting mine sites is the generation of big amount of waste, like the finely ground tailings and waste-rock piles. Meteoric water drains these accumulations but interacts with them differently: if the fine grained nature of the tailings limits the rate of the infiltration water, in the heterogeneous waste rock piles water can flow through interconnected pores. Therein, interactions between infiltrate water, gas and solute take place, thus they become an important controlling factor in the piles drainage. Since the sulphide oxidation, which is also influenced by external forcing that acts on temperature and gas characteristic of the pile (Amos et al., 2009), is an exothermic reaction, the generated heat can establish thermally driven convective gas-transport cells, by which oxygen can be transferred deep inside the waste pile with the consequence that a greater volume of rock undergoes oxidation (i.e., Lefebvre et al., 2001; Ritchie, 2003). Then, oxidation products within the pile interact with other minerals in the waste (Smith et al., 2013) and can either neutralize acidic pore water or form secondary minerals and gases along flow path. The same reactions happen in mill tailing, but downward and laterally through the tailings.

1.3 Uranium

Uranium is a strong lithophile element, which means that it is concentrated in the silicate minerals of the crust, and it has affinity with the oxygen occurring often in the oxide minerals too. Despite the fact that uranium is the highest number element found naturally on Earth, it's not so uncommon as it was thought and it can be found associated with other minerals. The average abundance of uranium in the Earth's crust is estimated varying between about 2 and 4 ppm, similar to the values of arsenic or molybdenum, but higher than elements like silver, mercury or cadmium, with higher values in acidic igneous rocks and minor amount in the basic ones. Average U content in granites amounts to 4,5 ppm, while in peridotites is up to two orders lower. The range for metamorphic rocks is 0,5-3,0 ppm. Shale are the sedimentary rocks containing more uranium than others, reaching a 3,5 ppm content (Gupta & Singh, 2003), while the value that can be found in the literature about its concentration in seawater is 3,3 ppb (e.g. Ku et al., 1977) and in common surface waters it presents temporal and spatial variability strongly dependent on the local redox conditions (Plater et al., 1991). The most common valence states of uranium are the tetravalent (IV) and the hexavalent (VI) states, even if it exists until the bivalent form, then the best-known minerals containing tetravalent uranium are uraninite and pitchblende, oxides having different content in UO_2, that form uranium ore deposits. Other important uranium minerals are phosphates like autunite and torbernite, simple and hydrated silicates like coffinite, uranothorite and uranophane, as well as vanadates and arsenates like carnotite and zeunerite respectively. Uranium is a radioactive element occurring with different isotopes, two of whom ,^{238}U and ^{235}U, have long half-life (4,471 x 10^9 y and 7,04 x 10^8 y respectively) and establish U-series radioactive disequilibria, a very widely used tool for dating a variety of processes. Isotopic studies of U in river waters were undertaken and it has been suggested

that the U isotopic ratios of river waters could depend on the lithological nature of the formations constituting the watersheds (Sarin et al., 1990; Plater et al., 1992); therefore, $^{234}U/^{238}U$ activity ratios could be very useful to investigate hydrological processes and as tracers of rock weathering (Riotte & Chabaux, 1999).

1.4 Thorium

The abundance of thorium in the Earth's crust is relatively high, it amounts to 6 ppm. Monazite and thorite, a phosphate and a silicate respectively, are the most common ores of thorium, though this element occurs in uranothorite, thorianite and it can be found as significant trace element in minerals like zircon, titanite, gadolinite and betafite. Thorium is composed of several isotopes, all of them radioactive with different half-lives: 24 days for ^{234}Th, 1,9 years for ^{228}Th, 7,5 x 104 years for ^{230}Th. The most stable isotope is ^{232}Th, which represents almost all naturally occurring uranium, with a half-life of 14,05 billion years after which it decays in radium by alpha-decay and can go on in its decay chain, until the stable ^{208}Pb. The fact that Th(IV) is the only stable oxidation state under all redox conditions in natural waters, and that these ions are extremely particle reactive, makes Th a very useful tracer of several oceanographic processes (Santschi et al., 2006). It is a strongly insoluble element in a wide variety of environmental conditions, indeed ^{232}Th concentration in seawater amounts to pM order, further other Th isotopes, e.g. ^{234}Th, ^{230}Th, ^{228}Th, are also present in seawater at very low concentration, due primarily to natural radioactive decay of uranium isotopes that are soluble in seawater (Bacon & Anderson, 1982; Moore, 1981). Its solubility is high in hydrochloric acid, at room temperature thorium reacts not so quickly with oxygen, in contrast to higher temperatures conditions where it reacts with oxygen faster, forming thorium dioxide (ThO_2) which has the highest melting point of any oxide (3300°C). Thorium in natural waters is typically complexed with inorganic ligands, such as sulphate, fluoride, phosphate and hydroxide, as well as with organic anions, all of which lead to the increase of the solubility of Th minerals and the mobility of this elements in surface (Langmuir & Herman, 1980). Thorium can be present in solution as Th^{4+} only in very acidic waters (Rai & Serne, 1978).

1.5 U-series

Weathering usually fractionates U-series nuclides determining the radioactive disequilibria in the decay chain. Chabaux et al. (2008) summarize the three main parameters which come into play on the behaviour of U-series nuclides in natural waters:

1) the chemical speciation of radionuclides in solution
2) their interactions with mineral and organic solids
3) their reactions with colloids.

1.5.1 Chemical speciation of radionuclides in solution

The chemical speciation of uranium in solution has been extensively studied and depends on redox conditions, pH and aqueous solution composition (fig. 8).
Uranium in natural water is usually complexed with inorganic ligands like phosphate, sulphate and fluoride, as well as carbonates and organic ligands, all forms that enhance its

solubility; so this ability of uranium to form complexes influences dissolution, sorption on minerals and colloids surface and the form in which U may precipitate. Among the two more frequent form, the hexavalent one has the highest mobility in the environment in the form of UO_2^{2+}, while U(IV) is stable in extremely reducing conditions for pH<5.

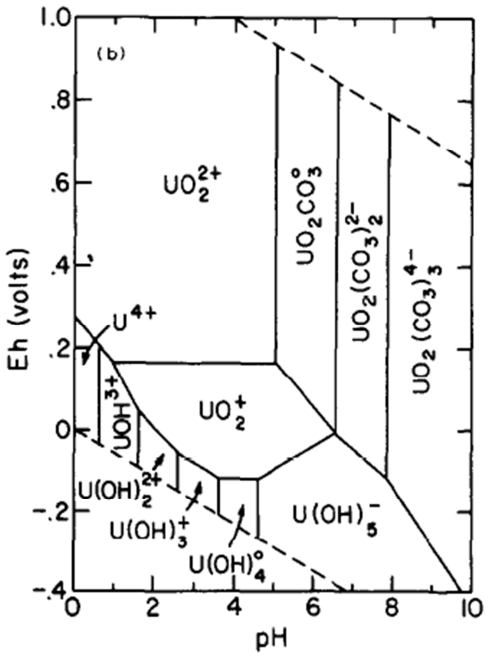

Fig. 8 - Eh-pH diagram for the system U-C-H-O at 25° and 1 atm with ΣU = 1 mm/L and $P_{CO2} = 10^{-2}$ atm (from Langmuir, 1978)

Thermodynamic data show that even U(V) as UO_2^+ has a considerable field of stability in reduced water, resulting in a vastly increase of the mobility of uranium for a wide range of natural conditions. During water-rock interactions and their transport in solution, each of other nuclides of the U-series behave differently than U: for instance, Th is known to be a very insoluble element for pH>3. This variability can led to significant geochemical fractionation among these nuclides, since, except in highly reducing or highly ligand-rich solutions, fluid phase will be generally enriched in U and the residual solid phases in Th (Chabeaux et al., 2008).

1.5.2 Interactions with solids

The mobility in solution of radionuclides is controlled by their reactivity with mineral surfaces and organic compounds. Carbonate anions form strong complexes with actinides in solution, consequently carbonate minerals are the best to make their surfaces available for actinide sorption. But in general the entity of this process depends on the nature of nuclide and of the interacting solids. Duff et al. (2002) show how the adsorption on mineral surfaces is controlled by mechanisms like surface complex formation, precipitation of U-bearing phases on mineral surfaces as well as structural incorporation of U in mineral host phase. Concentration of radionuclides takes an important role in their removing from solution by adsorption on minerals, because of its influences on the way how the radionuclides can be incorporated, together with the mineral growth rate and the bacterial activity.

1.5.3 Reactions with colloids

Colloids have an important influence in determining the mobility of U-series nuclides, especially of U and Th, because their presence, both as organic and inorganic form, modify the metal ion sorption onto mineral surfaces. More details are illustrated in the section 1.6.

1.5.4 Recoil

The fractionation of the U-series nuclides in solution can also take place due to a process induced by radioactive decay called "recoil". This process is defined as the motion acquired by an atomic nucleus during its emission of particles in radioactive decay, or during its collision with another particle, and determine a displacement called recoil range(δ) whose entity depends on the decay energy and the density of the solid phase. Typical values of the recoil range in mineral phases vary between 40 and 70 nm, but in air will amount up to 50 μm (three orders of magnitude larger). This displacement is influenced by grain size(r) and the difference in range has important consequences for the mobilization of daughter nuclide: when the grain size is large ($\delta/r<<1$) the effect will be negligible, while if the grain size is small the recoil will fractionate significantly the parent nuclide and its daughter. For example, let's take in account a δ = 19 nm for quartz, with the decay of ^{238}U that produces ^{234}Th. If it happens in sand with a grain size of 250 μm, the ejection factor (that is the fraction of daughter atoms ejected relative to that produced) will results in $7,6 \times 10^{-5}$. If it happens in silt or in clay, having grain radius r = 30 μm and r = 1 μm respectively, the ejection factor will be $6,3 \times 10^{-3}$ and $1,9 \times 10^{-2}$ respectively, with the latter that becomes significant. Other complications may come out based on the saturation of the porous medium and on the distribution of the parent nuclides. Thereby the amount of recoil nuclides that are effectively reject into solution will depend strongly on these factors, as well as on the surface from which daughter nuclides can be expelled. Another aspect to be mentioned was suggested by Kigoshi (1971) and was experimented by Fleischer (1982, 1983, 1988): even if these recoil nuclides are not emitted in the pore spaces, their displacement due to recoil makes them more easily to be removed from their sites in the mineral, so they are preferentially leached and the shorter-lived nuclides they are, the more is the leaching efficiency because if the leaching occurs in a time-scale longer than the time required for the annealing, it will be not efficient (Eyal & Olander, 1990).

1.6 U-series disequilibria in rivers

In rivers, weathering controls the fractionation and it is the main player governing the mass balance, since it provides the new bedrock material weathered as input in the system, as well as it provides the output represented by dissolved and weathered particulate material. Regardless the uranium in the bedrock, we need to assume that $^{234}U/^{238}U$ activity ratio is in secular equilibrium to affirm that in a steady-state context these two elements are equal; under secular equilibrium, the activity of the parent radionuclide undergoes insignificant changes during the half-life of its decay products. If it is not in secular equilibrium, it is necessary to take into account the contribution of daughter nuclides given by the uranium decay. ^{234}U-^{238}U disequilibrium is related to the recoil process, which causes release of ^{238}U

decay product from the solid into the solution and the perturbation of the crystal network where ^{234}U is located, promoting preferential leaching of ^{234}U respect to ^{238}U. This process is time-depended, this is the reason why U-series disequilibrium is an excellent tool and a chronometer of weathering processes. U-series disequilibrium in rivers gives information about weathering processes at the scale of watershed (Chabaux et al., 2008), so U-series isotope analyses have been used to investigate various issues, such as the contribution of rivers to the seawater U budget (Sarin et al., 1990), the behaviour of U-series isotopes during weathering and transport in rivers (Plater et al., 1992; Porcelli et al., 1997; Andersson et al. 1998) or the sources of dissolved flux, in particular groundwater contributions (Riotte & Chabaux, 1999; Riotte et al., 2003), as well as the nature of erosion, the estimation of its timescale and its related sediments production and transport rates (Dosseto et al., 2006). The control of the intensity of weathering on the magnitude of $^{234}U/^{238}U$ activity ratios of river waters was proved by Robinson et al. (2004), while Sarin et al. (1990) observed the control of the lithology on the $^{234}U/^{238}U$ fractionation during rock weathering. Uranium concentration in rainwater range from 0,5 ng/L to 50 ng/L, so U input from the atmosphere to rivers is generally considered insignificant. However, other potential sources of U nuclides in the environments are anthropic activities. Further processes called for the explanation of anomalous activity ratios are adsorption of dissolved radionuclides onto particles (Chabeaux et al., 2008), or mobilization of particulate Th through complexation with organic colloids (Plater et al., 1992; Dosseto et al., 2006). Organic and inorganic colloids are an important component of the < 0,2 μm fraction and play a critical role in Th and U mobility (Swarzenski et al., 1995) and thereby on radioactive disequilibria (Dosseto et al., 2006).

1.7 Fundamentals of colloids

The exact definition of colloids has been discussed for many years and it is still debated because of nomenclature divergences in view of different disciplines involved in their study. Environmental colloids are relative dilute dispersion of solid phase (sometimes liquid or gas) within a water or atmospheric gas (Lead & Wilkinson, 2007). Regard to a size-based definition, colloids can be conventionally defined as dispersed phase with sizes ranging between 1 nm and 1000 nm, boundaries that though are not so rigid (Everett, 1998). Thus they are macromolecules and nanoparticles with the upper size limit that shall be considered as the point at which particle-particle interactions are no longer dominated by Brownian motion, whereas the lower limit is more vague since it depend on the chemical species. Then, as can be seen in fig. 9, colloids in aquatic system comprehend macromolecular organic matter, microorganisms, viruses, aggregates and nanoparticles such as clay minerals and oxides of iron, aluminium and manganese coated with or sorbed on organic matter (Guo & Santschi, 1997; Buffle et al., 1998; Gustafsson et al., 2000; Taillefert et al., 2000).

The most common inorganic colloids found in oxic waters are aluminosilicates, silica and iron oxyhydroxyde particles (Pizarro et al., 1995; Buffle et al., 1998). In circum-neutral pH range, the majority of them have low zero point charge so they are negatively charged, excepting Fe-oxyhydroxydes with them neutral or positive charge (fig. 10). But this is not the case of Río Tinto area, where pH values are very low with the consequent elevated zeta potential values for amorphous oxy-hydroxides of iron and aluminium, that keep this colloidal system in a stable state. The other inorganic colloids change in positively charged with low zeta

potential value, then repulsion forces are not so strong, so they get the ability to come together catching other particles to growth in an aggregate. For natural nanoparticles, its nucleation is related to a geological fluid that becomes supersaturated with a mineral phase. For a given saturation degree (Ω), the critical size of nuclei (r*) is determined by

$$r* = \frac{2\gamma Vm}{RT \ln \Omega}$$

where γ is the surface energy, V_m is the volume of a formula unit of the solid, R is the gas constant, T is the absolute temperature (Steefel & Van Cappellen, 1990). Consequently, for a given mineral phase, the higher is the saturation degree, the smaller is the particle size.

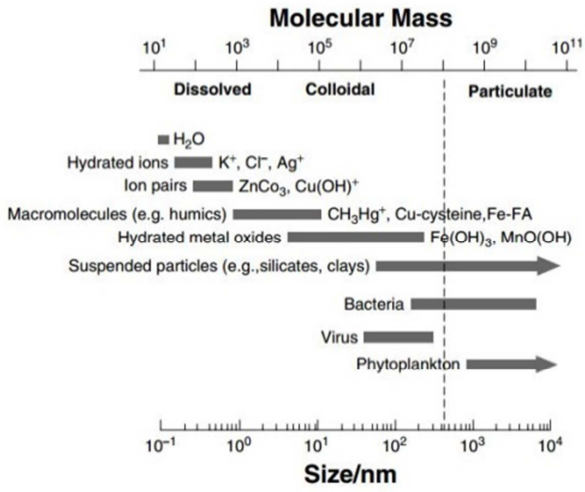

Fig. 9 - Size spectrum of chemical species in aquatic system. From Guo & Santschi (2007), reproduced from Wen et al. (1999).

nature of solid	pH_{zpc}	site density[c] (nm^{-2})	specific surface area ($m^2\ g^{-1}$)
am-SiO_2	3.0–3.5	4.5–12	40–260
am-FeOOH	7.9–8.1	0.1–0.9 mol/ mol of Fe	160–700
am-Al_2O_3	≈9.4	2–12[d]	
am-MnO_2	≈2.3	6–20[d]	260
allophanes		0.4–1.2	500–700
kaolinite	3.3–4.6[b]	0.6–3.6	10–20
chlorite		0.6–2.4	92–97
illite		0.9–2.7	90–130
smectites	≤2.5[b]	0.5–1.0	750–800
vermiculites		0.9–1.6	750–800

[a] Values are taken from refs *6* and *26*. Values are given for amorphous phases of metal oxides that should be more representative of natural colloids. [b] Values of pH at the isoelectric point and not at the zero point of charge (=pH_{zpc}). [c] Site density corresponds to the maximum negative charge density for pH ≫ pH_{zpc}. [d] Values for crystalline forms of Al_2O_3 or MnO_2.

Fig. 10 - Characteristics of inorganic colloids

1.7.1 Previous data.

Aquatic colloids are abundant in natural waters, so various works have been focused on their isolation and characterization (Guo & Santschi, 2007 and references therein). To know the partition of different elements between dissolved and colloidal phase, the most frequently used technique is the tangential (or cross-flow) ultrafiltration, by which it could be possible collect information about the concentration and the behaviour in different environments (e.g. Guo & Santschi, 1996; Gustafsson et al., 1996; Guo et al., 2000; Guo et al., 2001;). This technique will be exposed in section 2.2.1.
Previous studies demonstrated how U is associated with large particles and colloids (Porcelli et al., 1997; Andersson et al., 1998; Andersson et al., 2001). Andersson et al. (1998) found high concentration of Fe in river and brackish particles showing a strongly enrichment in U, especially related to the secondary Fe-oxyhydroxides, that, on the contrary of the Mn-oxyhydroxides, are largely responsible for the particle uptake of U. Even if U is highly soluble, they reported its different behaviour controlled by the differences in abundance and composition of colloidal fractions at different stage of changing in conditions of the system. However, the isotope composition is generally controlled by a significant isotopic exchange developed in a mineral-fluid system among their isotopes, as was suggested by Henderson & Burton (1999) and Dosseto et al. (2006). In their work, they show that isotope equilibrium will be achieved according to the transport rate (diffusion or surface reaction) relative to the advective transport time. Yamamoto et al. (2010) investigated radioactive disequilibrium in the uranium decay series in acid mine drainage system and in neutral surface waters from surrounding rivers in Japan, finding in the strongly acidic waters a high ^{238}U concentration, together with high concentrations of heavy metals, and an extremely high value of $^{234}U/^{238}U$ activity ratio (10-15). Here, ^{234}Th concentration was at similar level to that of ^{238}U, as expected as the result of its expulsion by recoil related to ^{238}U α-decay, and ^{230}Th is a daughter nuclide of ^{234}U, that instead was very low respect to its parent nuclide. Taking this into account, the authors concluded that deeper water is not in acidic condition, so the high $^{234}U/^{238}U$ activity ratio is probably due to the preferential leaching of ^{234}U, produced from the ^{234}Th adsorbed on the surface of mineral particles, in the underground water under neutral and reducing conditions. In addition, the elevated $^{234}U/^{238}U$ activity ratio could result if ^{234}U and ^{238}U are distributed differently within the solid matrix and if the ^{234}U is present in more labile sites, then preferential leaching of ^{234}U will be possible (Ketterer et al., 2011).

1.7.2 Colloidal uranium

Several investigations on colloidal U in natural waters were pursued, reporting considerable variability in the colloidal U percentage (table 1):

Table 1 - Reported colloidal uranium in natural waters

Location	Salinity	U (nmol/kg)	size fraction	colloidal U (%)	reference
river waters	-	0,076 ± 0,043	0,5 kDa - 10 kDa	53 ± 10	Tanazaki et al. (1992)
river waters	-	0,076 ± 0,043	10 kDa – 0,45 µm	12 ± 9	Tanazaki et al. (1992)
Amazon river	0,32	0,504	10 kDa – 0,45 µm	83	Swarzensky et al. (1995)
Amazon river	9,74	1,85	10 kDa – 0,45 µm	34	Swarzensky et al. (1995)
Amazon shelf	35,44	13,8	10 kDa – 0,45 µm	14	Swarzensky et al. (1995)

Table 1- continued

Location	Salinity	U (nmol/kg)	size fraction	colloidal U (%)	reference
Surface and ground waters	-	-	10 kDa – 5 µm	<3	Harnish et al. (1996)
Kalix river	-	0,46 -0,75	10 kDa – 0,45 µm	20 - 90	Porcelli et al. (1997)
Lake Pavin	-	0,17	> 1kDa	78	Alberic et al. (2000)
Lake Pavin	-	0,17	> 10 kDa	18	Alberic et al. (2000)
Jiulong river estuary	29,6	12,8	10 kDa – 0,22 µm	<2	Chen et al. (2000)
Kalix river estuary	~3	1,37	3 kDa – 0,2 µm	4 - 6	Andersson et al. (2001)
Kalix river estuary	~2	0,99	3 kDa – 0,2 µm	19 - 41	Andersson et al. (2001)
Kalix river estuary	0,8 - 1,4	0,66	3 kDa – 0,2 µm	33 - 88	Andersson et al. (2001)
Groundwater	<0,2	0,004 - 0,05	10 kDa – 0,45 µm	47 - 94	Tricca et al. (2001)
Coastal seawater	-	29,1 ± 13,0	0,5 kDa – 0,22 µm	~80	Singhal et al. (2004)
Galveston Bay	0	3,36	>1 kDa	15	Guo et al. (2007)
Galveston Bay	8,6	4,76	>1 kDa	12	Guo et al. (2007)
Galveston Bay	21,6	8,12	>1 kDa	~0	Guo et al. (2007)
Jiulong river estuary	1,1 - 31	1,19 - 11,8	10 kDa – 0,45 µm	<1	Lu et al. (2008)
Río Tinto	-	4650	> 5kDa	9	Casas-Ruiz & Barbero (2015)

1.7.3 Colloidal thorium

Most of previous studies were developed on ^{234}Th distribution in marine environment, because of its peculiarities that make it a widely used tracer for natural processes, like biological or scavenging processes. It has a half-life of 24,1 days and it's produced in constant rate from ^{238}U dissolved in seawater. Furthermore this radionuclide associates strongly with particles. Organic marine collides have high affinity for hydrolytic trace elements such as Th(IV). Therefore Th isotopes of different half-lives may be used as natural tracers for the DOM cycling in marine environments (Baskaran et al., 1992; Guo et al., 1997; Chen et al., 2000). Detailed size fractionation of other Th isotopes in both dissolved and particulate phase is scarce, but it could be reported available results about ^{230}Th, useful for the aim of this work (table 2):

Table 2 - reported ^{230}Th data in natural waters.

Regions	Phase	Salinity	^{230}Th concentration(mBq/L)	reference
Narragansett Bay	Total	26,4-32,2	0,07–0,27	Santschi et al. (1979)
	< 0,45 µm		0,01–0,05	
Northwest Pacific	> 0,45 µm	no data	0,001–0,004	Hirose & Sugimura (1993)
Baltic Sea brackish water	< 0,45 µm	2,5-24	0,01–0,34	Andersson et al. (1995)
Western Mediterranean Sea	Total	no data	0,003–0,014	Roy-Barman et al. (2002)
	< 0,2 µm		0,002–0,003	
	> 0,6 µm		0,0001	
Jiulong River estuary	Total	1,1-31,4	2,2–13,8	Zhang et al. (2005)
	< 0,4 µm		0,05–0,70	

2 - MATERIALS AND METHODS

2.1 Sampling and on-site analyses

To investigate the variations in water characteristics, the sampling was performed on 26 April 2016 at six different points: AC-1 from Río Tinto water before other water contribution; AC-2 drainage from waste pile of Peña de Hierro mine; AC-3 at the confluence of these two kind of water; AC-4 from the eastern natural river; AC-5 after this branch joins the just contaminated Río Tinto waters; AC-6 from a more upstream position along this branch, where life forms, e.g. frogs, and lusher vegetation appear again. Sampling points are shown in fig. 11 e fig. 12. From each point, fifteen litres of water were collected in a 20 L polyethylene tank without filtration. The pH, Eh, conductivity and temperature was immediately measured with a calibrated multiparametric probe (Hanna equipped with probes HI 9025C, HI9033 and HI9025), resulting in the values listed in table 3, section 3.1. It was not necessary acidify the samples, because of no carbonate content of the water. Colorimetric analyses on iron content, chloride content and alkalinity were carried out on the most contaminated AC-2 water, testing an aliquot of it with Hanna Instruments Test Kits. For iron content, the reduction of all the Fe^{3+} to Fe^{2+} takes place by means of the reaction with sodium sulphate, resulting in an orange-coloured solution due to the mixing of fenantrolina with the ferrous iron; the intensity of the colour of the solution identify Fe-content, then, as expected, it resulted in the maximum intensity, testifying the extremely high concentration of Fe due to the waste pile leaching. Chloride content was detected using mercury nitrate, which reacts with chlorine ions to form mercury chloride; when Hg ions-content is too high, Diphenylcarbazide is added to form a violet solution, since this changing in colour determines the end of Cl counting. The amount set out for the test wasn't enough to reach violet colour, maybe because Cl could exist not as free ion but as complex compound (e.g. $FeCl_2$, $FeCl_3$). Alkalinity test follows two steps: the Phenolphthalein Alkalinity measures total hydroxide ions content, after sample is neutralized at pH=8,3 using a dilute hydrochloric acid solution, with Phenolphthalein as indicator; the neutralization process convert hydroxide ions in water and carbonate ions in bicarbonate:

$$OH^- + HCl \rightarrow H_2O + Cl^-$$

$$CO_3^{2-} + HCl \rightarrow HCO_3^- + Cl^-$$

This measurement provides only half carbonate contribution because bicarbonate is converted in carbonic acid by adding hydrochloric acid. To obtain total conversion of bicarbonate, more hydrochloric acid is added since pH falls to 4,5 due to the following reaction:

$$HCO_3- + HCl \rightarrow H_2CO_3 + Cl^-$$

giving back Total Alkalinity. It was not possible operate with this kind of water due to its too high Fe-content. The samples were transported to the Earth Science laboratory of the International Excellence Campus CEI·MAR, Faculty of Marine and Environmental Science, University of Cádiz, where subsequent experiments of ultrafiltration and isotopic analyses were carry on, starting with the day after.

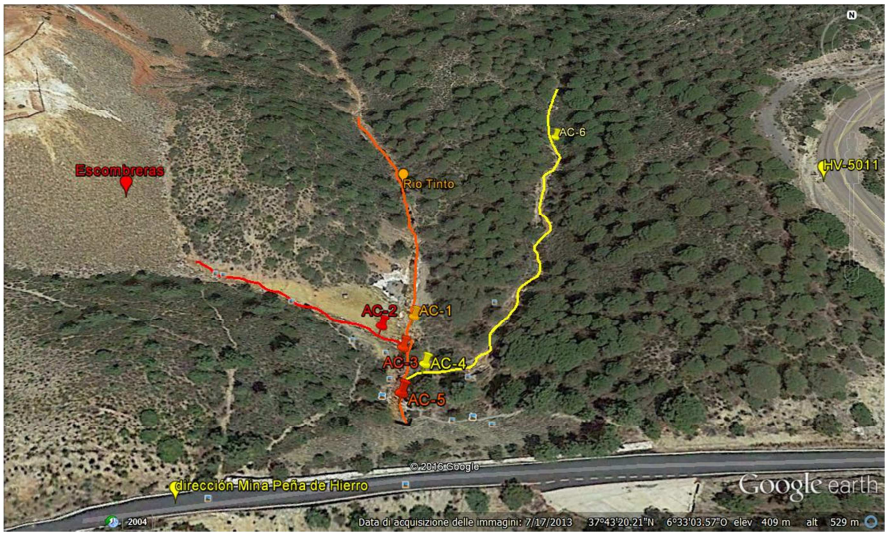

Fig. 11 - Panoramic of study area and sampling point on Google earth image.

Fig. 12 - Pictures taken on-site during the sampling, showing the different collected water; a: AC-1; b: on-site measurement of AC-2 parameters; c: AC-4; d: it can be seen the change in colour after the water sampled as AC-4 joins Río Tinto waters; e: AC-6 sampling.

2.2 Ultrafiltration experiments

Collected samples were filtered using standard technique through a pre-cleaned 0,45 µm and 0,2 µm cellulose nitrate membrane into a pre-washed 20 L container, in order to isolate the coarser retained colloidal fraction for a future work on its characterization (fig. 13). To analyse the characteristics of the investigated elements in natural Río Tinto water with distinct size particle-content and how they could part between dissolved and colloidal phase, an amount of 0,2 µm filtred water of AC-1 sample underwent to ultrafiltration experiments. The restricted budget and the short time available for the analyses let us work only on just one of collected samples. Other samples will be further analysed by the active research team of the University of Cádiz that is still carrying on the projects wherein I took part.

2.2.1 Ultrafiltration procedure

A cross-flow ultrafiltration (CFUF) was performed on the selected pre-filtered water sample AC-1. This technique isolates colloids from the water in a relatively short time and provides the feed flow travels tangentially across the surface of the filter, with the main advantages that the substances detained by filter are constantly washing away preventing the filter-cake formation. The ultrafiltration system used is a Masterflex L/S system with a Vivaflow 200 PES (polyethersulfone) membrane with an active membrane area of 200 cm^2 (fig. 13). The Masterflex L/S peristaltic pump system includes fixed and variable speeds, with a flow range from 0,0006 to 3400 mL/min, that providing high accuracy drives for precise flow control. Setting the recirculation rate to approximately 300 mL/min, permeate flow rate results in 5 mL/min. All ultrafiltration experiments were performed in an acid-cleaned polycarbonate (PC) container and polyethylene (PE) tubing. In order to separate extremely small particles and dissolved molecules in fluids, different ultrafiltration membranes with different molecular weight cut-offs (MWCOs) were employed. The Vivaflow 200 membrane system was firstly pre-cleaned following the cleaning procedure implemented on the employed membrane at the end of each ultrafiltration experiment: the system was rinsing with 200 ml of distilled water without recirculation, then 250 ml of cleaning solution, that is 0,5 mM NaOCl in 0,5 M NaOH, recirculate during 30-40 minutes with a rate of 50-100 mL/min, followed by the recirculation of distilled water for 5-10 minutes and ending with a rising with 500 ml of distilled water; for every step, the solution need to be discarded. Thanks to this cleaning procedure, the membrane could be reused more times. It's important to carry out all of the ultrafiltration experiment under rigorous cleaning and strict protocols, in order to assess correctly the mass balance and obtain accurate and reproducible results. Ultrafiltration was carried out using concentration factor (ratio of the initial volume respect to the retentate volume) from 1,07 to 1,73, with the aim to investigate if a permeation model, already proved for higher concentration factor, could be applied for lower values too.

Fig. 13 – AC-1 during the standard filtration (on the left) and during the ultrafiltration experiment (on the right) with a Masterflex L/S system with a Vivaflow 200 PES

2.2.2 Molecular weight cut-off and retention characteristics

The molecular weight cut-off (MWCO) defines the equivalent spherical size of macromolecules that can be retained by a specific membrane and it is usually expressed in kDa or atomic (molar) mass unit (amu). The nominal MWCO is estimated as the rejection rate of ~90% for specific globular molecules (fig. 14) and define the rated pore size for ultrafiltration membrane.

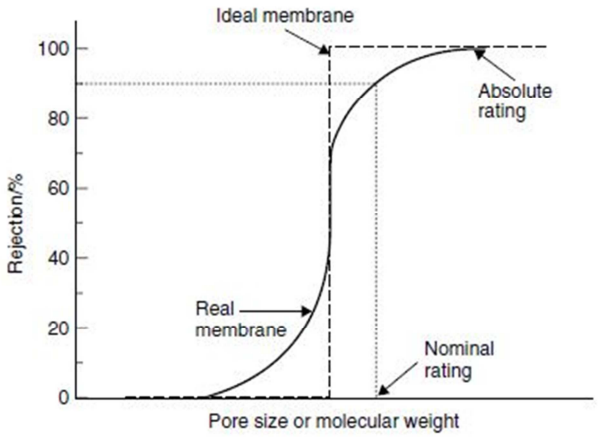

Fig. 14 - Membrane pore size distribution and ratings of ideal and real membranes. From Guo e Santschi (2007).

The experiments were carried out using 50, 10, 5 and 3 kDa PES membranes. The result of each ultrafiltration experiment is the partitioning of molecules of different size between a retentate solution and a permeate solution. Chemical species that have molecular size lesser than the MWCO pass through the membrane, while the concentration of the compounds rejected by the membrane will increase in the remaining solution over time. Thus the permeate solution will be free of particles between 0,2 µm and the MWCO of the membrane used, meanwhile components larger than the pore size are rejected at the membrane surface determining a constant enrichment in their concentration in the bulk solution. Studies on the retention characteristics of ultrafiltration membranes show that, as we can see in fig. 14, a certain percentage of compounds smaller than the rated cut-off can be retained by the membrane, and a varying fraction of higher molecular weight macromolecules can pass through the membrane, depending on the concentration factor and the bulk concentration (Guo & Santschi, 1996). These observations are likely related to electrostatic attraction and repulsion, the slow breakthrough of a small percentage of HMW molecules, steric effects and other physicochemical interactions between the species in solution and the membrane (Buesseler et al., 1996).

2.2.3 Ultrafiltration permeation model

The typical application of CFUF technique provides the concentration method, where the pre-filtered sample is concentrated from a single sample reservoir, so the concentration factor (CF) can be obtained from:

$$CF=(\text{Initial sample volume})/(\text{Retentate volume})$$

Recently, to interpret size fractionation data properly, the permeation and retention behaviour of chemical species have been investigated (e.g. Guo & Santschi, 1996; Dai et al., 1998; Guo et al., 2000; Guo et al., 2001). Since compounds with larger size than the MWCO of a selected ultrafiltration membrane are quantitatively retained and the those having lower molecular weight pass through without retention, a relation between the concentration of a specific element in the permeate (C_p) and the CF can be explained by the following permeation model:

$$\ln C_p = \ln(P_c \times C_f^0) + (1-P_c) \times \ln(CF)$$

where P_c is the permeation coefficient, defined as the ratio of C_p to C_f (concentration in the feed solution) at any given point of the ultrafiltration and C_f^0 is the initial concentration of permeable species in the upstream feed solution. The model works assuming negligible sorption and constant retention characteristics of the membrane, other than a constant partitioning across the membrane for high and low MW solutes. When the element behaves with a constant permeation, a linear relationship between $\ln C_p$ and lnCF can be found. The slope of the derived equation ($1-P_c$) gives the P_c value, which is related to the rejection coefficient R_c by $P_c = 1- R_c$, and could be equal to 1 when there is no retention for that element, resulting in the same concentration of that element in both permeate solution and feed solution at any time of the ultrafiltration. If instead $P_c < 1$, that means that retention occurs at each ultrafiltration cycle, with the consequence that the concentration of any chemical species in the permeate will increase with increasing CF (Guo & Santschi, 1996). The membrane theory (Johnson & Wangersky, 1985) describes how the interaction between particles and membrane works: any particle or molecule with a gyration radius R_p lesser than membrane pore size R_m, can pass through the membrane at a permeation rate proportional to $(R_m-R_p)^2/R_m^2$. R_p is always >0, so for the LMW the ratio $(R_m-R_p)^2/R_m^2$ will be always <100%, with the result that macromolecules P_c values will always result <1. This means that all of macromolecules will be retained to a certain extent (Guo & Santschi, 2007) according to the $R_c = 1- C_p/C_f$, that is defined as the fractional reduction in the feed concentration C_f through the membrane. As the P_c value can be calculated from the slope ($1-P_c$) derived from a linear relationship between $\ln C_p$ and lnCF, the estimation of initial feed concentration (C_f^0) is allowed due to a combination of the values of the intercept ($\ln(P_c \times C_f^0)$) and the slope. Using the estimated C_f^0, the initial colloidal fraction can be predicted as $1- C_f^0/C_T^0$ where C_T^0 is the measured total dissolved concentration.

2.3 Concentration of U and Th

The concentration of the investigated elements in the solution were find out by ICP-MS analysis, using an internal method that requires a calibration fitting the values of an internal standard with different known concentration versus distinct measured concentrations of the investigated elements. The report of the analysis Ref. 3471341328210616 is illustrated in the annex 1.

2.4 Radionuclide activities determination

2.4.1 Preparation of samples

The procedures for preparation of water samples for determination of radionuclide activities by ICP-MS were devised by Michael E. Ketterer, professor at Metropolitan State University of Denver, and can be applied on mine drainage samples, like the Río Tinto ones or similar, either filtered or un-filtered. The first procedural step is the lab-fabrication of the Eichrom Tech. TRU (*TRansUranic*) resin columns, whom purpose is the extraction chromatography. Columns were packed using 3 ml transfer pipets, cutting the top of their bulb and inserting into them small glass wool, in a way that the wool won't be neither too tightly (the flow through the column will be very slow) nor too loose (the resin will leak through). Then the columns were cleaned rinsing with several full volume of warm 2 M HNO_3, allowing it to drain each time. 30±2 mg of TRU resin, whose was mixed with distilled water and then added by pipetting this slurry, were transferred into each column, ensuring that the resin is completely wet and uniformly packed on the top of the glass wool. After ultrafiltration, 10 ml of each sample were pipetted in a pre-cleaned 125 ml polyethylene cups and then acidified with 1 ml of HNO_3 69% (16 moles/liter). 150 µg of ^{229}Th were accurately added to each sample. The spike is a solution containing a known concentration of a particular element, whose isotopic composition has been changed by the enrichment of one of its isotopes. The sample to be analysed contains an unknown concentration of the element whose isotopic composition is known, so, when a known amount of spike is mixed with a known weight of a sample, the isotopic composition of the solution can be used to calculate the amount of the element in the sample. This is the base of the isotope dilution analysis, that leads to the determination of the isotopic composition of an element in a sample. In this case a 2 x 10^{11} atoms ^{229}Th spike and a 5 x 10^{11} atoms ^{233}U spike were used. After adding the ^{229}Th-^{233}U spike, the samples were heated at 75°C for 2-3 hours to ensure complete equilibration of the mixture (fig. 15). The following step was the sample loading on the columns: the acidified sample solution was extremely carefully poured through the appropriate column, in order that the TRU resin could act and remove saline matrix and pre-concentrates Th and U. Subsequently the extraction of Th and U was performed using appropriate acid: when all the water sample passed through the TRU resin column, each column was rinsed three times with 1 ml of 2 M HNO_3, allowing the complete drainage of each rinse and discarding them. Then Th was eluted by passing six times 1 ml of 1 M HCl and collecting all of them. The Th fractions were completely evaporated by placing the un-capped tubes in a convection oven held at 85-90° C until evaporation was complete. After the completely removal of 1 M HCl, 300 µL of 2 M HNO_3 and 2,7 mL of distilled water were added to each tube; the tubes were capped and heated at 85-90°C for 1 hour to re-dissolved Th. Before U extraction, each column was rinsed again three times with 1 mL of 2 M HNO_3 that were discarded, in order to clean the columns. The U fraction was obtained by collecting in sequence 1 mL of distilled water, 1 mL of 0,05 M ammonium oxalate, and 1 mL of distilled water. In order to gain a controlled and more accurate analyse, replicate samples and standard materials were included, as well as blanks prepared with distilled water and acidified. The standard used was a preparation containing marine coral, which has a known $^{234}U/^{238}U$ equal to 1,148 ± 0,002.

2.5 ICP-MS analyses

Inductively Coupled Plasma Mass Spectrometry is the best technique to investigate the isotopic composition of elements. It has several advantages, including a very high sensitivity and a superior detection capability, as well as the high temperature of ICP-MS source that minimize matrix interferences. A mass spectrometer separate charged atoms and molecules on the basis of their mass using a magnetic field. it consists in three essential part, all of them maintained at high vacuum: the plasma source that converts the atoms into ions, the magnetic sector mass analyser and the ion collector. The source is an ICP torch, wherein argon gas flows in its concentric channels (fig. 16). A radio-frequency is generated to supply energy to the load coil, leading to an oscillating electric and magnetic field in the torch. This oscillating field will capture the ions generated by the reaction that takes place when the argon gas is sparked: electrons are separated from the argon atoms and the ions formed collide with other argon atoms, forming the plasma. The sample is introduced through a small orifice in the nebulizer that reduces the solution into an aerosol, which is brought into the torch. Here the aerosol is fragmented due to the high gas pressure and the atoms will ionized toward the end of plasma, travelling together with it. Plasma is an optimal source because of its temperature of 6000-10000°K , but it doesn't allow determinations of negative ions because its typically positively ions composition. To get a stable signal, it's important that the amount of the sample joining the plasma is constant, so an injector system (e.g. a cyclonic chamber, an ultrasonic injector) is needed. Other fundamental component is the peristatic pump, to ensure the sample will be pushed in the system with extreme stability. Since all the elements of the sample are converted into ions, they are accelerated and reach the mass spectrometer as a narrow ion beam, entering the magnetic field whose field lines result perpendicular to the direction of travel of the ions. Now the ions are deflected by the magnetic field into a curved path of radius r, according to following equation:

$$\frac{m}{z} = \frac{B^2 r^2}{2U}$$

where m/z is the ionic mass/charge ratio, B is the magnetic flux density, U the acceleration voltage (several kV) through which ions pass. So, the heavier ions are deflected less than the lightest ones. The resulting separated ion beams move onwards and the magnetic sector analyser focuses ions of the selected mass on the collector slit. Here, in the collector assembly, they can be detected and processed in a signal: it needs to be amplified to be measured by a digital or analogic voltmeter, that records the numbers of ions arriving at the collector during a given interval. The measurement is passed to the computer for isotope ratio calculations and other analytical outputs. To analyse several isotopes of an element, either the magnetic field or the accelerating voltage can be varied, in a way that the separated ion beams reach the collector successively. The mass spectrum of the element resulting from processing is a series of peaks and valley that represents a distinct mass/charge ratio that identifies each isotope in the mass spectrum, with the height of the peaks proportional to the isotopes relative abundance.

Th and U isotopes were measured with a Thermo Scientific XSERIES 2 quadrupole ICP-MS equipped with a CETAC 5000 ultrasonic nebulizer (fig. 16). The system was tuned and

calibrated by the technician, then was cleaned with milli-q water and a cleaning solution of HNO_3 2%. The acquisition parameters were for U 100 ms dwell time, 50 sweeps in 25 seconds and a timing washout between 10 and 220 seconds, for Th 20 ms dwell time, 200 sweeps in 17 seconds and a timing washout of 10-300 seconds. Three sequential integrations of each sample was acquired. In order to monitor the sensibility of the analyses, a tune 0,2 ppb for U and the cleaning solution of HNO_3 2% were random tested together with the samples. A tune for Th was not available, so the analysis were monitored just using the cleaning solution HNO_3 2%. The instrumentation exhibited a very stable mass discrimination behaviour.

2.5.1 Mass bias factor

This is the process of mass discrimination, that occurs because the ion transport efficiency is not the same for all masses. Light masses or heavy masses will be transported with greater efficiency, in reality. So, instead the measure of the effective value, for example a ratio value of 1,000, the instrumentation gives a slightly different results, such as 1,015 or 0,985. The mass bias factor can be calculated to correct the raw results. For U and Th it is not functional to measure an internal ratio, but it is practical measure $^{238}U/^{235}U$ in a sample of naturally occurring U source, like a marine coral. The measured ratio needs to be corrected for the blank values and then it is compared to the true $^{238}U/^{235}U$ ratio, that is constant in nature (137,88). The effect of MBF is cumulative and it is necessary to use exponent to adjust the formulae for the difference between the involved isotopes.

2.5.2 $^{234}U/^{238}U$ activity ratio

With the spectrometer, the activity of the isotopes is measured. But in terms of ratio between them, a problem will arise because of the $^{234}U/^{238}U$ atom ratio will be very small (0,00005472 at secular equilibrium). To get through this problem, it is possible to measure the much larger $^{234}U/^{235}U$ ratio, and then cross-multiply. This works because $^{235}U/^{238}U$ in nature is constant (1/137,88). To calculate $^{234}U/^{238}U$ AR, ^{234}U and ^{235}U measurements, to which the blank signal is subtracted, are needed. Their ratio is then corrected for the MBF and the result is divided for 0,0075448, that is $(^{234}U/^{238}U)nature*(^{238}U/^{235}U)nature$ = (0,00005472)*(137,88), obtaining the value of $^{234}U/^{238}U$ AR.

2.5.3 ^{230}Th activity with ^{229}Th tracer

The signals at masses of the isotopes ^{230}Th and ^{229}Th are needed. After blank-subtract to ^{230}Th signal, the ratio $^{230}Th/^{229}Th$ is calculated and then corrected using the MBF. The subsequent step is the calculation of the number of ^{230}Th atoms, multiplying the $^{230}Th/^{229}Th$ corrected for the amount of ^{229}Th atoms in the spike. Finally the number of ^{230}Th atoms is converted to mass of ^{230}Th and in activity of ^{230}Th using the specific activity of ^{230}Th (7,624 x 10^8 Bq/g). The concentration of ^{229}Th is determined using the known activity of the solution, the mass of the spike solution added and the specific activity of ^{229}Th (7,868 x 109 Bq/g). An example of ^{230}Th calculation is shown below:

- Amount of ^{229}Th spike added = (0,15 g solution)*(200 mBq ^{229}Th /g solution) = 0,03 Bq ^{229}Th
- Mass ^{229}Th = (0,03 Bq ^{229}Th) * 1 g ^{229}Th / 7,868 x 10^{9} Bq ^{229}Th = 3,813 x 10^{-12} g ^{229}Th
- Atoms ^{229}Th = 3,813 x 10^{-12} g ^{229}Th * (1 mole/229,03 ^{229}Th) * (6,022 x 10^{23} atoms /1 mole) = 1,0026 x 10^{10} atoms ^{229}Th

sample 44:

- (^{230}Th/^{229}Th)$_{measured}$ = (43,8 – 0,6125) / 1933,806 atoms ^{230}Th = 0,022332902
- (^{230}Th/^{229}Th)$_{corrected}$ = 0,022332902 * MBF = 0,022332902 * 1,0017 = 0,022370955 atoms ^{230}Th/ atoms ^{229}Th
- Atoms ^{230}Th = (0,022370955 atoms ^{230}Th/ atoms ^{229}Th) *(1,0026 x 10^{10} atoms ^{229}Th) = 224279616,7 atoms ^{230}Th
- Mass ^{230}Th = (224279616,7 atoms ^{230}Th)*(1 mole/6,022 x 10^{23} atoms)*(230,03 g / 1 mole) = 8,56709 x 10^{-14} g ^{230}Th
- Activity of ^{230}Th = (8,56709 x 10^{-14} g ^{230}Th) * (7,624 x 10^{8} Bq ^{230}Th / 1 g ^{230}Th) = 6,53155 x 10^{-05} Bq ^{230}Th

2.5.4 ^{234}U activity with ^{233}U tracer.

This calculation could not be performed, due to a likelihood contamination occurred during the critical preparation of the samples for the radionuclide determination that led to its determination failure.

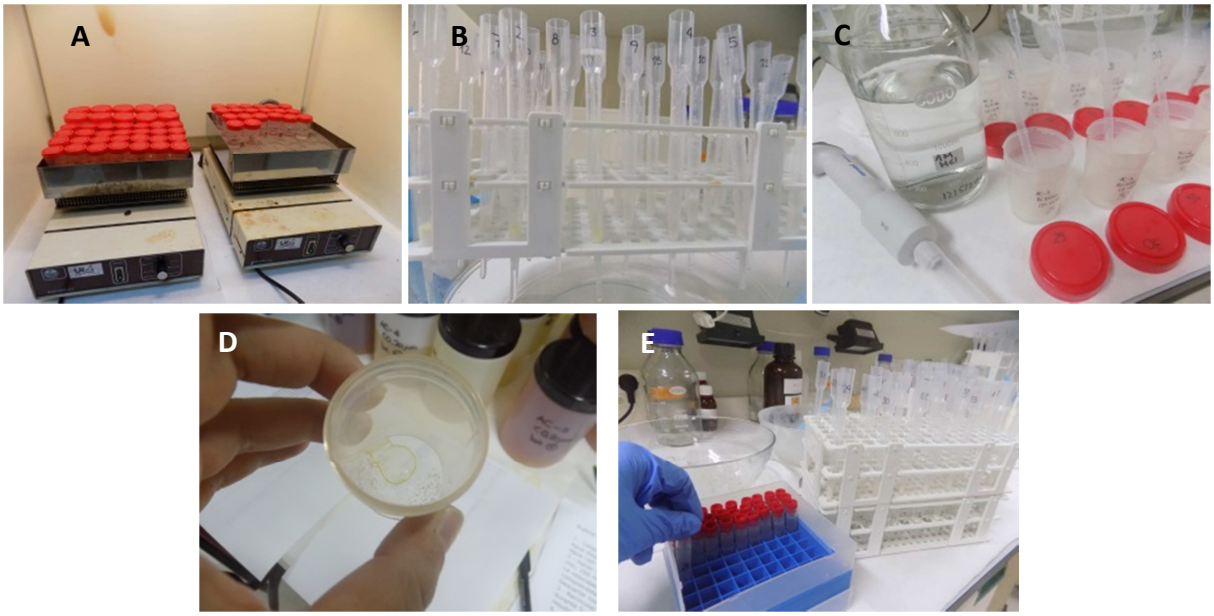

Fig. 15 – Preparing samples for radionuclide determination is a critical procedure and requires several steps. In A the samples are heating in order to equilibrate the mixture after adding the ^{229}Th-^{233}U spike. TRU columns shown in B were used to extract Th (image C) and U. Th fractions were completely evaporated, it can be seen the residue into the un-capped tube (D). Image E shows the collection of U fraction, ready for the ICP-MS analysis .

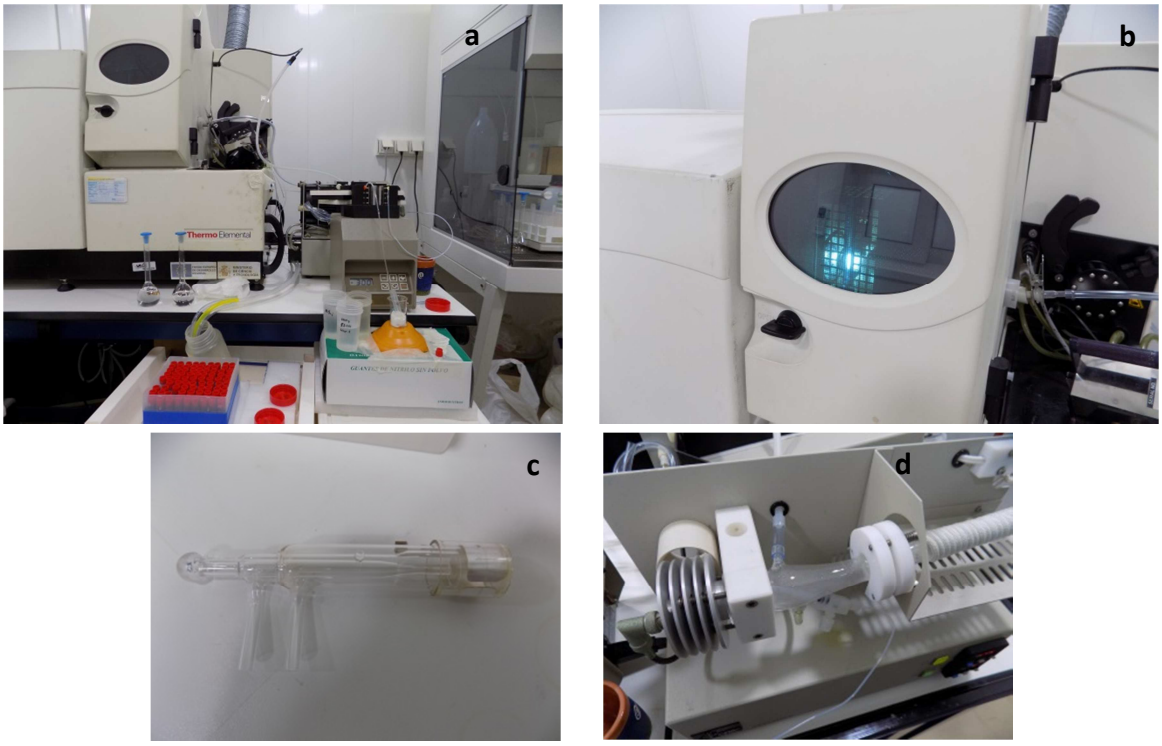

Fig. 16 - Thermo Scientific XSERIES 2 quadrupole ICP-MS (a) equipped with a CETAC 5000 ultrasonic nebulizer (d). The plasma source (b) is an ideal source, it can reach temperature of 6000-10000°K. c: the ICP torch, wherein argon gas flows in its concentric channels.

3 - RESULTS AND DISCUSSION

3.1 On-site measurements

The measured on-field parameters are listed below in table 3:

Table 3 - Collected samples and respective parameters measured on field using a calibrated multiparametric probe.

Sample	pH	Redox potential (mV)	Conductivity (µS/cm)	Temperature (°C)
AC-1	2,88	469	4480	26,0
AC-2	1,63	640	22900	27,6
AC-3	2,16	538	12370	22,4
AC-4	5,39	71,7	2140	19,5
AC-5	2,35	502	7270	24,5
AC-6	5,65	163,2	175,1	16,1

As it can be seen, the highest redox potential, equal to 640 mV, and the highest conductivity, that is 22900 µS/cm, correspond to sample AC-2 with pH equal to 1,63, the lowest one. This sample was collected from the waste pile of Peña de Hierro mine. Its water is the more acidic one just because it results from the weathering of a big rock-pile storage of prevailing pyritic waste, whose oxidation leads to the release of a high amount of acidity (H^+), sulphate (SO_4^{2-}), iron and other related trace metals. As expected when AC-4 and AC-6 was sampled, their pH is the highest one due to the water flows from the opposite side of the mountain, where a possible longer way of this little river or a more carbonatic composition of the drained rocks let the water be more alkaline. Within this condition, vegetation and life forms as frogs may develop therein. Where this alkaline water join the main river, precipitation of Fe-oxyhydroxides and secondary sulphates takes place due to the pH rises. The characterization and the quantification of the colloidal particles formed right here could be an interesting subject of further investigation.

3.2 Filtration and ultrafiltration experiments

Filtration was carried out to free the water from the coarser particles and get the first qualitative information about the water with highest particles-content. AC-1 had the more slowly progression in the 0,2 µm filtration process, so it could be considered the sample with the highest content in particles larger than 0,2 µm. Used filters with retained particles were stored for further investigation on particles characterization. At present, it could be presumed that this colloidal material > 0,2 µm consists in inorganic compounds, possibly mainly Fe-oxyhydroxydes, as could be expected in acid mine drainage rivers. Ultrafiltration experiments were carried out on AC-1 using membranes of different MWCO and obtaining a permeate and a retentate solution from each selected concentration factor of each experiments (table 4). Samples were prepared in order to obtain low concentration factors (CFs). They were calculated taking into account that 15 ml of volume of solution would remain into the ultrafiltration tubing system. During the first ultrafiltration experiment, where a 50 kDa membrane was employed, slightly different CFs result because of the shorter intake tubing system, which didn't allow the complete aspiration of the solution

from the reservoir and the consequent collection of sufficient amount of permeate volume needed to the radionuclide determination by ICP-MS analyses. Just for this experiment, in the course of which it was not possible to change the intake tubing system, larger initial volume of solution was placed into the reservoir and consequent larger volume of permeate solution was collected, resulting in CF a little different from the ones obtained from the followed ultrafiltration experiments. Ultrafiltration is a time-consuming procedure, so a longer intake tube replaced the shorter one before starting the 10 kDa ultrafiltration experiment, since the adequate permeate volume to prepare the samples for the radionuclide determination is 20 ml and the collection of this amount is shorter, especially when membranes with lower MWCO are involved. For the fact that 15 ml of solution were retained from the ultrafiltration tubing system, it was not possible to collect the retentate solution for the highest CF, because the difference between the initial volume and the permeate volume of the solution was exactly 15 ml.

Table 4 - List of samples obtained from ultrafiltration experiment developed on AC-1 sample. MWCO is the molecular weight cut-off of the membranes used in the experiments, expressed in kDa; V_i and V_p are the initial volume and the permeate volume of the solution, respectively, and the concentration factor CF is calculated as V_i/V_r, with the volume of retentate solution $V_r = V_i - V_p$. P and R mean permeate and retentate solution. Due to technical difficulties, the volumes involved in the 50 kDa ultrafiltration experiment are slightly distinct from the others and it was not possible to collect the retentate solution for the highest CF (explanation in the text).

MWCO (kDa)	V_i (ml)	V_p (ml)	CF	P sample number	R sample number
50	315	20	1,07	1	7
50	115	20	1,21	2	8
50	95	20	1,27	3	9
50	135	40	1,42	4	10
50	95	40	1,73	5	11
50	55	40	3,67	6	-
10	315	20	1,07	12	18
10	115	20	1,21	13	19
10	95	20	1,27	14	20
10	75	20	1,36	15	21
10	55	20	1,57	16	22
10	35	20	2,33	17	-
5	315	20	1,07	23	29
5	115	20	1,21	24	30
5	95	20	1,27	25	31
5	75	20	1,36	26	32
5	55	20	1,57	27	33
5	35	20	2,33	28	-
3	315	20	1,07	34	40
3	115	20	1,21	35	41
3	95	20	1,27	36	42
3	75	20	1,36	37	43
3	55	20	1,57	38	44
3	35	20	2,33	39	-

3.3 Permeation behaviour

As provided by the permeation model, if there is a constant permeation, log of concentration of U and Th in the permeate solution plotted versus log CF should result in a linear relationship described in the equation:

$$\ln C_p = \ln(P_c \times C_f^0) + (1-P_c) \times \ln(CF)$$

where P_c is the permeation coefficient of LMW of the investigated element. On the basis of this model, it can be possible calculate its value from the slope ($1-P_c$) and estimate the amount of the retention for that chemical species at each ultrafiltration cycle. Furthermore, C_f^0 can be derived from the combination of the intercept(*b*) and the P_c value, using $\exp(b)/P_c$, while the concentration of colloidal fraction of the element is given by calculating the difference between C_f^0 and the initial measured dissolved concentration (C_t^0) of the chemical specie under discussion (Guo & Santschi, 1996; Guo et al., 2000).

3.3.1 U discussion

The application of the permeation model using U concentration in the permeate samples produces a moderately good explanation of the behaviour of the LMW U interacting with the two membranes, with a coefficient of determination R^2= 0,658 and R^2= 0,694 for the 50 kDa membrane and for the 3 kDa membrane respectively (fig.15). We have few values in the data set, but R^2 could be increased repeating the experiments and operating with more and different CF, so that the regression will seem to fit better the data. The constant permeation coefficients are P_c = 0,813 for U ultrafiltered with 50 kDa membrane and P_c = 0,626 for U ultrafiltered through 3 kDa membrane. It means that, for each cycle of ultrafiltration, the 50 kDa membrane let 81 % of LMW U pass through it and 19 % will be retained as compounds with a molecular size higher than 50 kDa., while a 63% of U can pass through the 3 kDa membrane which retains 37 % of U. Previous results about U behaviour ultrafiltered at 5 kDa gave a value of P_c = 0,847 (Casas-Ruiz & Barbero, 2015), so the permeation behaviour of U resulting from our experiment can be considered the same even at low concentration factors. Although previous works mention artifactual retention of the dissolved species at low concentration factors, due to the retention of LMW molecules in the retentate, that leads to overestimate the colloidal concentration (Guo et al., 2000; Guo et al., 2007), here the value of initial concentration derived from the model is higher than the one measured in the 0,2 μm sample, resulting in a negative value of estimated colloidal fraction. This could suggest a probable contamination or that large artifacts occurred among the membrane and the chemical species. As is illustrated in table 1 section 1.7.2, colloidal U fractions in natural waters result considerably high. However, there is a lack of studies on colloidal U fraction in acidic environment as the Río Tinto one, but previous results show that the permeation model estimates around 9 % of U associated to 5 kDa colloidal fraction (Casas-Ruiz & Barbero, 2015).

3.3.2 Th discussion

Thorium reveals an opposite trend for the 50 kDa membrane ultrafiltration, showing a decrease in concentration of Th in the permeate solution with increasing the concentration factor (fig. 17). The permeation coefficient resulting from the model amounts to 1,944, but this is not a realistic value because of its effective meaning: P_c is defined as the ratio of C_p (concentration in the permeate) and C_f (feed concentration) and is related to the rejection coefficient R_c by $P_c = 1 - R_c$. P_c is equal to 1 when the concentration in the permeate is the same of the one in the feed solution, meaning that there is no retention for that species (Guo & Santschi, 1996). A value > 1 for the P_c implies a negative value for R_c, that is, the membrane is not giving back truthful information and it is not retaining in quantitative form. With regard to the 3 kDa ultrafiltration experiment, behaviour of thorium can be described by a permeation model with a P_c = 0,369, that means the membrane retain 63 % of Th. Casas-Ruiz & Barbero (2015) reported a value of P_c = 0,812 for Th ultrafiltered at 5 kDa membrane. This time this disagreement could be explained with the artefactual retention of Th < 3 kDa by the membrane. Again, the permeation model returns a negative estimation of the colloidal fraction due to the value of initial concentration calculated from the model which is higher than the one measured in the 0,2 µm sample.
Casas-Ruiz & Barbero (2015) applied the traditional method on their sample and got a colloidal U fraction of 2,2 % and colloidal Th fraction of 6,3 % which indicates that the 5 kDa membrane does not retain dissolved U and Th as previously evidenced (Guo et al., 2007). The colloidal abundance is calculated from:

$$[\text{colloidal}] = \frac{[\text{retentate}] - [\text{permeate}]}{CF}$$

obtaining again negative values for both Th and U in the samples underwent to 50 kDa ultrafiltration, but values up to 0,6 % for U and up to 2,1 % for Th in the 3 kDa colloidal fraction. This results could be considered consistent with the previous ones.

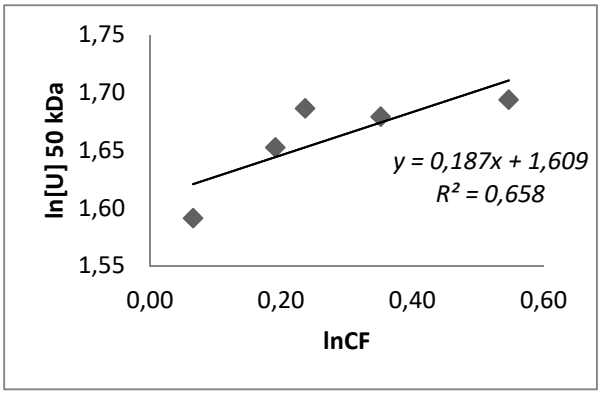

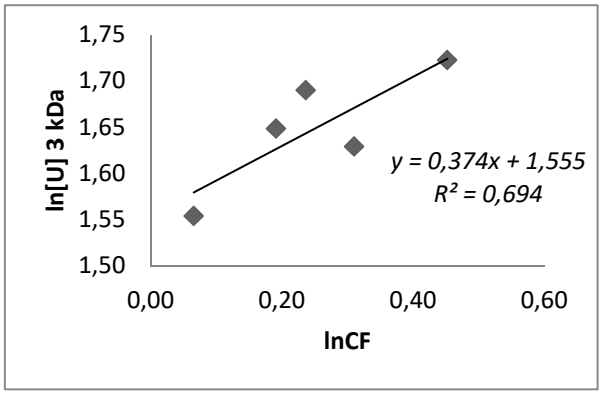

P_c U 50 kDa	0,813
C_f^0	6,14
C_t^0	5,30
estimated colloidal fraction (%)	-15,90

P_c U 3 kDa	0,626
C_f^0	7,57
C_t^0	5,30
estimated colloidal fraction (%)	-42,74

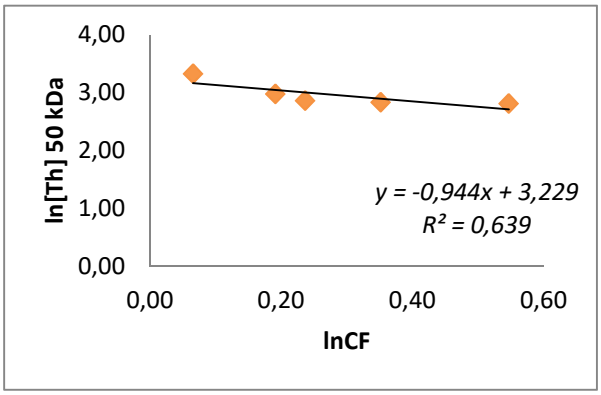

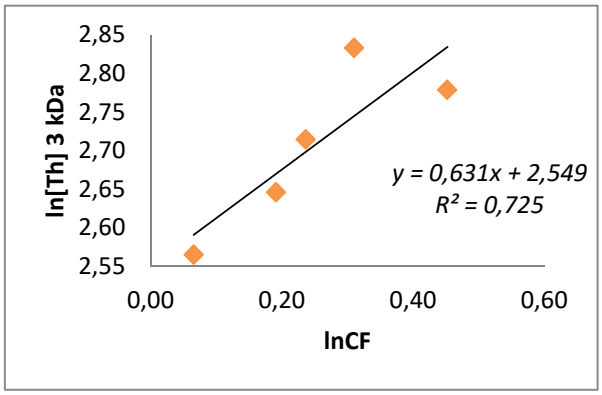

P_c Th 50 kDa	1,944
C_f^0 µg/L	13,0
C_t^0 µg/L	20,2
estimated colloidal fraction (%)	35,55

P_c Th 3 kDa	0,369
C_f^0 µg/L	34,7
C_t^0 µg/L	20,2
estimated colloidal fraction (%)	-72,02

Fig. 17 - Permeation models for U and Th with 50 kDa and 3kDa membrane. Explanation in the text. Results about Th 50 kDa could be not considered truthful. P_c is the permeation coefficient, C_f^0 is the initial feed concentration, both derived from the model. C_T^0 is the concentration measured in the pre-ultrafiltration sample.

Table 7 - Samples used for the permeation model with their concentration, calculated colloidal fraction and recovery. Type: p and r mean permeate and retentate solution respectively. CF is the concentration factor obtained from V_0/V_r where V_0 is the initial volume and V_r is the difference between initial volume and permeate volume (V_p). $Diss_f$ is the dissolved fraction, $Coll_f$ is the colloidal fraction, both at each point of ultrafiltration founded calculating the recovery (explanation in the text). C_0 is the measured initial concentration.

U - 50kDa membrane

Sample	Type	[U] µg/L	CF	V_p (ml)	$Diss_f$(%)		Sample	Type	[U] µg/L	V_r (ml)	$Coll_f$(%)	C_0 (µg/L)	V_0(ml)		recovery U (%)
1	p	4,91±0,11	1,07	20	5,88		7	r	4,81±0,20	295	85,00	5,30±0,33	315		90,88
2	p	5,22±0,30	1,21	20	17,13		8	r	5,41±0,30	95	84,32	5,30±0,33	115		101,45
3	p	5,40±0,10	1,27	20	21,45		9	r	5,30±0,10	75	78,95	5,30±0,33	95		100,40
4	p	5,36±0,12	1,42	40	29,97		10	r	5,31±0,12	95	70,50	5,30±0,33	135		100,47
5	p	5,44±0,40	1,73	40	43,22		11	r	5,30±0,30	55	57,89	5,30±0,33	95		101,11

U - 3kDa membrane

Sample	Type	[U] µg/L	CF	V_p (ml)	$Diss_f$(%)		Sample	Type	[U] µg/L	V_r (ml)	$Coll_f$(%)	C_0 (µg/L)	V_0(ml)		recovery U (%)
34	p	4,73±0,30	1,07	20	5,67		40	r	5,15±0,30	295	91,00	5,30±0,33	315		96,67
35	p	5,20±0,10	1,21	20	17,06		41	r	5,41±0,20	95	84,33	5,30±0,33	115		101,39
36	p	5,42±0,30	1,27	20	21,53		42	r	5,13±0,20	75	76,42	5,30±0,33	95		97,95
37	p	5,10±0,03	1,36	20	25,66		43	r	5,30±0,10	55	73,33	5,30±0,33	75		98,99
38	p	5,60±0,11	1,57	20	38,42		44	r	6,54±0,11	35	78,53	5,30±0,33	55		116,95

Th - 50kDa membrane

Sample	Type	[Th] µg/L	CF	V_p (ml)	$Diss_f$(%)		Sample	Type	[Th] µg/L	V_r (ml)	$Coll_f$(%)	C_0 (µg/L)	V_0(ml)		recovery Th (%)
1	p	28,0±0,2	1,07	20	8,81		7	r	14,2±0,6	295	65,83	20,2±1,2	315		74,82
2	p	19,7±1,3	1,21	20	16,96		8	r	16,0±1,2	95	65,43	20,2±1,2	115		82,39
3	p	17,5±0,5	1,27	20	18,24		9	r	15,0±0,5	75	58,62	20,2±1,2	95		76,86
4	p	17,1±0,7	1,42	40	25,08		10	r	15,2±0,4	95	52,95	20,2±1,2	135		78,03
5	p	16,7±1,2	1,73	40	34,81		11	r	15,7±1,4	55	45,00	20,2±1,2	95		79,81

Th - 3kDa membrane

Sample	Type	[Th] µg/L	CF	V_p (ml)	$Diss_f$(%)		Sample	Type	[Th] µg/L	V_r (ml)	$Coll_f$(%)	C_0 (µg/L)	V_0(ml)		recovery Th (%)
34	p	13,0±0,6	1,07	20	4,09		40	r	13,6±1,3	295	63,05	20,2±1,2	315		67,14
35	p	14,1±0,6	1,21	20	12,14		41	r	14,6±0,6	95	59,71	20,2±1,2	115		71,85
36	p	15,1±0,6	1,27	20	15,74		42	r	14,0±0,5	75	54,72	20,2±1,2	95		70,46
37	p	17,0±0,5	1,36	20	22,44		43	r	15,0±0,2	55	54,46	20,2±1,2	75		76,90
38	p	16,1±0,3	1,57	20	28,98		44	r	19,4±0,5	35	61,12	20,2±1,2	55		90,10

3.3.3 U and Th concentration

In general, both the investigated elements show no significant differences among the distinct samples obtained from the different experiments and the pre-ultrafiltration sample (filtered to 0,2 µm). The range of U concentration is 4,73 – 6,54 µg/L, extended among the solutions resulting from the 3 kD ultrafiltration experiments. The lowest value belongs to the permeate sample of 3 kDa membrane ultrafiltered with a CF=1,07, while the highest one is associated to the retentate solution after 3 kDa ultrafiltration experiment with CF=1,57. Th concentration covers a little more extended range, that is 13,0 – 28,0 µg/L. Another time the lowest value is given by the permeate sample from 3 kDa membrane with the lowest CF, but the highest one is detected in the solution permeated through the 50 kDa membrane. Uranium in seawater amounts to 3,3 ppb (e.g. Ku et al., 1977), while in common surface waters it presents temporal and spatial variability strongly dependent on the local redox conditions (Plater et al., 1992), but still predominantly in the order of ng/L (see table 1,

section 1.7.2).The extreme elevated value of U concentration results from acidic conditions of the study area, as a consequence of low pH (<3) surface water conditions that lead to the mobilization of high levels of natural radionuclides. Furthermore, the area is characterized by acidic volcanoclastic rocks (into which U is naturally concentrated), that under AMD suffer the continue dissolution of minerals and the subsequent release of the associated elements into the waters. Data on dissolved Th concentration in natural waters are lacking, but Langmuir & Herman (1980) reported previous measured values of dissolved thorium in surface waters, showing values of 0,001-1 ppb in fresh surface waters, which cover a pH range between 5 and 8, and a value of 0,00064 ppb in surface seawater, that have pH around 8. Th uses to be present not in dissolved form in natural water, but it should be noted that the samples show a Th concentration one order of magnitude higher than U, that on the contrary is commonly founded as dissolved form. This can be explained by the acidic environment of Río Tinto area that leads to the dissolution of solid phases, colloids included, and provides the conditions in which Th can exist in solution as Th^{4+} and in high concentrations. It can be supposed that such high concentrations of dissolved form of both the elements could emerge from the elevated zeta potential values of the particles > 0,2 µm, isolated by the classical filtration and expected to be amorphous oxy-hydroxides of iron and aluminium, with the consequence that the high charged ions will be rejected from the particles surfaces and could concentrate in the solution. Our results are consistent with previous data from Río Tinto data, that exhibits very high concentrations at pH below 2,5, as expected from the theoretical behaviour of these elements under low pH and oxidizing conditions, reaching values up to 200 µg/ L for U and up to 600 µg/L for Th (fig.18).

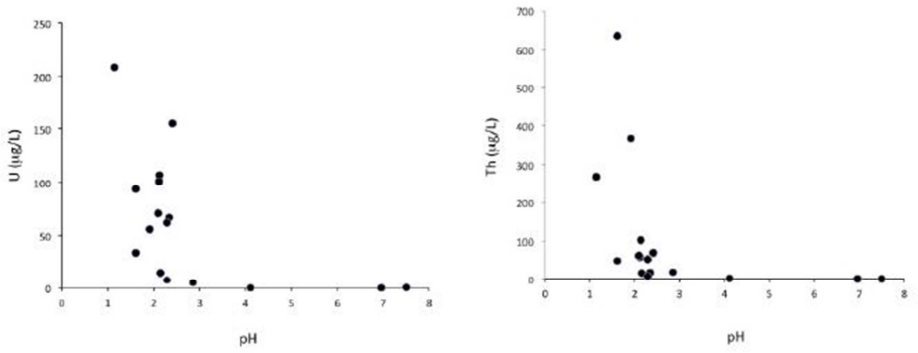

Fig. 18 - U and Th concentrations versus pH in Rio Tinto waters. From Casas-Ruiz & Barbero (2015).

3.3.4 Mass balance

A classic method to calculate colloidal fraction considers the measurements of all the fraction involved in each ultrafiltration experiment, and allows an accurate mass balance that is critical, even not very sensitive, to assess the recovery of the operations (Guo & Santschi, 1996). The mass balance is obtained using the following equation:

$$\text{Recovery (\%)} = \frac{(C_p \times V_p)+(C_r \times V_r)}{C_0 \times V_0} \times 100$$

where C_p, C_r and C_0 are the measured concentration in the permeate, retentate and initial solution respectively, and V_p, V_r and V_0 are the respective volumes involved in the ultrafiltration experiments. A recovery > 100 % indicates a contamination, while a recovery < 100 % means a loss of the element during the ultrafiltration process. Applying this method on the samples, dissolved and colloidal fractions for the ultrafiltration at each CF can be appreciated and are listed in table 7. It can be observed that U recovery results reasonably good. In contrast, the recovery of Th (mainly < 80%) reveals large losses of this element during ultrafiltration experiments. It might be due to the nature of Th, whose dissolved form as Th^{4+} is highly charged and physicochemical interactions with the ultrafiltration membranes, which, in general, are negatively charged, can be developed, with the consequent retention of Th. It seems that low CF for Th are inadequate to extract it and reach a permeate that will be representative of its actual permeation behaviour. This observation could explain the failure of the application of the permeation model for Th to the samples deriving from 50 kDa ultrafiltration experiments, which cannot describe quantitatively the ultrafiltration behaviour of Th in this so acidic waters.

3.4 ICP-MS results

3.4.1 $^{234}U/^{238}U$ activity ratio

The budget let us perform the ICP-MS analysis just on half of the ultrafiltered samples, so the samples deriving from the larger MWCO ultrafiltration experiment (50 kDa) and the ones from the lowest MWCO ultrafiltration experiment (3 kDa) were selected to carry out the analysis on them. Within these 22 samples, the 0,2 µm filtered sample (representing the initial solution whose concentration is investigated), 8 blanks, 6 coral solutions, 3 coral solutions diluted x 100, other than 2 replicates of the samples and a tune 0,2 ppb solution for U were submitted to the ICP-MS analysis, in order to carry out a monitored and more accurate analyse. Three measurements for each samples was acquired, with their mean, standard deviation and the RSD calculated by the computer. Then, in order to calculate the $^{234}U/^{238}U$ activity ratio, necessary corrections for each measurement were individually performed, and the mean, the standard deviation and the RSD of the final result can be calculated. The complete list of the analysed samples and the entire results of the analysis, with their corresponding corrections, are exposed in the annex 2 and 3 respectively.
The accuracy and precision of the instruments were verified by the analysis on the marine coral samples, which have a known value of $^{234}U/^{238}U$ activity ratio (AR) equal to 1,148 ± 0,002. The resulting calculated $^{234}U/^{238}U$ AR on the coral sample are about 1,15% less than the known value. This little difference is consistent with the typical bias of spectroscopy methods of investigation, that usually amounts as high as 2%. Calculated $^{234}U/^{238}U$ activity ratios are in a range with a minimum amounting at 1,761 and a maximum value of 2,060. The minimum value is given by a replicate of a sample whose measurement shows a $^{234}U/^{238}U$ activity ratio of 1,957. This deviation probably arises from an inaccuracy during the samples preparation process, because of the difficulties during their handling and their processing. Excluding this result, no significant variations can be seen in the activity ratio of

$^{234}U/^{238}U$ irrespectively of this is calculated neither for different pore size of the membrane nor in the retentate or in the permeate. Results are listed in table 5. Previous works in Río Tinto waters registered a $^{234}U/^{238}U$ AR ranging between 1,5 to 3 (Ketterer et al., 2011), explained as a consequence of weathering processes as well as the ones related to acid drainage, but it should be close to unity when the complete dissolution of the solid matrix occurs. Such a conclusion was found out by Barbero et al. (2014), with their leaching experiments on solid samples of the area that reveals their $^{234}U/^{238}U$ AR close to one, consistent to the secular equilibrium reached between ^{234}U and ^{238}U isotopes in the bulk material. Another acid mine drainage case that could be compared with Río Tinto one is the Ogoya Mine one in Japan, where Tedori and Kakehashi Rivers waters show a $^{234}U/^{238}U$ AR around 3,1 (Yamamoto et al., 2010). Here the authors attribute the exceptional high $^{234}U/^{238}U$ AR values (up to 16,8 ± 1,8), founded in samples closest to the mine zone, to the deeper underground water having high ^{234}U concentration due to preferential leaching of ^{234}U under the neutral and reducing conditions. Samples investigated in this work report a $^{234}U/^{238}U$ AR average of 2,002 ± 0,007 that is consistent with further results concerning dissolved matter from Río Tinto water and amounting to 2,01 ± 0,08 exposed by Hierro et al. (2013). The disequilibrium is imputable to the excess of ^{234}U related both to the recoil effect, enhanced by the weathering that leads to a reduction in the grain size, and the acidic water preferentially lixiviates ^{234}U respect to ^{238}U from minerals in the mining areas.

Table 5 - Calculated $^{234}U/^{238}U$ activity ratios. MWCO is the molecular weight cut-off of the membranes used, p and r mean permeate and retentate respectively, CF is the concentration factor.

sample	MWCO (kDa)	type	CF	$^{234}U/^{238}U$ AR	sample	MWCO (kDa)	type	CF	$^{234}U/^{238}U$ AR
M0	-	-	-	1,995 ± 0,038	34	3	p	1,07	2,021 ± 0,015
M0 bis	-	-	-	2,013 ± 0,052	35	3	p	1,21	2,050 ± 0,046
1	50	p	1,07	1,957 ± 0,053	36	3	p	1,27	2,060 ± 0,018
1 bis	50	p	1,07	1,761 ± 0,095	37	3	p	1,36	2,026 ± 0,005
2	50	p	1,21	2,010 ± 0,024	38	3	p	1,57	1,982 ± 0,063
3	50	p	1,27	2,030 ± 0,035	39	3	p	2,33	2,019 ± 0,016
4	50	p	1,42	2,016 ± 0,037	40	3	r	1,07	2,034 ± 0,016
5	50	p	1,73	2,034 ± 0,028	41	3	r	1,21	2,007 ± 0,015
6	50	p	3,67	2,027 ± 0,045	42	3	r	1,27	1,981 ± 0,030
7	50	r	1,07	2,039 ± 0,017	43	3	r	1,36	1,996 ± 0,003
8	50	r	1,21	2,051 ± 0,007	44	3	r	1,57	1,800 ± 0,053
9	50	r	1,27	2,037 ± 0,034					
10	50	r	1,42	2,042 ± 0,031					
11	50	r	1,73	2,054 ± 0,031					

3.4.2 ^{234}U activity

It was not possible carry out this information due to a likelihood contamination occurred during the handling and the processing of the samples for the radionuclide determination that led to the failure in its calculation.

3.4.3 ^{230}Th activity

The activity of ^{230}Th varies little in a range between 0,056 mBq/L and 0,169 mBq/L, with an average of 0,144 mBq/L . The lowest value belongs to the 50 kDa permeate sample resulting from the lowest CF, while the highest value is given by the sample 8, retentate obtained from the 50 kDa ultrafiltration experiment with a CF of 1,27. The typical ^{230}Th concentration in natural waters is one or more orders of magnitude lower than our results (see table 2, section 1.6.3).With the exception of the sample 44, it can be detected that the general trend is slightly lower ^{230}Th activity values in permeate samples and a bit higher values in the retentate ones. One might suppose this observation could be related to the typical behaviour of Th in the most of natural conditions i.e. in natural waters Th is mostly an insoluble elements and has affinity with solid phases, resulting in higher concentration in the retained fraction. But this is not the case of Río Tinto area, where pH is lower than 3 and even the most insoluble phases could not exist in solid form. Thorium can be present in solution as Th^{4+} only in very acidic waters (Rai & Serne, 1978). Thus, the acidic environment promotes the desorption of thorium from particles and colloids, while mineral phases undergo dissolution. Both these occurrences could be considered as further contributions of ^{230}Th into the solution, whose existence in solution is mainly related to the decay of ^{234}U (Osmond & Ivanovich, 1992), isotope that, as we discussed, determines its enrichment in the water due to the α-recoil and its subsequent easier leaching. In fact, the ^{230}Th/^{234}U ratio is almost exactly the same (0,127-0,146) testifying their direct correlation.

Table 6 - Calculated ^{230}Th activity. MWCO is the molecular weight cut-off of the membranes used, p and r mean permeate and retentate respectively, CF is the concentration factor. The determination of ^{230}Th/^{234}U ratio was useful to understand if ^{230}Th into the solution exists because mainly related to the decay of ^{234}U (explanation in the text).

sample	MWCO (kDa)	type	CF	^{230}Th activity (mBq/L)	^{230}Th/^{234}U	sample	MWCO (kDa)	type	CF	^{230}Th activity (mBq/L)	^{230}Th/^{234}U
M0	-	-	-	0,161 ± 0,003	0,145 ± 0,002	34	3	p	1,07	0,150 ± 0,006	0,135 ± 0,005
M0 bis	-	-	-	0,154 ± 0,003	0,142 ± 0,004	35	3	p	1,21	0,144 ± 0,004	0,136 ± 0,003
1	50	p	1,07	0,062 ± 0,003	0,145 ± 0,008	36	3	p	1,27	0,147 ± 0,009	0,135 ± 0,009
1 bis	50	p	1,07	0,056 ± 0,001	0,133 ± 0,010	37	3	p	1,36	0,156 ± 0,005	0,133 ± 0,003
2	50	p	1,21	0,153 ± 0,004	0,140 ± 0,002	38	3	p	1,57	0,149 ± 0,004	0,133 ± 0,003
3	50	p	1,27	0,142 ± 0,005	0,136 ± 0,001	39	3	p	2,33	0,155 ± 0,003	0,134 ± 0,003
4	50	p	1,42	0,158 ± 0,005	0,143 ± 0,004	40	3	r	1,07	0,160 ± 0,005	0,141 ± 0,003
5	50	p	1,73	0,157 ± 0,001	0,137 ± 0,002	41	3	r	1,21	0,159 ± 0,006	0,146 ± 0,009
6	50	p	3,67	0,159 ± 0,007	0,146 ± 0,006	42	3	r	1,27	0,155 ± 0,006	0,141 ± 0,005
7	50	r	1,07	0,157 ± 0,004	0,139 ± 0,001	43	3	r	1,36	0,149 ± 0,011	0,146 ± 0,010
8	50	r	1,21	0,169 ± 0,004	0,143 ± 0,004	44	3	r	1,57	0,067 ± 0,001	0,127 ± 0,005
9	50	r	1,27	0,160 ± 0,003	0,134 ± 0,005						
10	50	r	1,42	0,160 ± 0,013	0,132 ± 0,013						
11	50	r	1,73	0,158 ± 0,008	0,138 ± 0,005						

4 - SUMMARY AND CONCLUSIONS

The acid mine drainage environment of Río Tinto area presents the ideal conditions to evaluate the role of colloidal phase in the transport and the fate of trace elements like U and Th in aquatic system. The behaviour of these elements in natural waters is well known, but Río Tinto waters have a pH <3, there is no carbonate that can act as ligands for both investigated elements or neutralize the acidity of the water, and colloids are expected in very high concentrations into the water, due to their formation related to the increasing of pH occurring when clear water from precipitation or of no-contaminated tributary join Río Tinto waters.

Natural river waters underwent firstly to traditional filtration at 0,2 µm, process that, with its slowness, qualitatively reveals a high content in particles > 0,2 µm. Then, filtration at 0,45 µm proceeded, followed by ultrafiltration experiments for different membrane pore size and distinct concentration factors. Low increasing concentration factors were used to investigated if a permeation model is applicable even for low value.

U behaviour can be described by a permeation model that provides a permeation coefficient (P_c) of 0,813 for U < 50 kDa and P_c = 0,626 for U < 3 kDa. For both the ultrafiltration experiments, the value of initial concentration derived from the model is higher than the one measured in the 0,2 µm sample, resulting in a negative value of estimated colloidal fraction. This could suggest a probable contamination or that large artifacts occurred among the membrane and the chemical species. Using the traditional method to estimate U associated to the colloidal fraction for both the membrane pore sizes, again negative values for U in the samples underwent to 50 kDa ultrafiltration can be calculated, but values up to 0,6 % for U associated to 3 kDa colloidal fraction, that means the 3 kDa membrane does not retain dissolved U. Thus, the permeation model can just show that little retention for U occurs and that the permeation behaviour of U can be considered the same even at low concentration factors. But using low concentration factors, the colloidal concentration cannot be estimated by the permeation model.

The application of the permeation model on Th 50 kDa samples failed because the membrane was not retaining in quantitative form, but it could be possible derived a P_c = 0,360 for Th from the 3 kDa experiments. This low value could result from artefactual retention of Th <3 kDa by the membrane. A 6,3% of colloidal Th fraction is calculated from the traditional method, such a low value meaning the membrane doesn't retain dissolved Th.

Compared to the content of U and Th in common natural water (order of ng/L for U and far less for Th), concentrations of both elements are at least three orders higher, but with no appreciable differences among the concentrations in the permeate and the retentate solutions. The high values of the measurements were expected because of the nature of acid mine drainage condition: U derive from the dissolution of aluminosilicates by the leaching of the acidic volcanic lithologies present in the area, Th can stay as dissolved form in extreme acidic conditions, and colloids and all of solid phases, with which Th has high affinity, will be disintegrated.

It can be argued that the colloidal fraction >0,2 μm consist in amorphous oxy-hydroxides of iron and aluminium that, in acid mine drainage environment, get elevated zeta potential values and will not uptake the high charged U(VI) and Th(IV), rejecting them from the particles surfaces and leading to such high concentrations of dissolved form for both the elements. It is important carry out the characterization of the colloidal material for each size membrane experiment, in order to validate this scenario and understand how colloids composition affects the processes of elements uptake from the solution.

Recovery for U is excellent, while the membranes determined large losses of Th during each ultrafiltration experiments (recovery <80%). This could be due to interactions between the negatively charged membrane and the highly charged Th dissolved form. It seems that low CF for Th are inadequate to extract it and reach a permeate that will be representative of its actual permeation behaviour.

Using a standard material to assess more accuracy in the ICP-MS analysis, we found a 1,15% of uncertainty that can be accepted because of the spectroscopy methods can have upt to 2 % of bias. $^{234}U/^{238}U$ activity ratios range between 1,761 and 2,060. The disequilibrium among the ^{234}U and ^{238}U isotopes is attributable to the excess of ^{234}U related both to the recoil effect, and the acidic water preferentially lixiviates ^{234}U respect to ^{238}U from minerals in the mining areas.
The handling and the processing of the samples is a critical point to achieve a good success in all of the work, but difficulties and contamination occurred and led to problems in interpretation of some results and no less to failures in get some information, like the ^{234}U activity. On the other hand, we obtained a range between 0,056 mBq/L and 0,169 mBq/L for ^{230}Th activity, whose presence in solution is mainly related to the decay of ^{234}U. Again the acidic environment promotes the desorption of Th from particles and colloids, while mineral phases undergo dissolution. Both these occurrences could be considered as further contributions of ^{230}Th into the solution.

It would be interesting to investigate the behaviour of the other elements characterizing the AMD system, in order to better understand the relationships between them and U and Th associated, relations that can suggest and confirm these radionuclides derive from leaching of the host rock. Together with the characterization of the colloidal form, this will be the aim of the next project that the research team of the University of Cádiz will advance during the next months, and in which I will participate to carry on the investigation and improve the data on Río Tinto area.

ACKNOWLEDGMENT

I'd like to thank all of the people who supported me in the choice that got me where I am. My family: even just without one of them I wouldn't be able to achieve this objective. I really love each of them: my father, my mother, my brother, my two sisters and each respective partners. I realised how much they are important to me.
My Italian friends in Bologna: I am really grateful to their endurance with my impossible behaviour and bad mood during my always stressful time. Bianca, partner in a multitude of projects, I shared with her all of this university years, five years of studies, choices, sacrifices, angers, tears, joyful times, adventures and significant experiences together. Matteo and Carlotta, I don't know how they can still stand me, living with me was very hard. Thank you for staying close to me. Franz, his friendship and his support was essential for me, for both my university career and my personal life. Stiv, without his help I couldn't understand a lot of things. Sergio, Deiv, Greta, Pierfra, Richi, Marco, Matteo A,, Sara M., Siria, Sara V., Andre, Lu, Cri, Gio F., Gio M., Chiara, Miriana, Gabri L. and all of the others classmates that I shared the passion for geology with. I thank my friends I cannot mention every people met during my academic years, because they are so much, but I would like to say that professors, researchers, students and the staff of geology department, all of them have been like a family for me and I am fond of them. I want to remember Bruno Capaccioni, he left me a lot of teachings and good memories, I miss him.
I want to thank Enrico Dinelli, who promoted the participation in the Erasmus program and for being my supervisor.
Many thanks to my Spanish supervisor Luis Carlos Barbero González, who taught me everything about the work, how to face several coming out situations and their related problems. He had the patience to put up with me and my questions and doubts. I appreciated the support and the assistance from Melquiades Casas Ruiz, I thank him so much. I thank Antonio Benítez Rodriguez (Beni), who explained, showed and helped me in all of the ICP-MS operations. Special thanks to Micheal E. Ketterer, professor at Metropolitan State University of Denver, for his suggestions and comments coming from his great experiences about analytical, instrumental and radiochemistry.
I cannot forgot the support from my friends all along Chiara, Sara and Vale.
Last but not the least, I would like to thank all of the international people met thanks to the Erasmus program in Cádiz, each of them was lovely and surprising, cheering me every time that I needed. Especially all of the flatmates passed by Sagasta 22, I will never forget anybody. Among them, I need to mention Serena and Barbara, they have been so close to me in the worst and dispiriting moments, encouraging me despite everything.
Thanks to everybody.

BIBLIOGRAPHY

Alberic, P., Viollier, E., Jezequel, D., Grosbois, C. & Michard, G. (2000) - Interactions between trace elements and dissolved organic matter in the stagnant anoxic deep layer of a meromictic lake. Limnol. Oceanogr. 45: 1088-1096.

Amos, R.T., Blowes, D.W., Smith, L.& Sego, D.C. (2009) - Measurement of wind induced pressure gradients in a waste rock pile. Vadose Zone J. 2009. http://dx.doi.org/10.2136/vzj2009.0002 (published online 13.09.09).

Andersson, P. S., Wasserburg, G.J., Chen, J.H. & Papanastassiou, D.A. (1995) - ^{238}U–^{234}U and ^{232}Th–^{230}Th in the Baltic Sea and in river water. Earth Planet. Sci. Lett. 130: 217–234.

Andersson, P. S., Porcelli, D., Wasserburg, G. J. & Ingri, J. (1998) - Particle transport of ^{234}U-^{238}U in the Kalix River and in the Baltic Sea. Geochimica et Cosmochimica Acta 62: 385-392.

Andersson, P. S., Porcelli, D., Gustafsson, O., Ingri, J. & Wasserburg, G. J. (2001) - The importance of colloids for the behaviour of uranium isotopes in the low salinity zone of a stable estuary. Geochimica et Cosmochimica Acta 65(1): 13-25.

Bacon, M. P. & Anderson, R. F. (1982) - Distribution of thorium isotopes between dissolved and particulate forms in the deep ocean. Journal of Geophysical Research 87 (C3) : 2045-2056.

Balistrieri, L. S., Brewer, P. G. & Murray, J. W. (1981) - Scavenging residence times of trace metals and surface chemistry of sinking particles in the deep ocean. Deep-Sea Res. I 28: 101-121.

Ball, J.W. & Nordstrom, D.K. (1989) - Final revised analyses of major and trace elements from acid mine waters in the Leviathan mine drainage basin, California and Nevada—October 1981 to October 1982. U.S. Geol. Surv. Water-Resour. Investig. Rep., pp. 89-4138.

Barbero, L., Gasquez, M., Bolívar, J. P., Casas-Ruiz, M., Hierro, A., Baskaran, M. & Ketterer, M. E. (2014) - Mobility of Po and U-isotopes under acid mine drainage conditions: an experimental approach with samples from Río Tinto area (SW Spain). J. Environ. Rad. 138: 384-389.

Baskaran, M., Santschi, P., H., Benoit, G. & Honeyman, B. D. (1992) - Scavenging of thorium isotopes by colloids in seawater of the Gulf of Mexico. Geochim. Cosmochim. Acta 56: 3375-3388.

Borrego, J., Morales, J. A., de la Torre, M. L. & Grande, J. A. (2001) - Geochemical characteristics of heavy metal pollution in surface sediments of the Tinto and Odiel rivers estuary (SW Spain). Environ. Geol. 41: 785-796.

Buesseler, K. O., Bauer, J., Chen, R., Eglinton, T., Gustafsson, O., Landing, W., Mopper, K., Moran, S. B., Santschi, P. H., Vernon-Clark, R. & Wells, M. (1996) - An intercomparison of cross-flow filtration techniques used for sampling marine colloids: overview and organic carbon results, Mar. Chem. 55: 1–32.

Buffle, J., Wilkinson, K. J., Stoll, S., Filella, M. & Zhang, J. (1998) - A generalized description of aquatic colloidal interactions: the three-colloidal component approach, Environ. Sci. Technol. 32: 2887-2899.

Casas-Ruiz, M. & Barbero, L. (2015) - Dissolved versus colloidal U and Th under acid mine drainage conditions in Río Tinto area (Spain). Procedia Earth and Planetary Science 13: 72-75.

Chabaux, F., Bourdon, B. & Riotte, J. (2008) - U-series Geochemistry in Weathering Profiles, River Waters and Lakes. In: U-Th Series Nuclides in Aquatic Systems (S. Krishnaswami & J. K. Cochran editors), Radioactivity in the Environment, vol. 13, Elsevier, Oxford, pp 49-104.

Chase, Z., Anderson, R. F., Martin, Q., Fleisher, P. & Kubik, W. (2002) - The influence of particle composition and particle flux on scavenging of Th, Pa and Be in the ocean. Earth and Planetary Science Letters 204: 215-229.

Chen, J. Y., Ko, C. H., Bhattacharjee, S. & Elimelech, M. (2001) - Role of spatial distribution of porous medium surface charge heterogeneity in colloid transport. Colloids and Surfaces, A: Physico-chemical and engineering Aspects 191 (1-2 Special Issue SI): 3-15.

Chen, M., Guo, L., Huang, Y., Gao, Z., Cai, Y. & Cai, M. (2000): Application of the cross-flow ultrafiltration technique to examining colloidal uranium, thorium, radium isotopes and organic carbon in seawater. Acta Oceanol. Sin. 22 (5): 51-59.

Cheryan, M. (1998) - Ultrafiltration and Macrofiltration Handbook. Technomic, Lancaster.

Dai, M., Buesseler, K. O., Ripple, P., Andrews, J., Belastock, R. A., Gustafsson, O. and Moran, S. B. (1998): Evaluation of two cross-flow ultrafiltration membranes for isolating marine organic colloids, Mar. Chem. 62: 17–136.

Dold, B. & Fontboté, L. (2002) - A mineralogical and geochemical study of element mobility in sulfide mine tailings of Fe oxide Cu-Au deposits from the Punta del Cobre belt, northern Chile. Chemical Geology 189: 135-163.

Dosseto, A., Turner, S. P. & Douglas, G. B. (2006) - Uranium-series isotopes in colloids and suspended sediments: Timescale for sediment production and transport in the Murray-Darling river system. Earth and Planetary Science Letters 246: 418-431.

Doucet, F. J., Lead, J.R. & Santschi, P. H. (2007) - Colloid-trace element interactions in aquatic systems. In: K. J. Wilkinson and J. R. Lead (eds.): Environmental Colloids and Particles. IUPAC Series on Analytical and Physical Chemistry of Environmental Systems 10: 95-157.

Doyle, M. G. & Allen, R. L. (2003) - Subsea-floor replacement in volcanic-hosted massive sulfide deposits. Ore Geology Reviews 23: 183– 222.

Duff, M. C., Coughlin, J. U. & Hunter, D. B. (2002) - Uranium co-precipitation with iron oxide minerals. Geochimica et Cosmochimica Acta 66: 3533-3547.

Emsbo, P. (2009) - Geologic criteria for the assessment of sedimentary exhalative (sedex) Zn-Pb-Ag deposits: U.S. Geological Survey Open-File Report 2009−1209: 21 p.

Everett, D. H. (1988) - Basic principles of colloid chemistry. Royal Society of Chemistry.

Eyal, Y. & Olander, D. R. (1990) - Leaching of uranium and thorium from monazite: I. Initial leaching. Geochimica et Cosmochimica Acta 54: 1867-1877.

Faure, G. & Mensing, T. M. (2005) - Isotopes: principles and applications. Third edition, John Wiley & Sons, Inc., Hoboken, New Jersey, pp.68-72.

Filella, M. (2007) - Colloidal properties of submicron particles in natural waters. In: K. J. Wilkinson and J. R. Lead (eds.): Environmental Colloids and Particles. IUPAC Series on Analytical and Physical Chemistry of Environmental Systems 10: 17-93.

Fleischer, R. L. (1982) - Alpha-recoil damage and solution effects in minerals: uranium isotopic disequilibrium and radon release. Geochimica et Cosmochimica Acta 46: 2191-2201.

Fleischer, R. L. (1983) - Theory of alpha recoil effects on radon release and isotopic disequilibrium. Geochimica et Cosmochimica Acta 47: 779-784.

Fleischer, R. L. (1988) - Alpha-recoil damage: Relation to isotopic disequilibrium and leaching of radionuclides. Geochimica and Cosmochimica Acta 52: 1459-1466.

Franklin, J.M., Gibson, H.L., Jonasson, I.R. & Galley, A.G. (2005) - Volcanogenic massive sulfide deposits, in Hedenquist, J.W., Thompson, J.F.H., Goldfarb, R.J. & Richards, J.P., eds.,

Economic Geology 100th anniversary volume, 1905–2005: Littleton, Colo., Society of Economic Geologists, pp. 523–560.

Goldfarb, R.J., Nelson, S.W., Taylor, C.D., d'Angelo, W.M. & Meier, A.M. (1996) - Acid mine drainage associated with volcanogenic massive sulphide deposits, Prince William Sound, Alaska. In: Dumoulin, J.A., Gray, J.E. (Eds.), Geologic Studies in Alaska by the U.S. Geological Survey 1995: U.S. Geol. Surv. Prof. Pap. 1574: 3–18.

González-Toril, E., Llobet-Brossa, E., Casamayor, E.O., Amann, R. & Amils, R., (2003) - Microbial ecology of an extreme acidic environment, the Tinto River. Applied and Environmental Microbiology 69 (8): 4853–4865.

Guo, L. & Santschi, P. H. (1996) - A critical evaluation of the cross-flow ultrafiltration technique for sampling colloidal organic carbon in seawater. Mar. Chem., 55: 113-127.

Guo, L. & Santschi, P. H. (1997) - Composition and cycling of colloids in marine environments, Rev. Geophy., 35: 17-40.

Guo, L. & Santschi, P. H. (2007) - Ultrafiltration and its application to sampling and characterization of aquatic colloids. In: K. J. Wilkinson and J. R. Lead (eds.): Environmental Colloids and Particles. IUPAC Series on Analytical and Physical Chemistry of Environmental Systems 10: 159-221.

Guo, L., Hunt, B. J. & Santschi, P. H. (2001) - Ultrafiltration behaviour of major ions (Na, Ca, Mg, F, Cl, and SO_4) in natural waters. Water Res. 35: 1500-1508.

Guo, L., Santschi, P. H. & Baskaran, M. (1997) - Interaction of thorium isotopes with colloidal organic matter in oceanic environments. Colloids Surf. A 120: 255-272.

Guo, L., Warnken, K. W. & Santschi, P. H. (2007) - Retention behaviour of dissolved uranium during ultrafiltration: Implications for colloidal U in surface waters. Mar. Chem. 107: 156-166.

Guo, L., Wen, L., Tang, D. & Santschi, P.H. (2000) - Re-examination of cross-flow ultrafiltration for sampling aquatic colloids: evidence from molecular probes. Mar. Chem. 69: 75-90.

Gupta, C. & Singh, H. (2003) - Uranium resource processing: secondary resources. Springer Science & Business Media.

Gustafsson, O., Buesseler, K.O. & Gschwend, P.M. (1996) - On the integrity of cross-flow filtration for collecting marine organic colloids. Mar. Chem. 55: 93-111.

Gustafsson, O., Widerlund, A., Anderson, P., Ingri, J., Roos, P. & Ledin, A. (2000) - Colloid dynamics and transport of major elements through a boreal river-brackish bay mixing zone, Mar. Chem. 71: 1-21.

Harnish, R. A., McKnight, D. M., Ranville, J. F., Stephens, V.C. & Orem, W.H. (1996) - Particulate, Colloidal and Dissolved-phase Associations of Plutonium, Americium, and Uranium in Water Samples from well 1587 and Surface-water Sites SW-51 and SW-53 at the Rocky Flats plant, Colorado, Water-Resources Investigations Report, 96-4067, 43 p.

Henderson, G. M. & Burton, K. W. (1999) - Using ($^{234}U/^{238}U$) to assess diffusion rates of isotope tracers in ferromanganese crusts. Earth and Planetary Science Letters 170: 169-179.

Hierro, A., Bolívar, J.P., Vaca, F. & Borrego, J. (2011) - Behaviour of natural radionuclides in surficial sediments from an estuary impacted by acid mine discharge and industrial effluents in Southwest Spain. J. Environ. Radioact. 110: 13-23.

Hierro, A., Martín, J.E., Olías, M., García, C. & Bolívar, J.P. (2013) - Uranium behavior during a tidal cycle in an estuarine system affected by acid mine drainage (AMD). Chem. Geol. 342: 110-118.

Hirose, K. & Sugimura, Y., (1993) - Chemical speciation of particulate ^{238}U, ^{239},^{240}Pu and Th isotopes in seawater. Sci. Total Environ. 130/131: 517–524.

Jamieson, H. E., Walker, S. R. & Parsons, M. B. (2015) - Mineralogical characterization of mine waste. Appl. Geochem. 57: 85-105.

Jamieson, H. E., Robinson, C., Alpers, C. N., McCleskey, R. B., Nordstrom, D. K. & Peterson, R. C. (2005) - Major and trace element composition of copiapite-group minerals and coexisting water from the Richmond mine, Iron Mountain, California. Chemical Geology 215: 387-405.

Johnson, B.D. & Wangersky, P.J., (1985) - Seawater filtration: particle flow and impact considerations. Limnol. Oceanogr. 30: 966–971.

Ketterer, M., Hierro, A., Barbero, L., Olías, M., Bolívar, J. P., Casas-Ruiz, M. & Baskaran, M. (2011) - ^{230} Th- ^{234}U- ^{238}U disequilibria along the river catchments from the Iberian Belt (Spain) affected by acid mine drainage (AMD). In: Mineralogical Abstracts, Goldschmidt 2011, Prague Czech Republic.

Kigoshi, K. (1971) - Alpha-Recoil Thorium-234: Dissolution into Water and the Uranium-234/Uranium-238 Disequilibrium in Nature. Science 173: 47-48.

Kirby, C.S. & Elder Brady, J.A., (1998) - Field determination of Fe(II) oxidation rates in acid mine drainage using a continuously stirred tank reactor. Appl. Geochem. 13(4): 509–520.

Kirby, C.S., Thomas, H.M., Southam, G. & Donald, R. (1999) - Relative contributions of abiotic and biological factors in Fe(II) oxidation in mine drainage. Appl. Geochem. 14: 511–530.

Ku., T. L., Knauss, K. G. & Mathieu, G. G. (1977) - Uranium in open ocean: concentration and isotopic composition. Deep-Sea Research 24: 1005-1017.

Langmuir, D. (1978) - Uranium solution-mineral equilibria at low temperatures with applications to sedimentary ore deposits. Geochimica et Cosmochimica Acta 42: 547-569.

Langmuir, D. & Herman, J. S. (1980) - The mobility of thorium in natural waters at low temperatures. Geochim. Cosmochim. Acta 44: 1753-1766.

Lao, Y., Anderson, R. F., Broecker, W. S., Hofmann, H. J. & Wolf, W. (1993) - Particulate fluxes of 230Th, 231Pa and 10Be in the Northeastern Pacific Ocean, Geochim. Cosmochim. Acta 57: 205-217.

Lead, J. R. & Wilkinson, K. J. (2007) - Environmental Colloids and Particles: Current knowledge and Future Development. In: K. J. Wilkinson and J. R. Lead (eds.): Environmental Colloids and Particles. IUPAC Series on Analytical and Physical Chemistry of Environmental Systems 10: 1-15.

Lefebvre, R., Hockley, D., Smolensky, J. & Gelinas, P. (2001) - Multiphase transfer processes in waste rock piles producing acid mine drainage 1. Conceptual model and system characterization. J. Contam. Hydrol 52: 137–164.

López-Archilla, A.I.& Amils, R., (1999) - A comparative ecological study of two acidic rivers in southwestern Spain. Microbial Ecology 38: 146–156.

López-Archilla, A.I., Marin, I. & Amils, R. (2000) - Microbial community composition and ecology of an acidic aquatic environment: The Tinto river, Spain. Microbial Ecology 41: 20–35.

Lotze, F. (1945) - Zur Gliederung der Varisciden der Iberischen Mesetas. Geoth. Porsch 6: 78-92.

Lu, E., Zhang, L., Chen, M., Xing, N., Yang, W. F., Li, Y. P. & Huang, Y. P. (2008) - Size-fractionated uranium isotopes in surface waters of the Jiulong River estuary. Acta Oceanol. Sin. 27(1): 29-41.

Luo, S. & Ku, T. (2004) - On the importance of opal, carbonate, and lithogenic clays in scavenging and fractionating ^{230}Th, ^{231}Pa and ^{10}Be in the ocean. Earth and Planetary Science Letters 220: 201-211.

Menor-Salván, C., Tornos, F., Fernández-Remolar, D. & Amils, R. (2010) - Association between catastrophic paleovegetation changes during Devonian–Carboniferous boundary and the formation of giant massive sulfide deposits, Earth Planet. Sci. Lett. 299: 398-408.

Mitjavila, J., Martí, J. & Soriano, C. (1997) - Magmatic evolution and tectonic setting of the Iberian Pyrite Belt volcanism. Journal Petrology 38: 727-755.

Moore, W. S. (1981) - The thorium isotope content of ocean water. Earth and Planetary Science Letters 53: 419-426.

Moreno, C. (1993) - Postvolcanic paleozoic of the Iberian Pyrite Belt: An example of basin morphologic control on sediment distribution in a turbidite basin. Journal Sedimentary Petrology 63: 1118-1128.

Moreno, C., Sierra, S. & Saez, R. (1996) - Evidence catastrophism at the Famennian-Dinantian boundaryin the Iberian Pyrite Belt, in Recent Advances in Lower Carboniferous Geology, edited by P. Strongen, I. D. Sommerville, and G. L. Jones, Geol. Soc. Spec. Publ. 107: 153–162.

Morgan, L.A. & Schulz, K.J. (2012) - Physical volcanology of volcanogenic massive sulfide deposits in volcanogenic massive sulfide occurrence model: U.S. Geological Survey Scientific Investigations Report 2010–5070 –C, chap. 5, 36 p.

Munhá, J. (1990) - Metamorphic evolution of the South Portuguese/Pulo do Lobo Zone. In: Dallmeyer, R. D. & Martinez García E. (eds) Pre-Mesozoic Geology of Iberia. Berlin: Springer-Verlag, pp. 363-369.

Navarro Vásquez, D. & Ramírez Copeiro del Villar, J. (1982) - Mapa geológico y Memoria de la Hoja nº 938 (Nerva). Mapa Geológico de España E. 1:50.000. Segunda Serie (MAGNA), Primera edición. IGME.

Nordstrom, D. K. (1985) - The rate of ferrous iron oxidation in a stream receiving acid mine effluent. In: Selected Papers in the Hydrologic Sciences, U.S. Geological Survey Water Supply Paper 2270. Washington D.C., 113-119.

Nordstrom, D. K. (2011) - Hydrogeochemistry processes governing the origin, transport and fate of major and trace elements from mines waters and mineralized rock to surface waters. Appl. Geochem. 57: 3-16.

Nordstrom, D.K. & Alpers, C.N. (1999) - Geochemistry of acid mine waters. In: Plumlee, G.S., Logsdon, M.J. (Eds.), The Environmental Geochemistry of Mineral Deposits, Part A. Processes, Techniques, and Health Issues: Society of Economic Geologists, Rev. Econ. Geol. 6A: 133–156.

Nordstrom, D. K., Blowes, D. W. & Ptacek, C. J. (2015) - Hydrogeochemistry and microbiology of mine drainage: An update. Appl. Geochem. 57: 3-16.

Olías Álvarez, M., Donaire Romero, T, Fernández Rodríguez, C., Mayoral Alfaro, E., Morales González, J. A., Alonso Chaves, F. M. & Ruiz de Almodóvar Sel, G. (Coords): "Geología de Huelva : lugares de interés geológico". 2ª ed. Huelva : Universidad de Huelva, (2008), 184 p.

Onézime J., Charvet J., Faure M., Bourdier J.-L. & Chauvet A. (2003) - A new geodynamic interpretation for the South Portuguese Zone (SW Iberia) and the Iberian Pyrite Belt genesis. *Tectonics*, American Geophysical Union (AGU), 22 (4): 1027 p., doi:10.1029/2002TC001387.

Osmond, J. K. & Ivanovich, M. (1992) - Uranium-series mobilization and surface hydrology. In Uranium Series Disequilibrium: Application to Earth, Marine and Environmental Sciences, second edition (eds M. Ivanovich and R. S. Harmon). Clarendon Press, Oxford (United Kingdom) pp. 259-289.

Osthols, E. (1995) - Thorium sorption on amorphous silica. Geochim. Cosmochim. Acta 59: 1235-1249.

Pizarro, J., Belzile, N., Filella, M., Leppard, G. G., Negre, J. C., Perret, D. & Buffle, J. (1995) - Coagulation/sedimentation of submicron iron particles in a eutrophic lake. Water Res. 29: 617-632.

Plater, A. J., Ivanovich, M. & Dugdale, R. E. (1992) - Uranium series disequilibrium in river sediments and waters: the significance of anomalous activity ratios. Applied Geochemistry 7: 101-110.

Plumlee, G.S., Smith, K.S., Montour, M.R., Ficklin, W.H. & Mosier, E.L. (1999) - Geologic controls on the composition of natural waters and mine waters draining diverse mineral deposit types. In: Filipek, L.H., Plumlee, G.S. (Eds.), The Environmental Geochemistry of Mineral Deposits, Part B. Case Studies and Research Topics: Society of Economic Geologists, Rev. Econ. Geol. 6B: 373–432.

Porcelli, D., Andersson, P. S., Wasserburg, G. J., Ingri, J. & Baskaran, M. (1997) - The importance of colloids and mires for the transport of uranium isotopes through the Kalix River watershed and the Baltic Sea. Geochim. Cosmochim. Acta 61: 4095-4113.

Quesada, C. (1996) - Estructura del sector español de la Faja Pirítica: implicaciones para la exploración de yacimientos. Boletin Geologico Minero 107: 3-4, 65-78.

Rai, D. & Serne, R., J. (1978) - Solid Phases and Solution Species of Different Elements in Geologic environments. Battelle, PNL-265 I /UC-70.

Riotte, J. & Chabaux, F. (1999) - ($^{234}U/^{238}U$) Activity ratios in freshwaters as tracers of hydrological processes: The Strengbach watershed (Vosges, France). Geochimica et Cosmochimica Acta 63(9): 1263-1275.

Riotte, J., Chabaux, F., Benedetti, M., Dia, A., Gérard, M., Boulégue & J. Etamé, J. (2003) - Uranium colloidal transport and origin of the $^{234}U–^{238}U$ fractionation in surface waters: new insights from Mount Cameroon. Chemical Geology 202: 365-381.

Ritchie, A.I.M. (2003) - Oxidation and gas transport in piles of sulfidic material. In: Jambor, J.L., Blowes, D.W., Ritchie, A.I.M. (Eds.), Environmental Aspects of Mine Wastes. Mineral. Assoc. Can. Short Course 31: 73–94.

Robinson, L. F., Henderson, G. M., Hall, L. & Matthews, I. (2004) – Climatic control of riverine and seawater uranium-isotope ratios. Science 305: 851-854.

Roy-Barman, M.R., Coppola, L. & Souhaut, M. (2002) - Thorium isotopes in the western Mediterranean Sea: an insight into the marine particle dynamics. Earth Planet. Sci. Lett. 196: 161–174.

Sáez, R., Almodovar, G.R. & Pascual, E. (1996) - Geological constraints on massive sulphide genesis in the Iberian Pyrite Belt. Ore Geology Reviews 11: 429-451.

Sánchez España, F. J., López-Pamo, E., Santofimia, E., Aduvire, O., Reyes, J. & Barettino, D. A. (2005) - Acid mine drainage in the Iberian pyrite Belt (Odiel river watershed, Huelva, SW Spain): geochemistry, mineralogy and environmental implications. Appl. Geochem. 12: 269-298.

Sánchez España, F. J., López-Pamo, E. & Santofimia, E. (2007) - The oxidation of ferrous iron in acidic mine effluents from the Iberian Pyrite Belt (Odiel Basin, Huelva, Spain): Field and laboratory rates. Journal of Geochemical Exploration 92: 120–132.

Santschi, P.H., Li, Y.H. & Bell, J.J. (1979) - Natural radionuclides in Narragansett Bay. Earth Planet. Sci. Lett. 47: 201–213.

Santschi, P. H., Murray, J. W., Baskaran, M., Benitez-Nelson, C. R., Guo, L. D., Hung, C. C., Lamborg, C., Moran, S. B., Passow, U. & Roy-Barman, M. (2006) - Thorium speciation in seawater. Marine Chemistry 100: 250-268.

Sarin, M. M., Krishnaswami, S., Somayajulu, B. L. K. & Moore, W. S. (1990) - Chemistry of U, Th, and Ra isotopes in the Ganga-Brahmaputra river system: Weathering processes and fluxes to the bay of Bengal. Geochim. Cosmochim. Acta 54: 1387–1396.

Singhal, R. K., Joshi, S. N. & Hedge, A. G. (2004) - Association of uranium with colloidal and suspended particulate matter in Arabian sea near the west coast of Maharashtra (India). J. Radioanal. Nucl. Chem. 261: 263-267.

Smith, L.J.D., Bailey, B.L., Blowes, D.W., Jambor, J.L., Smith, L. & Sego, D.C. (2013) - The Diavik Waste Rock Project: initial geochemical response from a low sulphide waste rock pile. Appl. Geochem. 36: 210–221.

Steefel, C.I. & Van Cappellen, P. (1990) - A new kinetic approach to modeling water–rock interaction: The role of nucleation, precursors, and Ostwald ripening. Geochim. Cosmochim. Acta 54: 2657–2677.

Swarzenski, P. W., McKee, B.A. & Booth, J. G. (1995) - Uranium geochemistry on the Amazon shelf: chemical phase partitioning and cycling across a salinity gradient. Geochim. Cosmochim. Acta 59: 7-18.

Taillefert, M., Lienemann, C. P., Gaillard, J.F. & Perret, D. (2000) - Speciation, reactivity, and cycling of Fe and Pb in a meromictic lake, Geochim. Cosmochim. Acta 64: 169-183.

Tanazaki, Y., Shimokawa, T. & Nakamura, M. (1992) - Physicochemical speciation of trace elements in river waters by size fractionation. Environ. Sci. Technol. 26: 1433-1444.

Tornos, F. (2006) - Environment of formation and styles of volcanogenic massive sulfides: The Iberian Pyrite Belt. Ore Geology Reviews 28: 259-307.

Tornos Arroyo, F.(2008) - La Geología y Metalogenia de la Faja Pirítica Ibérica. Macla 10: 13-23.

Tornos, F. & Conde, C. (2002) - La influencia biogénica en la formación de sulfuros masivos de la Faja Pirítica Ibérica. Geogaceta 32: 235–238.

Tornos, F., López Pamo, E. & Sánchez España, F. J. (2009) - The Iberian Pyrite Belt . In: García Cortés, A. (ed. pr.); Águeda Villar, J., Palacio Suárez-Valgrande, J. & Salvador González, C.I. (eds.) - SPANISH geological frameworks and geosites: an approach to Spanish geological heritage of international relevance . Madrid: Instituto Geológico y Minero de España, pp. 56-64.

Tricca, A., Wasserburg, G. J., Porcelli, D. & Baskaran, M. (2001) - The transport of U- and Th-series nuclides in a sandy unconfined aquifer. Geochim. Cosmochim. Acta 65: 1187-1210.

Turekian, K. K. (1977) - The fate of metals in the ocean. Geochim. Cosmochim. Acta 41: 1139-1144.

Wang, Y. (2014) - Nanogeochemistry: Nanostructures, emergent properties and their control on geochemical reactions and mass transfer. Chemical Geology 378/379: 1-23.

Wen, L. S., Santschi, P. H., Paternostro, C. & Gill, G. (1999) - Eustarine trace metal distribution in Galveston Bay I: importance of colloidal forms in the speciation of the dissolved phase, Mar. Chem. 63: 185-212.

Williamson, M. A., Kirby, C.S. & Rimstidt, J.D. (1992) - The kinetics of acid mine drainage. In: Program and Abstracts, V. M. Goldschmidt Conference, Reston VA

Yamamoto, M., Sakaguchi, A. & Kofuji, H. (2010) - Uranium in acidic mine drainage at the former Ogoya Mine in Ishikawa Prefecture of Japan. J. Radioanal. Nucl. Chem. 283: 699-705.

Zänker, H., Moll, H., Richter, W., Brendler, V., Henning, C., Reich, T., Kluge, A. & Hüttig, G. (2002) - The colloid chemistry of acid rock drainage solution from an abandoned Zn-Pb-Ag mine. Appl. Geochem. 17: 633-648.

Zhang, L., Chen, M., Yang, W., Xing, N., Li, Y., Qiu, Y. & Huang, Y. (2005) - Size-fractionated thorium isotopes (228Th, 230Th, 232Th) in surface waters in the Jiulong River estuary, China. Journal of Environmental Radioactivity 78: 199–216.

http://www.hannainst.es/catalogo-productos/test-kits/alcalinidad/test-kit-de-alcalinidad--fenolftaleina-y-total--110-test-hi-3811

http://www.hannainst.es/catalogo-productos/test-kits/cloruros/test-kit-cloruro-110-test-hi-3815

http://www.hannainst.es/catalogo-productos/test-kits/hierro/test-kit-de-hierro-50-test-hi-3834

http://www.lenntech.com/periodic/elements/th.htm.

Annex 1

UCA Universidad de Cádiz

Servicios Centrales de Investigación Científica y Tecnológica

División de Espectroscopia(ICP-AAS)

Campus Universitario del Rio San Pedro
Apartado 40. 11510 Puerto Real.Cádiz.
Tel. 956016184. Fax.956016397
http://www2.uca.es/serv/cent_ciencia_tecnologia/

INFORME DE ANÁLISIS Ref: 3471341328210616

Puerto Real, 4 de Julio de 2016

Análisis de 23 muestras líquidas suministradas por D. Luís Carlos Barbero González (Departamento de Ciencias de la Tierra de la UCA). El suministrador identifica las muestras como aguas ácidas filtradas, proporcionándolas en recipientes de plástico.

- FECHA DE RECEPCIÓN: 21/06/16.
- ANÁLISIS REQUERIDO: Elementos: U y Th.
- ANALISTA: Antonio Benítez Rodríguez. Técnico División de Espectroscopía (AAS-ICP).
- INSTRUMENTAL: : Espectrómetro ICP-MS serie X2 de Thermo Elemental.
- TRATAMIENTO PREVIO REALIZADO A LA MUESTRA: Dilución por duplicado de dos muestras y el resto una réplica.

Los resultados son los siguientes:

Muestra	[Th] µg/L	[U] µg/L	Muestra	[Th] µg/L	[U] µg/L
0 (a)	21,1 ± 1,0	5,40 ± 0,23	*34*	13,0 ± 0,6	4,73 ± 0,30
0 (b)	19,2 ± 0,2	5,20 ± 0,10	*35*	14,1 ± 0,6	5,20 ± 0,10
1	28,0 ± 0,2	4,91 ± 0,11	36	15,1 ± 0,6	5,42 ± 0,30
2	19,7 ± 1,3	5,22 ± 0,30	37	17,0 ± 0,5	5,10 ± 0,03
3	17,5 ± 0,5	5,40 ± 0,10	38	16,1 ± 0,3	5,60 ± 0,11
4	17,1 ± 0,7	5,36 ± 0,12	39	14,2 ± 0,6	5,21 ± 0,13
5	16,7 ± 1,2	5,44 ± 0,40	40 (a)	13,5 ± 0,6	5,10 ± 0,10
6	15,6 ± 0,8	5,23 ± 0,10	40 (b)	13,7 ± 0,7	5,20 ± 0,20
7	14,2 ± 0,6	4,81 ± 0,20	41	14,6 ± 0,6	5,41 ± 0,20
8	16,0 ± 1,2	5,41 ± 0,30	42	14,0 ± 0,5	5,13 ± 0,20
9	15,0 ± 0,5	5,30 ± 0,10	43	15,0 ± 0,2	5,30 ± 0,10
10	15,2 ± 0,4	5,31 ± 0,12	44	19,4 ± 0,5	6,54 ± 0,11
11	15,7 ± 1,4	5,30 ± 0,30			

Resultado expresado como el valor medio de tres medidas instrumentales ± desviación estándar.

P. O. A. Benítez

Fdo. Carolina Mendiguchia Martínez
RESPONSABLE CIENTÍFICO DE LA
DIVISIÓN DE ESPECTROSCOPÍA

Annex 2

Sample number	description	permeate or retentate	CF
M0	AC-1 <0,20 µm	-	-
1	AC-1 P<50 kDa	p	1,07
2	AC-1 P<50 kDa	p	1,21
3	AC-1 P<50 kDa	p	1,27
4	AC-1 P<50 kDa	p	1,42
5	AC-1 P<50 kDa	p	1,73
6	AC-1 P<50 kDa	p	3,67
7	AC-1 R<50 kDa	r	1,07
8	AC-1 R<50 kDa	r	1,21
9	AC-1 R<50 kDa	r	1,27
10	AC-1 R<50 kDa	r	1,42
11	AC-1 R<50 kDa	r	1,73
34	AC-1 P<3 kDa	p	1,07
35	AC-1 P<3 kDa	p	1,21
36	AC-1 P<3 kDa	p	1,27
37	AC-1 P<3 kDa	p	1,36
38	AC-1 P<3 kDa	p	1,57
39	AC-1 P<3 kDa	p	2,33
40	AC-1 R<3 kDa	r	1,07
41	AC-1 R<3 kDa	r	1,21
42	AC-1 R<3 kDa	r	1,27
43	AC-1 R<3 kDa	r	1,36
44	AC-1 R<3 kDa	r	1,57
B17	blank	-	-
B18	blank	-	-
B19	blank	-	-
B20	blank	-	-
B21	blank	-	-
B22	blank	-	-
B23	blank	-	-
B24	blank	-	-
C1	marine coral	-	-
C2	marine coral	-	-
C3	marine coral	-	-
C4	marine coral	-	-
C5	marine coral	-	-
C6	marine coral	-	-
Cd1	marine coral dilute x100	-	-
Cd2	marine coral dilute x100	-	-
Cd3	marine coral dilute x100	-	-

Sample AC-1
collected on 26/04/2016 h. 11:00
pH = 2,88
T 26°C
mV 469
mS/cm 4,48
x kDa: pore size of the membrane
CF: factor de concentración
TRU resin columns
added spike: ^{229}Th 200 mBq/g
U collection: distilled water and 0,05M ammonium oxalate
Th collection: elution with 1M HCl, evaporation and re-dissolution using 300 µl 2 M HNO_3 and 2,7 ml distilled water

Run	Time	229Th	230Th	234U	235U	i234c	i235c	i234235	i234235c	AR234238	i230c	i230229	i230229c	230atoms	230mass	230activity
Rinse solution 24/06/2016 10:07:14																
1	10.07.14	13,4	0	0,1	3,4											
2	10.08.02	7,2	0	0	2,7											
3	10.08.51	6,5	0	0	3,7											
x		9,033	0	0,033	3,267											
s		3,798	0	0,058	0,513											
%RSD		42,042	0	173,205	15,709											
B24 24/06/2016 10:12:03																
1	10.12.03	841,239	0,3	0,4	39,4											
2	10.12.52	840,739	0,3	1,1	42,3											
3	10.13.41	829,438	0,2	0,5	40,4											
x		837,139	0,267	0,667	40,7											
s		6,674	0,058	0,379	1,473											
%RSD		0,797	21,651	56,789	3,619											
B23 24/06/2016 10:15:49																
1	10.15.49	1060,462	0,3	0,7	36,9											
2	10.16.38	1082,464	0,4	0,4	34,4											
3	10.17.26	1019,157	0,4	0,8	30,5											
x		1054,028	0,367	0,633	33,933											
s		32,14	0,058	0,208	3,225											
%RSD		3,049	15,746	32,868	9,505											
C6 24/06/2016 10:18:37																
1	10.18.37	57,7	0,7	2666,191	306041,7	2650,392	305916,4	0,008664	1,148311	1,14635784	0,0875	0,001516	0,00151905	15229192,76	5,81729E-15	4,4351E-06
2	10.19.25	46,1	0,1	2770,622	321392,1	2754,823	321266,9	0,008575	1,136528	1,13459452	-0,5125	-0,01112	-0,01113608	-111644565,6	-4,26463E-14	-3,2514E-05
3	10.20.14	40,3	0,5	2954,88	338293,6	2939,081	338168,3	0,008691	1,151943	1,1499834	-0,1125	-0,00279	-0,00279632	-28034455,16	-1,07087E-14	-8,1643E-06
x		48,033	0,433	2797,231	321909,1	2781,432	321783,9	0,008643	1,145594	1,14364525	-0,1795	-0,00374	-0,00374338	-37529206,72	-1,58459E-14	-1,2081E-05
s		8,86	0,306	146,172	16132,14	146,1724	16132,14	6,08E-05	0,008059	0,00804506	-0,3065	-0,03459	-0,03465262	-347409268,5	2,46368E-14	1,87831E-05
%RSD		18,445	70,501	5,226	5,011	5,255292	5,013348	0,703458	0,703458	0,70345765	69,8885	3,789021	3,79547751	38051493185	-155,4776312	-155,477631
C5 24/06/2016 10:22:06																
1	10.22.06	28,4	0,4	2717,206	313655,4	2701,407	313530,1	0,008616	1,141992	1,14004927	-0,2125	-0,00748	-0,00749514	-75142430,47	-2,87031E-14	-2,1883E-05

Run	Time	229Th	230Th	234U	235U	i234c	i235c	i234235	i234235c	AR234238	i230c	i230229	i230229c	230atoms	230mass	230activity
2	10.22.55	24,4	0,6	2705,102	314459,1	2689,303	314333,8	0,008556	1,133968	1,13203942	-0,0125	-0,00051	-0,00051317	-5144756,57	-1,96521E-15	-1,4983E-06
3	10.23.43	24,1	0,5	2773,223	319481,3	2757,424	319356	0,008634	1,144407	1,14246082	-0,1125	-0,00467	-0,004676	-46879192,65	-1,7907E-14	-1,3652E-05
x		25,633	0,5	2731,844	315865,3	2716,045	315740	0,008602	1,140123	1,13818317	-0,1125	-0,00439	-0,00439635	-44075548,82	-1,61918E-14	-1,2345E-05
s		2,401	0,1	36,343	3157,26	36,343	3157,263	4,12E-05	0,005465	0,00545556	-0,5125	-0,21345	-0,21381643	-2143612858	1,34512E-14	1,02552E-05
%RSD		9,366	20	1,33	1	1,338085	0,999957	0,479322	0,479322	0,47932172	19,3875	2,069987	2,07351423	20787980520	-83,0743652	-83,0743652
C4 24/06/2016 10:25:32																
1	10.25.32	24,3	0,3	3556,195	411736,2	3540,396	411610,9	0,008601	1,140032	1,13809326	-0,3125	-0,01286	-0,01288199	-129148210,2	-4,93324E-14	-3,7611E-05
2	10.26.21	18,6	0,6	3179,556	369117,3	3163,757	368992	0,008574	1,136419	1,13448571	-0,0125	-0,00067	-0,00067319	-6749035,501	-2,57802E-15	-1,9655E-06
3	10.27.10	18,1	0,4	3195,461	369850,7	3179,662	369725,5	0,0086	1,139866	1,13792725	-0,2125	-0,01174	-0,01176034	-117903040,1	-4,50369E-14	-3,4336E-05
x		20,333	0,433	3310,404	383568,1	3294,605	383442,8	0,008592	1,138772	1,13683541	-0,1795	-0,00883	-0,00884306	-88655898,6	-3,23158E-14	-2,4638E-05
s		3,444	0,153	213,01	24397,06	213,0098	24397,06	1,54E-05	0,00204	0,00203659	-0,4595	-0,13342	-0,13364778	-1339883431	2,58431E-14	1,97027E-05
%RSD		16,939	35,251	6,435	6,361	6,465411	6,362634	0,179145	0,179145	0,17914529	34,6385	2,044896	2,04838068	20536004587	-79,97040339	-79,9704034
44 24/06/2016 10:29:26																
1	10.29.26	1933,806	43,8	366,007	26688,52	350,208	26563,25	0,013184	1,74742	1,74444725	43,1875	0,022333	0,02237095	224279616,7	8,56709E-14	6,53155E-05
2	10.30.14	1714,462	39,8	310,605	21208,51	294,806	21083,24	0,013983	1,853324	1,85017127	39,1875	0,022857	0,02289597	229543150,6	8,76815E-14	6,68484E-05
3	10.31.03	1608,642	38	312,905	21913,98	297,106	21788,71	0,013636	1,807308	1,80423403	37,3875	0,023242	0,02328125	233405812,1	8,9157E-14	6,79733E-05
x		1752,303	40,533	329,839	23270,34	314,04	23145,06	0,013601	1,802684	1,79961752	39,9205	0,022782	0,02282055	228787035,8	8,75031E-14	6,67124E-05
s		165,852	2,969	31,344	2981,174	31,34351	2981,174	0,000401	0,053103	0,05301298	2,3565	0,014208	0,01423266	142689289,3	1,74986E-15	1,33409E-06
%RSD		9,465	7,324	9,503	12,811	9,980738	12,88039	2,945792	2,945792	2,94579176	6,7115	0,709086	0,71029431	7121043193	1,999763538	1,999763538
43 24/06/2016 10:32:46																
1	10.32.46	1576,037	75,6	546,516	35308,84	530,717	35183,56	0,015084	1,999288	1,99588763	74,9875	0,04758	0,04766085	477823065	1,8252E-13	0,000139153
2	10.33.35	1502,824	83,2	538,816	34875,17	523,017	34749,89	0,015051	1,99487	1,99147669	82,5875	0,054955	0,05504851	551887860,8	2,10812E-13	0,000160723
3	10.34.23	1531,529	77,5	569,618	36807,86	553,819	36682,59	0,015098	2,00106	1,99765623	76,8875	0,050203	0,05028864	504167863	1,92583E-13	0,000146826
x		1536,797	78,767	551,65	35663,96	535,851	35538,68	0,015078	1,998406	1,99500685	78,1545	0,050855	0,0509421	510719133,8	1,95305E-13	0,00014890
s		36,889	3,955	16,03	1014,107	16,02995	1014,106	2,41E-05	0,003188	0,00318253	3,3425	0,09061	0,09076406	909953453	1,43408E-14	1,09334E-05
%RSD		2,4	5,021	2,906	2,844	2,991494	2,853529	0,159525	0,159525	0,15952487	4,4085	1,836875	1,84000484	18446936264	7,342748597	7,342748597
42 24/06/2016 10:35:54																
1	10.35.54	1368,603	74,1	522,815	33810,96	507,016	33685,69	0,015051	1,994934	1,99154071	73,4875	0,053695	0,05378676	539238174	2,0598E-13	0,000157039
2	10.36.43	1256,887	64	482,513	31837,15	466,714	31711,88	0,014717	1,950658	1,94733995	63,3875	0,050432	0,05051807	506468026,1	1,93462E-13	0,000147495
3	10.37.31	1234,384	68	494,713	31735,3	478,914	31610,02	0,015151	2,008098	2,00468263	67,3875	0,054592	0,05468503	548243769,5	2,0942E-13	0,000159662

Run	Time	229Th	230Th	234U	235U	i234c	i235c	i234235	i234235c	AR234238	i230c	i230229	i230229c	230atoms	230mass	230activity
x		1286,625	68,7	500,014	32461,14	484,2147	32335,86	0,014973	1,984563	1,98118776	68,0875	0,052919	0,05300963	531447105,8	2,02954E-13	0,000154732
s		71,881	5,086	20,667	1170,09	20,66726	1170,09	0,000227	0,030092	0,03004053	4,4735	0,062235	0,06234085	624997061,1	8,39811E-15	6,40272E-06
%RSD		5,587	7,404	4,133	3,605	4,268202	3,618552	1,516289	1,516289	1,51628889	6,7915	1,21559	1,217661	12207638985	4,137944151	4,137944151
41 24/06/2016 10:39:36																
1	10.39.36	1313,695	70,4	513,014	32627,95	497,215	32502,67	0,015298	2,027577	2,0241283	69,7875	0,053123	0,05321358	533491786,7	2,03785E-13	0,000155365
2	10.40.25	1365,603	73,8	533,516	34404,68	517,717	34279,41	0,015103	2,001757	1,99835219	73,1875	0,053594	0,05368486	538216607	2,05589E-13	0,000156741
3	10.41.13	1420,811	81,2	533,916	34434,49	518,117	34309,22	0,015101	2,001563	1,99815841	80,5875	0,056719	0,05681601	569607916,1	2,1758E-13	0,000165883
x		1366,703	75,134	526,815	33822,37	511,0163	33697,1	0,015167	2,010299	2,00687963	74,5215	0,054526	0,05461938	547585682,2	2,08985E-13	0,00015933
s		53,567	5,522	11,954	1034,511	11,95398	1034,511	0,000113	0,014964	0,01493809	4,9095	0,091652	0,09180774	920416898,6	7,49847E-15	5,71683E-06
%RSD		3,919	7,35	2,269	3,059	2,339256	3,070029	0,744344	0,744344	0,74434426	6,7375	1,719189	1,72211788	17265062646	3,588044937	3,588044937
40 24/06/2016 10:43:17																
1	10.43.17	1453,916	83,2	587,019	36961,69	571,22	36836,41	0,015507	2,055315	2,05181861	82,5875	0,056803	0,05690028	570452710,1	2,17903E-13	0,000166129
2	10.44.05	1375,104	74	544,816	34750,49	529,017	34625,22	0,015278	2,02502	2,02157574	73,3875	0,053369	0,05345963	535958535,6	2,04727E-13	0,000156084
3	10.44.54	1332,898	72,5	527,715	33525,91	511,916	33400,63	0,015327	2,031404	2,02794852	71,8875	0,053933	0,05402513	541628000,7	2,06893E-13	0,000157735
x		1387,306	76,567	553,184	35079,36	537,3843	34954,09	0,015371	2,037246	2,03378096	75,9545	0,0547S	0,05484292	549826779,4	2,09841E-13	0,000159983
s		61,425	5,793	30,524	1741,34	30,52459	1741,34	0,00012	0,01597	0,01594274	5,1805	0,084339	0,08448233	846976102,2	7,06557E-15	5,38679E-06
%RSD		4,428	7,566	5,518	4,964	5,680215	4,981793	0,783896	0,783896	0,78389645	6,9535	1,570348	1,57302349	15770319447	3,367109147	3,367109147
39 24/06/2016 10:46:48																
1	10.46.48	1454,316	76	589,619	37404,49	573,82	37279,22	0,015392	2,040146	2,03667523	75,3875	0,051837	0,05192541	520577271,9	1,98852E-13	0,000151604
2	10.47.37	1401,808	76	568,118	36435,97	552,319	36310,7	0,015211	2,01608	2,01265016	75,3875	0,053779	0,0538704	540076712,2	2,063E-13	0,000157283
3	10.48.25	1479,62	79,8	607,72	39143,59	591,921	39018,32	0,01517	2,010701	2,00728071	79,1875	0,053519	0,05361	537466107,6	2,05303E-13	0,000156523
x		1445,248	77,267	588,486	37661,35	572,6867	37536,08	0,015258	2,022309	2,0188687	76,6545	0,053039	0,05312937	532647535,5	2,03485E-13	0,000155137
s		39,691	2,194	19,826	1371,964	19,82531	1371,964	0,000118	0,01568	0,01565287	1,5815	0,039845	0,0399132	400149058,3	4,04336E-15	3,08265E-06
%RSD		2,746	2,839	3,369	3,643	3,461808	3,655053	0,775329	0,775329	0,77532857	2,2265	0,810816	0,81219728	8142669550	1,987055904	1,987055904
B22 24/06/2016 10:50:51																
1	10.50.51	1044,96	2,4	9,5	695,127	-6,299	569,854	-0,01105	-1,46508	-1,46258432	1,7875	0,001711	0,001713506	17178728,97	6,56198E-15	5,00285E-06
2	10.51.39	1019,457	0,5	5,2	331,606	-10,599	206,333	-0,05137	-6,8084S	-6,79687222	-0,1125	-0,00011	-0,000110541	-1108225,794	-4,23323E-16	-3,2274E-07
3	10.52.28	1074,564	1,9	4,2	366,707	-11,599	241,434	-0,04804	-6,36758	-6,356748433	1,2875	0,001198	0,001200202	12032603,19	4,59625E-15	3,50418E-06
x		1046,327	1,6	6,3	464,48	-9,499	339,207	-0,028	-3,71164	-3,705322278	0,9875	0,000944	0,000945386	9477947,874	3,5783E-15	2,7281E-06
s		27,579	0,985	2,816	200,515	-12,983	75,242	-0,17255	-22,87	-22,83114183	0,3725	0,013507	0,013529668	135641444,5	3,60219E-15	2,74631E-06

Run	Time	229Th	230Th	234U	235U	i234c	i235c	i234235	i234235c	AR234238	i230c	i230229	i230229c	230atoms	230mass	230activity
%RSD		2,636	61,555	44,699	43,17	28,9	-82,103	-0,352	-46,6542	-46,57487761	60,942S	23,11931	23,15870242	2,32177E+11	100,6676048	100,6676048
B21 24/06/2016 10:55:39																
1	10.55.39	1076,564	2,2	1,9	104,301	-13,899	-20,972	0,662741	87,84074	87,69132087	1,587S	0,001475	0,001477111	14808754,2	5,65669E-15	4,31266E-06
2	10.56.28	966,451	0,7	1,4	77,1	-14,399	-48,173	0,298902	39,61694	39,54954983	0,087S	9,05E-05	9,06917E-05	909228,1163	3,47309E-16	2,64789E-07
3	10.57.16	879,343	0,5	1	56	-14,799	-69,273	0,213633	28,31527	28,26710161	-0,112S	-0,00013	-0,000128154	-1284809,844	-4,90775E-16	-3,7417E-07
x		974,119	1,133	1,433	79,134	-14,366	-46,139	0,311363	41,26862	41,19842282	0,520S	0,000534	0,000535239	5366033,299	1,83774E-15	1,40109E-06
s		98,834	0,929	0,451	24,214	-15,348	-101,059	0,151872	20,12932	20,09507817	0,316S	0,003202	0,003207796	32159699,77	3,33375E-15	2,54165E-06
%RSD		10,146	81,984	31,46	30,599	15,661	-94,674	-0,16542	-21,9251	-21,88777768	81,371S	8,020057	8,033722496	80541943986	181,4046061	181,4046061
Cleaning 24/06/2016 10:59:39																
1	10.59.39	34,3	1,6	1,6	85,2	-14,199	-40,073	0,354328	46,96325	46,88336862	0,987S	0,02879	0,028839143	289126319,7	1,10441E-13	8,42004E-05
2	11.00.28	29,8	0,9	1,2	80,5	-14,599	-44,773	0,326067	43,2174S	43,14394159	0,287S	0,009648	0,00966409	96887160,65	3,70092E-14	2,82158E-05
3	11.01.16	31,1	1,2	1,1	70,5	-14,699	-54,773	0,268362	35,56915	35,50865049	0,587S	0,018891	0,018922863	189710830,7	7,24663E-14	5,52483E-05
x		31,733	1,233	1,3	78,734	-14,499	-46,539	0,311545	41,2927	41,22246031	0,620S	0,019554	0,019587094	196370071,3	7,33056E-14	5,58882E-05
s		2,316	0,351	0,265	7,508	-15,534	-117,765	0,131907	17,48314	17,45339712	-0,261S	-0,11291	-0,113102577	-1133907902	3,67232E-14	2,79978E-05
%RSD		7,298	28,475	20,352	9,535	4,553	-115,738	-0,03934	-5,21404	-5,205165983	27,862S	3,817827	3,824331976	38340773150	50,09606774	50,09606774
C3 24/06/2016 11:03:05																
1	11.03.05	109,401	2,3	2270,584	263066,8	2254,785	262941,6	0,008575	1,136575	1,134641845	1,687S	0,01542S	0,015451187	154905605,5	5,91713E-14	4,51122E-05
2	11.03.54	34,8	0,7	2372,309	272689,1	2356,51	272563,9	0,008646	1,145917	1,143968133	0,087S	0,002514	0,002518652	25250701,79	9,64533E-15	7,3536E-06
3	11.04.43	25,1	0,5	2405,218	280069,2	2389,419	279943,9	0,008535	1,131289	1,129364634	-0,112S	-0,00448	-0,004489709	-45011495,73	-1,71936E-14	-1,3108E-05
x		56,434	1,167	2349,37	271941,7	2333,571	271816,4	0,008585	1,137927	1,135991537	0,554S	0,009826	0,009842379	98674596,8	1,72077E-14	1,31191E-05
s		46,127	0,987	70,187	8525,777	70,187	8525,781	5,59E-05	0,007407	0,007394714	0,374S	0,008119	0,008132723	81534470,64	3,874E-14	2,95354E-05
%RSD		81,736	84,564	2,987	3,135	3,007708	3,136595	0,650948	0,650948	0,650948008	83,951S	1,027106	1,028855639	10314774162	225,1324841	225,1324841
38 24/06/2016 11:06:41																
1	11.06.41	1443,315	73,4	579,318	39129,43	563,519	39004,16	0,014448	1,914917	1,911659651	72,787S	0,050431	0,050516708	506454368,7	1,93457E-13	0,00014749
2	11.07.30	1440,814	76,1	572,418	36881,56	556,619	36756,29	0,015144	2,007144	2,003730344	75,487S	0,052392	0,05248153	526152655,5	2,00981E-13	0,000153228
3	11.08.19	1426,112	71,7	551,117	34998,54	535,318	34873,27	0,01535	2,034565	2,031103796	71,087S	0,049847	0,049932001	500592398,8	1,91218E-13	0,000145784
x		1436,747	73,734	567,618	37003,18	551,8187	36877,9	0,014981	1,985542	1,982164597	73,121S	0,050894	0,050980508	511104184,6	1,95219E-13	0,00014883S
s		9,295	2,219	14,701	2068,129	14,70056	2068,129	0,000473	0,062681	0,062574252	1,606S	0,172835	0,17312935	1735705260	5,11465E-15	3,89941E-06
%RSD		0,647	3,009	2,59	5,589	2,66402	5,608043	3,156865	3,156865	3,156864583	2,396S	3,704019	3,710329804	37197846374	2,619961883	2,619961883

Run	Time	229Th	230Th	234U	235U	i234c	i235c	i234235	i234235c	AR234238	i230c	i230229	i230229c	230atoms	230mass	230activity
37	24/06/2016 11:10:30															
1	11.10.30	1577,637	88	654,224	41894,71	638,425	41769,44	0,015285	2,025832	2,022386459	87,3875	0,055391	0,055485767	556271584,4	2,12486E-13	0,000161999
2	11.11.18	1667,553	87,6	681,826	43498,42	666,027	43373,15	0,015356	2,035275	2,031813432	86,9875	0,052165	0,052253642	523867971,7	2,00109E-13	0,000152563
3	11.12.07	1469,919	77,5	599,02	38270,59	583,221	38145,31	0,015289	2,026489	2,023041893	76,8875	0,052307	0,05239643	525299491,3	2,00655E-13	0,00015298
x		1571,703	84,367	645,023	41221,24	629,2243	41095,97	0,01531	2,029199	2,025747262	83,7545	0,053289	0,053379811	535158357,3	2,04417E-13	0,000155847
s		98,951	5,95	42,163	2678,196	42,16275	2678,196	3,98E-05	0,005273	0,00526367	5,3375	0,053941	0,054032749	541704376,5	6,99372E-15	5,33201E-06
%RSD		6,296	7,053	6,537	6,497	6,70075	6,516931	0,259838	0,259838	0,259838431	6,4405	1,022951	1,024694081	10273052535	3,421304572	3,421304572
36	24/06/2016 11:13:50															
1	11.13.50	1613,843	87,4	616,121	39029	600,322	38903,73	0,015431	2,045245	2,041765946	86,7875	0,053777	0,053868547	540058168,5	2,06293E-13	0,000157278
2	11.14.39	1555,033	75,4	603,32	37559,93	587,521	37434,66	0,015695	2,080184	2,076645812	74,7875	0,048094	0,048175781	482985452,3	1,84492E-13	0,000140657
3	11.15.28	1494,823	74,2	569,718	35675,66	553,919	35550,39	0,015581	2,065162	2,061649279	73,5875	0,049228	0,049312116	494377755,1	1,88844E-13	0,000143974
x		1554,566	79	596,386	37421,53	580,5873	37296,26	0,015569	2,06353	2,060020346	78,3875	0,050424	0,050509958	506386702,3	1,9321E-13	0,00014730
s		59,512	7,299	23,966	1680,946	23,96594	1680,947	0,000132	0,017527	0,017496894	6,6865	0,112355	0,112546933	1128337305	1,15375E-14	8,79619E-06
%RSD		3,828	9,24	4,019	4,492	4,127879	4,507011	0,849355	0,849355	0,849355421	8,6275	2,253788	2,257628095	22633810875	5,971495197	5,971495197
35	24/06/2016 11:17:19															
1	11.17.19	1481,421	72,6	538,416	34708,63	522,617	34583,36	0,015112	2,002943	1,999536174	71,9875	0,048594	0,048676345	488003839,1	1,86409E-13	0,000142118
2	11.18.07	1386,606	71	529,315	32672,91	513,516	32547,64	0,015777	2,091158	2,087600771	70,3875	0,050762	0,050848931	509785066,3	1,94729E-13	0,000148461
3	11.18.56	1464,618	70,9	544,616	34032,78	528,817	33907,51	0,015596	2,067101	2,063585191	70,2875	0,04799	0,0480721	481945992,2	1,84095E-13	0,000140354
x		1444,215	71,5	537,449	33804,78	521,65	33679,5	0,015495	2,053734	2,050240712	70,8875	0,049084	0,049167392	492926824,6	1,88411E-13	0,000143645
s		50,593	0,954	7,696	1036,838	7,696198	1036,839	0,000344	0,045601	0,045523616	0,3415	0,00675	0,006761447	67786766,7	5,59257E-15	4,26377E-06
%RSD		3,503	1,334	1,432	3,067	1,475357	3,078545	2,220403	2,220403	2,220403494	0,7215	0,205966	0,206317259	2068430066	2,968279032	2,968279032
34	24/06/2016 11:20:51															
1	11.20.51	1391,206	72,6	543,616	34636,06	527,817	34510,78	0,015294	2,027126	2,023678263	71,9875	0,051745	0,051832841	519649236,2	1,98497E-13	0,000151334
2	11.21.39	1400,208	69,6	546,916	35161,17	531,117	35035,89	0,015159	2,009228	2,005810577	68,9875	0,049269	0,049353416	494791803	1,89002E-13	0,000144095
3	11.22.28	1441,714	77,1	563,017	35711,51	547,218	35586,23	0,015377	2,038124	2,034657317	76,4875	0,053053	0,053143568	532789913,3	2,03517E-13	0,000155161
x		1411,043	73,1	551,183	35169,58	535,384	35044,3	0,015277	2,024826	2,021382053	72,4875	0,051372	0,051459106	515902362,8	1,97005E-13	0,000150197
s		26,941	3,775	10,381	537,774	10,38052	537,7738	0,00011	0,014585	0,014559809	3,1625	0,117386	0,117586154	1178857921	7,37142E-15	5,61997E-06
%RSD		1,909	5,164	1,883	1,529	1,938892	1,534554	0,72029	0,72029	0,720289822	4,5515	2,384233	2,388295063	23943810268	3,741738652	3,741738652
11	24/06/2016 11:24:43															
1	11.24.43	1602,441	84,5	630,522	39625,37	614,723	39500,1	0,015563	2,062688	2,059179398	83,8875	0,05235	0,05243902	525726474	2,00818E-13	0,000153104

Run	Time	229Th	230Th	234U	235U	i234c	i235c	i234235	i234235c	AR234238	i230c	i230229	i230229c	230atoms	230mass	230activity
2	11.25.31	1526,828	80,6	610,52	39065,96	594,721	38940,69	0,015272	2,02424	2,020796556	79,9875	0,052388	0,052477286	526110114,5	2,00965E-13	0,000153216
3	11.26.20	1513,726	87	615,621	38258,84	599,822	38133,56	0,01573	2,084814	2,081267486	86,3875	0,057069	0,057166684	573123583	2,18923E-13	0,000166907
x		1547,665	84,034	618,888	38983,39	603,0887	38858,12	0,015522	2,057247	2,053747813	83,4215	0,053902	0,053993365	541309535,1	2,06902E-13	0,000157742
s		47,888	3,225	10,393	686,999	10,39343	686,9991	0,000231	0,030651	0,030599182	2,6125	0,054554	0,054647332	547865866,3	1,04108E-14	7,9372E-06
%RSD		3,094	3,838	1,679	1,762	1,723366	1,767968	1,489919	1,489919	1,489919152	3,2255	1,042502	1,044277929	10469390060	5,031753086	5,031753086
10 24/06/2016 11:28:24																
1	11.28.24	1339,999	71,1	577,918	36751,34	562,119	36626,06	0,015348	2,034184	2,030724146	70,4875	0,052603	0,052692281	528265534,6	2,01788E-13	0,000153843
2	11.29.13	1358,302	71,3	584,019	36329,85	568,22	36204,57	0,015695	2,080201	2,076662784	70,6875	0,052041	0,05212975	522625897	1,99634E-13	0,000152201
3	11.30.01	1317,295	79,4	550,817	35218,99	535,018	35093,72	0,015245	2,020651	2,017213854	78,7875	0,05981	0,059911975	600646458,2	2,29437E-13	0,000174922
x		1338,532	73,934	570,918	36100,06	555,119	35974,78	0,015429	2,045012	2,041533595	73,3215	0,054778	0,054870883	550107070,2	2,10286E-13	0,000160322
s		20,542	4,735	17,673	791,596	17,67323	791,596	0,000236	0,031217	0,031163712	4,1225	0,200686	0,201028347	2015406167	1,66195E-14	1,26707E-05
%RSD		1,535	6,405	3,096	2,193	3,183684	2,200419	1,526485	1,526485	1,526485386	5,7925	3,773616	3,780045478	37896779642	7,903295887	7,903295887
9 24/06/2016 11:32:03																
1	11.32.03	1636,747	89,5	693,326	43764,69	677,527	43639,42	0,015526	2,057785	2,054284375	88,8875	0,054307	0,05439995	545385744,4	2,08328E-13	0,000158829
2	11.32.52	1567,335	88,1	638,922	41408,19	623,123	41282,92	0,015094	2,000579	1,997175826	87,4875	0,055819	0,055914383	560568666	2,14128E-13	0,000163251
3	11.33.41	1637,247	88,4	681,926	42942,28	666,127	42817,01	0,015558	2,06202	2,058512966	87,7875	0,053619	0,053710332	538471995,7	2,05687E-13	0,000156816
x		1613,777	88,667	671,391	42705,06	655,5923	42579,78	0,015392	2,040128	2,036657722	88,0545	0,054564	0,054657202	547964820,7	2,09381E-13	0,000159632
s		40,22	0,737	28,691	1196,027	28,69117	1196,027	0,000259	0,034316	0,034257632	0,1245	0,003095	0,003100749	31086507,23	4,31766E-15	3,29178E-06
%RSD		2,492	0,831	4,273	2,801	4,376374	2,808909	1,682051	1,682051	1,682051497	0,2185	0,087681	0,087829976	880537887	2,062106187	2,062106187
8 24/06/2016 11:35:28																
1	11.35.28	1495,723	84,9	622,921	39344,86	607,122	39219,58	0,01548	2,051754	2,048263819	84,2875	0,056352	0,056448364	565922087,7	2,16172E-13	0,00016481
2	11.36.17	1346	80,4	556,017	34835,21	540,218	34709,94	0,015564	2,062849	2,059340123	79,7875	0,059277	0,059378491	595298024,5	2,27394E-13	0,000173365
3	11.37.06	1328,397	77,6	554,517	34957,48	538,718	34832,21	0,015466	2,0499	2,04641342	76,9875	0,057955	0,058053939	582018748,5	2,22321E-13	0,000169498
x		1390,04	80,967	577,818	36379,19	562,0193	36253,91	0,015503	2,054834	2,051339121	80,3545	0,057807	0,057905827	580533851,7	2,21962E-13	0,000169224
s		91,946	3,683	39,067	2569,075	39,06725	2569,075	5,28E-05	0,007002	0,006990567	3,0705	0,033395	0,033451502	335367447,2	5,61914E-15	4,28404E-06
%RSD		6,615	4,549	6,761	7,062	6,95123	7,08634	0,340781	0,340781	0,340780662	3,9365	0,595087	0,596100889	5976199008	2,531575389	2,531575389
7 24/06/2016 11:39:0																
1	11.39.08	1444,815	79,4	577,218	36336,57	561,419	36211,3	0,015504	2,054922	2,051426133	78,7875	0,054531	0,054624118	547633140,7	2,09186E-13	0,000159484
2	11.39.57	1278,09	69,8	514,915	32398,63	499,116	32273,36	0,015465	2,049791	2,046304548	69,1875	0,054134	0,05422575	543639300,7	2,07661E-13	0,000158321
3	11.40.45	1350,1	70,8	523,915	33414,1	508,116	33288,82	0,015264	2,023097	2,019655746	70,1875	0,051987	0,05207547	522081711,5	1,99426E-13	0,000152043

Run	Time	229Th	230Th	234U	235U	i234c	i235c	i234235	i234235c	AR234238	i230c	i230229	i230229c	230atoms	230mass	230activity
x		1357,668	73,334	538,683	34049,77	522,8837	33924,49	0,015411	2,042603	2,039128809	72,7215	0,053564	0,053654804	537915291,5	2,05424E-13	0,000156616
s		83,62	5,278	33,675	2044,483	33,6746	2044,483	0,000129	0,017087	0,017057485	4,6655	0,055794	0,055889136	560315548,8	5,25037E-15	4,00288E-06
%RSD		6,159	7,197	6,251	6,004	6,440171	6,026569	0,836508	0,836508	0,836508458	6,5845	1,069086	1,0709075	10736364360	2,555861981	2,555861981
6	24/06/2016 11:41:56															
1	11.41.56	1478,12	85,3	570,118	36062,08	554,319	35936,81	0,015425	2,044431	2,040953618	84,6875	0,057294	0,057391686	575379339,1	2,19785E-13	0,000167564
2	11.42.45	1365,803	72,4	514,815	33532,73	499,016	33407,46	0,014937	1,979809	1,976441414	71,7875	0,052561	0,052650213	527843783	2,01627E-13	0,000153721
3	11.43.33	1384,705	74,5	541,116	33810,96	525,317	33685,69	0,015595	2,066942	2,063426378	73,8875	0,05336	0,05345066	535868656,9	2,04693E-13	0,000156058
x		1409,543	77,4	542,016	34468,59	526,2173	34343,32	0,015319	2,030394	2,02694047	76,7875	0,054477	0,054569699	547087564,2	2,08702E-13	0,000159114
s		60,137	6,922	27,663	1387	27,66249	1386,999	0,000341	0,045231	0,045153873	6,3095	0,104919	0,105097539	1053653537	9,72009E-15	7,4106E-06
%RSD		4,266	8,943	5,104	4,024	5,256857	4,03863	2,227686	2,227686	2,227686181	8,3305	1,952766	1,956093364	19610779718	4,657412139	4,657412139
5	24/06/2016 11:45:21															
1	11.45.21	1413,11	76,6	575,418	36039,9	559,619	35914,62	0,015582	2,065254	2,061740646	75,9875	0,053773	0,053864862	540021226	2,06279E-13	0,000157267
2	11.46.10	1497,923	81,4	594,119	38261,25	578,32	38135,97	0,015165	2,009952	2,006532853	80,7875	0,053933	0,054024909	541625775	2,06892E-13	0,000157734
3	11.46.58	1453,616	78,5	590,219	37517,86	574,42	37392,59	0,015362	2,036087	2,032623625	77,8875	0,053582	0,053673193	538099654,8	2,05545E-13	0,000156707
x		1454,883	78,834	586,586	37273	570,7863	37147,73	0,015369	2,037097	2,033632375	78,2215	0,053765	0,053856414	539936534,1	2,06238E-13	0,000157236
s		42,421	2,417	9,866	1130,737	9,865825	1130,737	0,000209	0,027665	0,027617717	1,8045	0,042538	0,042610374	427189557,7	6,74365E-16	5,14136E-07
%RSD		2,916	3,066	1,682	3,034	1,728462	3,043892	1,358049	1,358049	1,358048655	2,4535	0,841392	0,842825962	8449736900	0,326983306	0,326983306
4	24/06/2016 11:48:47															
1	11.48.47	1155,774	64,5	456,211	28971,19	440,412	28845,92	0,015268	2,023611	2,020168989	63,8875	0,055277	0,055370996	555120949,5	2,12047E-13	0,000161664
2	11.49.36	1085,565	56,9	420,81	26252,15	405,011	26126,88	0,015502	2,05462	2,051125453	56,2875	0,051851	0,051939228	520715818,6	1,98904E-13	0,000151645
3	11.50.24	1074,363	59,1	417,71	27027,22	401,911	26901,94	0,01494	1,980152	1,976783696	58,4875	0,054439	0,054531994	546709548,1	2,08834E-13	0,000159215
x		1105,234	60,167	431,577	27416,85	415,778	27291,58	0,015236	2,019461	2,016026046	59,5545	0,053884	0,053975877	541134209,5	2,06595E-13	0,000157508
s		44,125	3,911	21,39	1400,77	21,3899	1400,77	0,000282	0,037407	0,037343637	3,2985	0,074754	0,074880913	750717282,2	6,85113E-15	5,2233E-06
%RSD		3,992	6,5	4,956	5,109	5,144549	5,132609	1,852339	1,852339	1,852338997	5,8875	1,474825	1,477337595	14811022147	3,316215797	3,316215797
3	24/06/2016 11:52:12															
1	11.52.12	1342,699	64,8	489,513	31394,32	473,714	31269,04	0,01515	2,007955	2,004539184	64,1875	0,047805	0,047886286	480083123,4	1,83383E-13	0,000139812
2	11.53.01	1445,615	73,6	549,117	34205,13	533,318	34079,86	0,015649	2,074153	2,07062473	72,9875	0,050489	0,05057492	507037973,6	1,9368E-13	0,000147661
3	11.53.50	1368,703	65,5	496,914	31703,08	481,115	31577,81	0,015236	2,019385	2,015950183	64,8875	0,047408	0,047488799	476098120	1,81861E-13	0,000138651
x		1385,672	67,967	511,848	32434,18	496,049	32308,9	0,015345	2,033831	2,030371366	67,3545	0,048608	0,048690646	488147218,5	1,86308E-13	0,000142041
s		53,515	4,891	32,487	1541,441	32,48734	1541,441	0,000267	0,035384	0,035324252	4,2785	0,07995	0,080085772	802898507,1	6,4292E-15	4,90162E-06

Run	Time	229Th	230Th	234U	235U	i234c	i235c	i234235	i234235c	AR234238	i230c	i230229	i230229c	230atoms	230mass	230activity
%RSD		3,862	7,196	6,347	4,753	6,549221	4,770949	1,739793	1,739793	1,739792637	6,583S	1,704687	1,707591297	17119426600	3,450839534	3,450839534
2 24/06/2016 11:55:46																
1	11.55.46	1358,602	71	520,815	33838,46	505,016	33713,19	0,01498	1,985444	1,982066558	70,387S	0,051809	0,051897048	520292942	1,98743E-13	0,000151522
2	11.56.3S	1486,021	77	571,318	36391,59	555,519	36266,32	0,015318	2,030241	2,026787989	76,387S	0,051404	0,051491639	516228519,4	1,9719E-13	0,000150338
3	11.57.24	1498,424	81,3	585,119	37393,45	569,32	37268,17	0,015276	2,024746	2,021302123	80,687S	0,053848	0,053939995	540774473,3	2,06567E-13	0,000157486
x		1447,682	76,434	559,084	35874,5	543,28S	35749,23	0,015191	2,013477	2,010052224	75,821S	0,052374	0,052463657	525973472,7	2,00833E-13	0,000153115
s		77,395	5,173	33,853	1833,036	33,85268	1833,036	0,000184	0,024433	0,024391018	4,560S	0,05892S	0,059025397	591758083,7	5,02545E-15	3,8314E-06
%RSD		5,346	6,768	6,055	5,11	6,23111	5,12748S	1,213452	1,213452	1,213451971	6,155S	1,151422	1,153383525	11563226297	2,502298683	2,502298683
1 24/06/2016 11:59:51																
1	11.59.51	1435,713	30,2	224,703	14701,48	208,904	14576,21	0,014332	1,899567	1,896335582	29,587S	0,020608	0,020643342	206959459,7	7,90549E-14	6,02715E-05
2	12.00.40	1341,799	28,3	216,003	13394,76	200,204	13269,49	0,015088	1,999728	1,996326125	27,687S	0,020635	0,02066977	207224415,6	7,91561E-14	6,03486E-05
3	12.01.28	1351,7	30,8	211,802	13245,14	196,003	13119,87	0,014939	1,980093	1,976724413	30,187S	0,022333	0,022371041	224280480,6	8,56713E-14	6,53158E-05
x		1376,404	29,767	217,503	13780,46	201,7037	13655,19	0,014786	1,959796	1,95646204	29,154S	0,021182	0,021217736	212718036,4	8,12941E-14	6,19786E-05
s		51,601	1,305	6,58	801,125	6,579947	801,1252	0,0004	0,053076	0,052985375	0,692S	0,01342	0,013443149	134774057,5	3,79106E-15	2,89031E-06
%RSD		3,749	4,38S	3,025	5,813	3,262185	5,86682	2,708224	2,708224	2,708224027	3,772S	1,006268	1,007982913	10105515018	4,66338992	4,66338992
M0 24/06/2016 12:03:27																
1	12.03.27	1232,784	66,9	469,112	30800,99	453,313	30675,72	0,014778	1,958645	1,955313313	66,287S	0,053771	0,053862191	539994448,2	2,06269E-13	0,000157259
2	12.04.16	1147,973	64,7	457,312	28875,69	441,513	28750,41	0,015357	2,035409	2,031946639	64,087S	0,055827	0,055921784	560642866,4	2,14156E-13	0,000163272
3	12.05.04	1236,984	68,8	492,213	31680,2	476,414	31554,93	0,015098	2,001103	1,997699617	68,187S	0,055124	0,055217921	553586294,6	2,1146E-13	0,000161217
x		1205,913	66,8	472,879	30452,29	457,08	30327,02	0,015077	1,998386	1,994986523	66,187S	0,054886	0,05497932	551194206,7	2,10628E-13	0,000160583
s		50,222	2,052	17,753	1434,406	17,75282	1434,406	0,00029	0,038454	0,038388635	1,439S	0,028663	0,028711576	287847398,9	4,00897E-15	3,05644E-06
%RSD		4,165	3,072	3,754	4,71	3,883964	4,729796	1,924255	1,924255	1,924255362	2,459S	0,590516	0,591522384	5930297284	1,903339338	1,903339338
Blanco tune0,25nit 24/06/2016 12:08:19																
1	12.08.19	3,3	0,3	1,3	102,301	-14,499	-22,972	0,63116	83,65492	83,51262757	-0,312S	-0,0947	-0,094858323	-951000456,9	-3,63266E-13	-0,00027695
2	12.09.07	11,3	0,7	1,3	98,901	-14,499	-26,372	0,549788	72,86975	72,74579404	0,087S	0,007743	0,007756557	77763223,21	2,97042E-14	2,26465E-05
3	12.09.56	1,5	0,1	0,4	32,5	-15,399	-92,773	0,165986	22,00003	21,96260366	-0,512S	-0,34167	-0,342248831	-3431209649	-1,31066E-12	-0,00099925
x		5,367	0,367	1	77,9	-14,799	-47,373	0,312393	41,40509	41,33466173	-0,245S	-0,04574	-0,045820441	-459372026,2	-5,48075E-13	-0,00041785
s		5,217	0,306	0,52	39,355	-15,279	-85,918	0,177832	23,57019	23,53009485	-0,306S	-0,05875	-0,058850344	-590003089,7	6,8903E-13	0,000525316
%RSD		97,204	83,32	51,962	50,519	36,163	-74,754	-0,48376	-64,1183	-64,0092769	82,707S	0,850865	0,852314975	8544868836	-125,7181633	-125,718163

Run	Time	229Th	230Th	234U	235U	i234c	i235c	i234235	i234235c	AR234238	i230c	i230229	i230229c	230atoms	230mass	230activity
B20 24/06/2016 12:13:51																
1	12.13.51	904,345	1,3	5,2	316,305	-10,599	191,032	-0,05548	-7,35379	-7,341278089	0,6875	0,00076	0,000761514	7634545,795	2,91626E-15	2,22336E-06
2	12.14.39	977,353	0,4	2,7	150,701	-13,099	25,428	-0,51514	-68,2776	-68,16145387	-0,2125	-0,00022	-0,000217794	-2183494,628	-8,34057E-16	-6,3589E-07
3	12.15.28	866,741	0,6	1,8	101,001	-13,999	-24,272	0,576755	76,44406	76,3140243	-0,0125	-1,4E-05	-1,44464E-05	-144832,2628	-5,53234E-17	-4,2179E-08
x		916,146	0,767	3,233	189,336	-12,566	64,063	-0,19615	-25,9981	-25,9539037	0,1545	0,000169	0,000168929	1693590,613	6,75628E-16	5,15099E-07
s		56,242	0,473	1,762	112,732	-14,037	-12,541	1,119289	148,3523	148,099993	-0,1395	-0,00248	-0,002484579	-24909103,39	1,97913E-15	1,50889E-06
%RSD		6,139	61,641	54,483	59,541	38,684	-65,732	-0,58851	-78,0022	-77,86950858	61,0285	9,941114	9,958052797	99834283669	292,9315559	292,9315559
B19 24/06/2016 12:18:04																
1	12.18.04	1098,166	0,3	2,1	84,9	-13,699	-40,373	0,339311	44,97282	44,89632052	-0,3125	-0,00028	-0,00028505	-2857766,046	-1,09162E-15	-8,3225E-07
2	12.18.53	1060,362	0,2	0,7	76,3	-15,099	-48,973	0,308313	40,86427	40,79475996	-0,4125	-0,00039	-0,00038968 1	-3906739,388	-1,49231E-15	-1,1377E-06
3	12.19.42	1014,457	0,2	1,4	63,3	-14,399	-61,973	0,232343	30,79513	30,74275029	-0,4125	-0,00041	-0,000407314	-4083522,506	-1,55984E-15	-1,1892E-06
x		1057,662	0,233	1,4	74,834	-14,399	-50,439	0,285474	37,83713	37,77276441	-0,3795	-0,00036	-0,000359422	-3603375,512	-1,38125E-15	-1,0531E-06
s		41,92	0,058	0,7	10,875	-15,099	-114,398	0,131987	17,49371	17,46395723	-0,5545	-0,01323	-0,013250115	-132838792,8	2,53094E-16	1,92959E-07
%RSD		3,963	24,744	50	14,532	34,201	-110,741	-0,30884	-40,9339	-40,86422525	24,1315	6,0892	6,099575455	61151186748	-18,32352415	-18,3235241
B18 24/06/2016 12:21:24																
1	12.21.24	1026,758	0,3	1,1	66,2	-14,699	-59,073	0,248828	32,98003	32,92392994	-0,3125	-0,0003	-0,000304875	-3056515,272	-1,16754E-15	-8,9013E-07
2	12.22.13	989,454	0,2	1,4	59,9	-14,399	-65,373	0,220259	29,1935	29,14384324	-0,4125	-0,00042	-0,000417607	-4186711,045	-1,59925E-15	-1,2193E-06
3	12.23.02	1046,16	0,2	1,1	53,2	-14,699	-72,073	0,203946	27,03133	26,98535254	-0,4125	-0,00039	-0,000394971	-3959774,786	-1,51257E-15	-1,1532E-06
x		1020,791	0,233	1,2	59,767	-14,599	-65,506	0,222865	29,5389	29,4886529	-0,3795	-0,00037	-0,000372404	-3733529,539	-1,42645E-15	-1,0875E-06
s		28,82	0,058	0,173	6,501	-15,626	-118,772	0,131563	17,43757	17,40791094	-0,5545	-0,01924	-0,019272894	-193220062,3	2,28378E-16	1,74115E-07
%RSD		2,823	24,744	14,434	10,877	-1,365	-114,396	0,011932	1,581518	1,57882763	24,1315	8,548176	8,562740889	85845608602	-16,01019354	-16,0101935
B17 24/06/2016 12:24:46																
1	12.24.46	819,637	0,2	0,7	61,4	-15,099	-63,873	0,236391	31,33164	31,27834577	-0,4125	-0,0005	-0,000504129	-5054137,369	-1,93059E-15	-1,4719E-06
2	12.25.34	777,433	0,5	1,2	57,2	-14,599	-68,073	0,214461	28,425	28,37665002	-0,1125	-0,00014	-0,000144954	-1453229,465	-5,55109E-16	-4,2321E-07
3	12.26.23	796,935	0,2	0,9	61,4	-14,899	-63,873	0,23326	30,91662	30,86403561	-0,4125	-0,00052	-0,00051849	-5198112,758	-1,98559E-15	-1,5138E-06
x		798,002	0,3	0,933	60	-14,866	-65,273	0,227751	30,1865	30,13515716	-0,3125	-0,00039	-0,00039227	-3932698,8	-1,49043E-15	-1,1363E-06
s		21,122	0,173	0,252	2,425	-15,547	-122,848	0,126555	16,77377	16,74524145	-0,4395	-0,02081	-0,020843143	-208962562,3	8,10479E-16	6,17909E-07
%RSD		2,647	57,735	26,964	4,041	11,165	-121,232	-0,0921	-12,2066	-12,18580891	57,1225	21,58009	21,61686087	2,16719E+11	-54,37886082	-54,3788608
Tune blanco 24/06/2016 12:28:46																
1	12.28.46	29,6	0,7	12,8	1086,265	-2,999	960,992	-0,00312	-0,41363	-0,412935	0,0875	0,002956	0,002961118	29686635,89	1,13398E-14	8,64545E-06

Run	Time	229Th	230Th	234U	235U	i234c	i235c	i234235	i234235c	AR234238	i230c	i230229	i230229c	230atoms	230mass	230activity
2	12.29.34	4,8	0,1	0,8	49,4	-14,999	-75,873	0,197686	26,20157	26,15700135	-0,512S	-0,10677	-0,10695276	-1072253015	-4,09582E-13	-0,00031227
3	12.30.23	4,2	0	0,1	19,6	-15,699	-105,673	0,148562	19,69066	19,65716388	-0,612S	-0,14583	-0,146081818	-1464540704	-5,59429E-13	-0,00042651
x		12,867	0,267	4,567	385,088	-11,232	259,81S	-0,04323	-5,72987	-5,720128432	-0,345S	-0,0268S	-0,026897388	-269659294,9	-3,19224E-13	-0,00024338
s		14,495	0,379	7,139	607,419	-8,66	482,146	-0,01796	-2,38063	-2,376578861	-0,233S	-0,01611	-0,016136451	-161775707,9	2,95919E-13	0,000225608
%RSD		112,652	141,973	156,325	157,735	140,526	32,462	4,328938	573,7645	572,7885356	141,360S	1,254842	1,256980465	12601835609	-92,69937944	-92,6993794
C2 24/06/2016 12:32:49																
1	12.32.49	94,9	0,6	1838,086	213463,4	1822,287	213338,1	0,008542	1,132141	1,130215465	-0,012S	-0,00013	-0,000131942	-1322782,511	-5,0528E-16	-3,8523E-07
2	12.33.38	53,1	0,2	2173,46	253171,5	2157,661	253046,2	0,008527	1,130149	1,128226606	-0,412S	-0,00777	-0,007781598	-78014274,77	-2,98001E-14	-2,272E-05
3	12.34.27	37,3	0,5	2257,18	257887,4	2241,381	257762,1	0,008696	1,152521	1,1505607	-0,112S	-0,00302	-0,003021225	-30289237,07	-1,157E-14	-8,8209E-06
x		61,767	0,433	2089,575	241507,4	2073,776	241382,1	0,008588	1,13827	1,136334257	-0,179S	-0,00291	-0,002911034	-29184522,26	-1,39585E-14	-1,0642E-05
s		29,762	0,208	221,783	24401,03	221,7824	24401,03	9,34E-05	0,012382	0,012360528	-0,404S	-0,01359	-0,013614314	-136490070,3	1,47927E-14	1,1278E-05
%RSD		48,185	48,038	10,614	10,104	10,69461	10,10888	1,087755	1,087755	1,087754583	47,425S	0,984238	0,985914871	9884272245	-105,976996	-105,976996
C1 24/06/2016 12:36:58																
1	12.36.58	29,4	0,2	2083,139	241272,6	2067,34	241147,3	0,008573	1,136271	1,134337922	-0,412S	-0,01403	-0,014054519	-140903333	-5,38226E-14	-4,1034E-05
2	12.37.47	22,3	0,1	2128,049	248850,6	2112,25	248725,3	0,008492	1,125583	1,123668611	-0,512S	-0,02298	-0,023021222	-230798855,3	-8,81612E-14	-6,7214E-05
3	12.38.3S	21,6	0,1	2147,054	244417,5	2131,25S	244292,2	0,008724	1,15632	1,15435305	-0,512S	-0,02373	-0,02376728	-238278447,8	-9,10183E-14	-6,9392E-05
x		24,433	0,133	2119,414	244846,9	2103,61S	244721,6	0,008596	1,139391	1,137453194	-0,479S	-0,01963	-0,019658536	-197086310,9	-7,76674E-14	-5,9214E-05
s		4,31S	0,058	32,821	3807,213	32,82079	3807,217	0,000118	0,015604	0,015577625	-0,554S	-0,12851	-0,128724174	-1290521946	2,06995E-14	1,57813E-05
%RSD		17,662	43,301	1,549	1,555	1,560209	1,555734	1,369518	1,369518	1,369517873	42,688S	2,416969	2,421086893	24272564180	-26,65145818	-26,6514582
1bis 24/06/2016 12:40:59																
1	12.40.59	1427,212	27,8	237,303	17610,94	221,504	17485,67	0,012668	1,679004	1,676147567	27,187S	0,019049	0,019081836	191304607,3	7,30751E-14	5,57124E-05
2	12.41.47	1260,887	24,1	185,602	13014,41	169,803	12889,14	0,013174	1,746119	1,743148789	23,487S	0,018628	0,018659499	187070484	7,14577E-14	5,44793E-05
3	12.42.36	1260,887	25	189,802	12476,96	174,003	12351,68	0,014087	1,867166	1,863989685	24,387S	0,019342	0,019374499	194238698,4	7,41958E-14	5,65669E-05
x		1316,329	25,633	204,236	14367,44	188,4367	14242,16	0,01331	1,764096	1,761095347	25,020S	0,019008	0,019040173	190886923,6	7,29095E-14	5,55862E-05
s		96,028	1,93	28,714	2821,784	28,71405	2821,783	0,000719	0,095361	0,095198343	1,317S	0,01372	0,013743334	137783554,4	1,37655E-15	1,04948E-06
%RSD		7,29S	7,528	14,059	19,64	15,23804	19,81289	5,405633	5,405633	5,405632546	6,915S	0,947978	0,949593322	9520131193	1,888027286	1,888027286
M0bis 24/06/2016 12:44:24																
1	12.44.24	1242,485	64,9	456,711	29990,79	440,912	29865,52	0,014763	1,956745	1,953416342	64,287S	0,051741	0,051829229	519613022,5	1,98483E-13	0,000151324
2	12.45.13	1135,171	60,4	449,311	28337,2	433,512	28211,92	0,015366	2,03667	2,033205799	59,787S	0,052668	0,052758018	528924580,1	2,0204E-13	0,000154035
3	12.46.02	1093,366	59,4	430,61	26871,46	414,811	26746,18	0,015509	2,05561	2,052113411	58,787S	0,053767	0,053859062	539963086,2	2,06257E-13	0,00015725

Run	Time	229Th	230Th	234U	235U	i234c	i235c	i234235	i234235c	AR234238	i230c	i230229	i230229c	230atoms	230mass	230activity
x		1157,007	61,567	445,544	28399,81	429,745	28274,54	0,015213	2,016342	2,012911851	60,9545	0,052683	0,05277268	529071576,6	2,0226E-13	0,000154203
s		76,92	2,93	13,452	1560,609	13,45207	1560,608	0,000396	0,052474	0,052384741	2,3175	0,030129	0,030180041	302569474,6	3,89135E-15	2,96676E-06
%RSD		6,648	4,759	3,019	5,495	3,130245	5,519483	2,602436	2,602436	2,602435931	4,1465	0,623721	0,624784175	6263762793	1,923934432	1,923934432

coral diluted x 100 measurements for MBF calculation

Run	Time	235U	238U
Blank rinse 24/06/2016 12:52:08			
1	12.52.08	55,75	7674,038
2	12.52.57	58,15	8221,316
3	12.53.46	48,3	6655,836
x		54,067	7517,063
s		5,136	794,458
%RSD		9,5	10,569
Cd1_Coral 100x dil 24/06/2016 12:57:09			
1	12.57.09	1263,838	172939,14
2	12.57.58	1324,647	182628,84
3	12.58.46	1392,307	189152,21
x		1326,93	181573,4
s		64,265	8157,904
%RSD		4,843	4,493
Cd2_Coral 100x dil 24/06/2016 12:59:57			
1	12.59.57	1476,57	203388,87
2	13.00.45	1595,84	218037,54
3	13.01.33	1597,64	217790,52
x		1556,683	213072,31
s		69,386	8387,015
%RSD		4,457	3,936
Cd3_Coral 100x dil 24/06/2016 13:02:44			
1	13.02.44	1735,416	237673,8
2	13.03.33	1888,946	261324,61
3	13.04.21	1874,743	259022,31
x		1833,035	252673,57
s		84,839	13041,093
%RSD		4,628	5,161

238U	235U	238235	MBF
208256,03	1518,149	137,177596	1,00170389